University of Alberta

# Borehole-based investigations of subglacial hydrology

by

Shulamit Gordon

A thesis submitted to the Faculty of Graduate Studies and Research in partial fulfillment of the requirements of Master of Science

Department of Earth and Atmospheric Sciences

Edmonton, Alberta

Spring 1996

National Library of Canada

Acquisitions and Bibliographic Services Branch

395 Wellington Street
Ottawa, Ontario
K1A 0N4

Bibliothèque nationale du Canada

Direction des acquisitions et des services bibliographiques

395, rue Wellington
Ottawa (Ontario)
K1A 0N4

*Your file* *Votre référence*

*Our file* *Notre référence*

**The author has granted an irrevocable non-exclusive licence allowing the National Library of Canada to reproduce, loan, distribute or sell copies of his/her thesis by any means and in any form or format, making this thesis available to interested persons.**

**L'auteur a accordé une licence irrévocable et non exclusive permettant à la Bibliothèque nationale du Canada de reproduire, prêter, distribuer ou vendre des copies de sa thèse de quelque manière et sous quelque forme que ce soit pour mettre des exemplaires de cette thèse à la disposition des personnes intéressées.**

**The author retains ownership of the copyright in his/her thesis. Neither the thesis nor substantial extracts from it may be printed or otherwise reproduced without his/her permission.**

**L'auteur conserve la propriété du droit d'auteur qui protège sa thèse. Ni la thèse ni des extraits substantiels de celle-ci ne doivent être imprimés ou autrement reproduits sans son autorisation.**

ISBN 0-612-18267-3

Canada

**University of Alberta**

**Library Release Form**

**Name of Author**: Shulamit Gordon

**Title of Thesis:** Borehole-based investigations of subglacial hydrology

**Degree**: Master of Science

**Year this Degree Granted:** 1996

Permission is hereby granted to the University of Alberta Library to reproduce single copies of this thesis and to lend or sell such copies for private, scholarly, or scientific research purposes only.

The author reserves all other publication and other rights in association with the copyright in the thesis, and except as hereinbefore provided, neither the thesis nor any substantial portion thereof may be printed or otherwise reproduced in any material form whatever without the author's prior written permission.

21, Rosecroft Avenue,
London, NW3 7QA.
England.

31st May 1996

UNIVERSITY OF ALBERTA

FACULTY OF GRADUATE STUDIES AND RESEARCH

The undersigned certify that they have read, and recommend to the Faculty of Graduate Studies and Research for acceptance, a thesis entitled *Borehole Based Investigations of Subglacial Hydrology* submitted by Shulamit Gordon in partial fulfillment of the requirements for the degree of Master of Science.

M. J. Sharp
Supervisor

F. E. Hicks
External Examiner

R. B. Rains

Date: May 23 1996

## ABSTRACT

The nature and evolution of the subglacial drainage system under part of Haut Glacier d'Arolla, Switzerland was investigated over three summer observation periods using measurements of borehole water level and of the electrical conductivity and turbidity of basal meltwaters. Electrical conductivity profiles, salt traces and video recordings were also carried-out in boreholes to identify the water sources driving water level changes, and to determine patterns of water circulation within boreholes. This was necessary so that the basal water quality measurements could be understood and interpreted with confidence.

In each year, a variable pressure axis (VPA) was identified within the borehole array. Increasing base water levels and decreasing water level fluctuation amplitudes away from the centre of the VPA revealed the presence of a subglacial channel located within an extensive distributed system. A period of high subglacial water pressures following a heavy rainfall event, triggered re-organisation of the subglacial drainage system in the 1993 summer observation period which affected the water level behaviour in all observed boreholes. Subsequent to this, the evolution of a subglacial channel was demonstrated.

## ACKNOWLEDGEMENTS

Many thanks to Dr. Martin Sharp for his continued encouragement and support in my work over the past four years and for inviting me to come to the University of Alberta to undertake this Masters degree. It has been a privilege to work with, and learn from such a great mind.

Thank you to all of the now widely scattered members of the Arolla Glaciology Project for their company and continual entertainment in the field and for putting up with my singing (or not as the case may be); Ian (Ball or Aerosol?) Willis, Bryn (Dont mess with me) Hubbard, Martyn (Torchy) Tranter, Pete (Ploppy) Nienow, Douglas (Snoop) Mair, Mickey (Excellent!!!) Nielsen, Helen (Spaz) Lamb, Ben (Brown) Brock, Matt (Gum) Tulley, Luke (SAY it) Copland and Giles (Tasteful) Brown.

My deepest gratitude to the many, many people (too many to name or remember) who helped me probe the depths of Haut Glacier D'Arolla over the last four years. Thank you for putting up with the monotony. Special thanks to Brad Ketterling for the cheroots and probe advice, Ginny Catania for the gossip sessions, Bernd Kulessa for his tranquility (!) and Marie Minner for eating her chocolate.

Life in Edmonton has been made especially bearable thanks to the many fun, caring and helpful people I have gotten to know here...thanks to you all; Mandy (you're THE best), Anne, Wendy, Esther, Anthony, Colm, Skids, Scott L., Darren, Craig, Elisabeth, Amy (and all the rest from the dept.), Steph, Dave S., Pat, Darci, Shannon and all the squash crowd. To Janis (BBLH) for her honest friendship, for trying to share the light of the double edged sword with me and for her prayers. Finally, to all my family at home for their never ending love, support and thoughtfulness and for laughing at my thesis title.

Financial support for this thesis came from a Geological Society of America grant and funds from Dr. Sharp's NSERC grant.

## TABLE OF CONTENTS


CHAPTER 1 : **INTRODUCTION** . . . . . 1

1.1 Thesis rationale . . . . . 1

1.2 Field site . . . . . 6

1.3 Thesis outline . . . . . 9

CHAPTER 2: **INTRA- AND INTER-ANNUAL DISTRIBUTION OF BOREHOLE WATER LEVEL BEHAVIOUR** . . . . . 11

2.1 Introduction . . . . . 11

2.2 Water level measurements . . . . . 16

2.2.1 Manual WL measurements . . . . . 16

2.2.2 Automatic in-situ WL measurements . . . . . 16

2.3 Classification of water level behaviour . . . . . 17

2.4 Spatial distribution of classified WL behaviour . . . . . 22

2.4.1 Annual distribution of classified WL behaviour . . . . . 22

2.4.2 Inter-annual comparisons of WL behaviour patterns . . . . . 23

2.4.2.1 Width of connected zone . . . . . 23

2.4.2.2 WL behaviour in the connected zone . . . . . 23

2.5 Possible reasons for the observed distribution of borehole WL behaviour . . . . . 23

2.5.1 Meteorological Conditions . . . . . 24

2.5.2 Snowline position . . . . . 25

2.6 Discussion . . . . . 25

2.6.1 1993 . . . . . 29

2.6.2 1992 . . . . . 30

2.6.3 1995 . . . . . 32

2.7 Changing borehole WL behaviour over an observation season . . . . . 33

2.8 Summary . . . . . 36

CHAPTER 3 : **DETERMINATION OF BOREHOLE PLUMBING FOR THE INTERPRETATION OF BASAL WATER QUALITY MEASUREMENTS** .. 38

3.1 Introduction .... 38

3.2 Data sources .... 40

3.2.1 Drilling records .... 40

3.2.2 Continuous in-situ and manual WLs .... 41

3.2.3 Continuous in-situ EC measurements .... 42

3.2.4 Continuous in-situ Tu measurements .... 44

3.2.5 EC profiling .... 46

3.2.6 Borehole salt tracing .... 48

3.2.7 Borehole video imagery .... 48

3.3 Classification of borehole plumbing .... 50

3.4 Examples of borehole plumbing categories .... 53

3.4.1 Unconnected .... 53

3.4.1.1 Unstratified 92/2 .... 53

3.4.1.2 Stratified 92/7 .... 53

3.4.2 Englacially connected .... 53

3.4.2.1 93/39 .... 53

3.4.2.2 95/2 .... 55

3.4.3 Passively connected .... 55

3.4.4 Actively connected .... 58

3.4.4.1 93/37 .... 58

3.4.4.2 93/41 .... 61

3.4.4.3 92/14 .... 66

3.4.5 Anomalous behaviour .... 66

3.4.5.1 92/5 .... 66

3.4.5.2 65/16 .... 66

3.4.5.3 95/17 .... 68

3.5 Distribution of the classified boreholes .... 69

3.6 Summary .... 71

CHAPTER 4: **SEASONAL RE-ORGANISATION OF SUBGLACIAL DRAINAGE INFERRED FROM MEASUREMENTS IN BOREHOLES** . . . . 72

4.1 Introduction . . . . 72

4.2 Analysis of in-situ records . . . . 73

4.3 Water level and head difference records . . . . 89

4.4 In-situ water quality records . . . . 95

4.5 Borehole EC profiling . . . . 96

4.6 Possible explanations for the observed evolution of the subglacial drainage system . . . . 112

4.6.1 Evidence for channel formation . . . . 113

4.6.2 The character of the subglacial drainage system before channelisation . . . . 117

4.6.3 The character of the subglacial drainage system after channelisation . . . . 119

4.6.3.1 Direct Response . . . . 119

4.6.3.2 Lagged Response . . . . 120

4.6.3.3 Damped Response . . . . 121

4.6.3.4 Inverse Response . . . . 122

4.6.4 Summary . . . . 125

4.7 Summary . . . . 126

CHAPTER 5 : **CONCLUSION** . . . . 127

5.1 Implications . . . . 128

BIBLIOGRAPHY . . . . 130

APPENDICES . . . . 135

I Drilling procedure . . . . 135

II EC profilers . . . . 136

III In-situ water pressure, electrical conductivity and turbidity sensors . . . . 138

IV Video imagery system . . . . 141

## LIST OF FIGURES

Figure 1.1 Haut Glacier d'Arolla showing the location of the borehole array, GDSA intake and upper meteorological station . . . . . 7

Figure 1.2 Borehole arrays for a) 1992, b) 1993, and c) 1995 . . . . . 8

Figure 2.1 a) Longitudinal cross-section through an idealised glacier showing Shreve's equipotential surfaces, b) Plan view of an idealised glacier showing Shreve's equipotential contours and consequent water flow at the bed, c) Plan view of an idealised glacier showing Röthlisberger's 'valley' equipotential surfaces and consequent water flow at the bed, and d) Cross-section through an idealised glacier showing the effect of a channel at a pressure less than IOP on the piezometric surface and borehole water levels . . . . . 13

Figure 2.2 Distribution of all classified boreholes in 1992, 1993 and 1995 . . . . . 21

Figure 2.3 1993 a) temperature, b) precipitation, and c) discharge . . . . . 26

Figure 2.4 1992 a) temperature, b) precipitation, and c) discharge . . . . . 27

Figure 2.5 1995 a) temperature, b) precipitation, and c) discharge . . . . . 28

Figure 2.6 Distribution of classified boreholes in 1993 highlighting those holes that changed classification over the summer observation period . . . . . 34

Figure 3.1 Frequency histogram of in-situ EC measured in 1992, 1993 and 1995 . . . . . 45

Figure 3.2 92/7 EC profiles . . . . . 54

Figure 3.3 93/39 EC profiles . . . . . 54

Figure 3.4 95/2 in-situ WL and EC and EC profiles . . . . . 57

Figure 3.5 95/8 EC profiling and video log measurements. . . . . 57

Figure 3.6 93/37 a) in-situ WL and EC profiles and b) in-situ EC and Tu. . . . . 59

Figure 3.7 93/37 salt trace profiles conducted on JD 232 . . . . . 60

Figure 3.8 93/41 a) in-situ WL and EC profiles and b) in-situ EC and Tu. . . . . 62

Figure 3.9 a) 93/41 salt trace profiles conducted on JD 231, b) 93/41 in-situ EC and Tu measurements for JD 231-232. . . . . 63

Figure 3.10 92/14 EC profiles . . . . . 67

Figure 3.11 92/5 EC profiles . . . . . 67
Figure 3.12 95/17 in-situ WL and EC and EC profiles. . . . . 67
Figure 3.13 Distribution of classified boreholes; a) unconnected, b) actively connected, c) unconnected unstratified, d) unconnected stratified, e) englacial, and f) passively connected . . . . . 70
Figure 4.1 1993 borehole array highlighting the location of the seven boreholes discussed in this chapter . . . . . 74
Figure 4.2 1993 a) temperature, b) precipitation, and c) discharge from JD 198 to JD 233. . . . . 76
Figure 4.3 H35 WL from JD 203 to JD 233 . . . . . 78
Figure 4.4 H41 measurements from JD 203 to JD 233; a) WL, b) in-situ EC, c) in-situ Tu, and d) H35-H41 HD . . . . . 79
Figure 4.5 H34 measurements from JD 203 to JD 233; a) WL, b) in-situ EC, c) in-situ Tu, and d) H35-H34 HD . . . . . 80
Figure 4.6 a) H35 and H36 WL and b) H35-H36 HD from JD 203 to JD 233 . . . . 81
Figure 4.7 a) H35 and H42 WL from JD 203 to JD 233 and b) H35 and H40a WL from JD 203 to JD 220 . . . . . 82
Figure 4.8 Water level variation amplitudes in a) H35, H41 and H34 and b) H36, H42 and H40a from JD 203 to JD 233 . . . . . 83
Figure 4.9 Time (in decimal fractions of a day) at which daily peak WL was reached in a) H35, H41 and H34 and b) H36, H42 and H40a from JD 203 to JD 233 . . . . . 84
Figure 4.10 F-R plots for JD 206 in Period 1; a) H34 with H35, b) H42 with H40a, c) H36 with H35, d) H36 with H41, e) H42 with H41, and f) H40a with H34 . . . . . 87
Figure 4.11 F-R plots on JD 229 in Period 5; a) H29 with H35, b) H41 with H35, c) H34 with H35, d) H36 with H35, e) H42 with H35, and f) H40a with H35 (on JD 218) . . . . . 88
Figure 4.12 H35 WL and EC profiles for JD 204 to JD 214 . . . . . 97
Figure 4.13 H41 a) WL and EC profiles, b) H35-H41 HD, and c) in-situ Tu and EC on JD 218 . . . . . 101

Figure 4.14 H34 a) WL and EC profiles, b) H35-H34 HD, and c) in-situ Tu and EC on JD 218 . . . . . 103
Figure 4.15 a) H29 WL and H41 WL and EC profiles, b) H29-H41 HD, c) H41 in-situ Tu and EC, and d) H29 in-situ Tu and EC on JD 224 . . . . . 105
Figure 4.16 H34 a) WL and EC profiles, b) H29-H34 HD, and c) in-situ Tu and EC on JD 224 . . . . . 107
Figure 4.17 a) H29 WL and H41 WL and EC profiles, b) H29-H41 HD, c) H41 in-situ Tu and EC, and d) H29 in-situ Tu and EC on JD 229 . . . . . 109
Figure 4.18 H34 a) WL and EC profiles, b) H29-H34 HD, and c) in-situ Tu and EC on JD 229 . . . . . 110
Figure 4.19 Modelled moulin input hydrograph for a moulin located 350m upglacier from the borehole array in 1993 . . . . . 115
Figure II.1 EC profiler components . . . . . 137
Figure III.1 In-situ water pressure, electrical conductivity and turbidity sensor used in 1993 . . . . . 139
Figure III.2 In-situ EC sensor constructed in 1995 . . . . . 140
Figure IV.1 Components of the Geo Vision Micro™ video imagery system . . . . . 142

## LIST OF TABLES

Table 2.1 Symbols for classified WL behaviour . . . . . 18

Table 2.2 Classification of borehole WL behaviours for a five day period in the 1992, 1993 and 1995 observation seasons . . . . . 19

Table 3.1 Borehole drilling records. . . . . 41

Table 3.2 Boreholes monitored by in-situ EC and Tu sensors in 1993 and 1995 . 43

Table 3.3 Features seen in video logs from 11 boreholes drilled in 1995. . . . . 49

Table 3.4 Final classification of borehole plumbing based on all available data sources . . . . . 52

Table 4.1 Maximum cross-correlation coefficients and associated lags (hours) for pairs of borehole WL records for each of the five sub-periods of the 1993 melt season . . . . . 85

Table 4.2 Maximum cross-correlation coefficients and associated lags (hours) for pairs of temperature and borehole WL records for each of the five sub-periods of the 1993 melt season . . . . . 86

# CHAPTER 1: INTRODUCTION

## 1.1 THESIS RATIONALE:

The objective of this thesis is to describe and explain the nature and evolution of the subglacial drainage system of Haut Glacier d'Arolla, Switzerland. This will be undertaken by the analysis of water level (WL) and basal water quality measurements derived from an array of boreholes drilled to the glacier bed over three summer ablation seasons. Additional borehole-derived data such as electrical conductivity (EC) profiling, borehole salt tracing and borehole video imagery will be employed to improve the accuracy of the interpretations made from the WL and basal water quality measurements.

Knowledge of the configuration of subglacial drainage systems is of great significance to the study of the motion, erosion and weathering regimes of warm-based glaciers. Variations in glacier velocity have been linked to fluctuations in basal water pressure (e.g. Iken, 1981; Kamb et al., 1985), while changes in the chemical characteristics of bulk meltwaters have been associated with different through flow velocities (e.g. Gurnell and Fenn, 1985). Basal water pressure and through flow velocity are largely a function of the structure of the subglacial drainage system, the hydraulic geometry of the individual pathways, and the melt-water discharge (Sharp, 1991).

Subglacial drainage systems may be characterised as being either channelized or distributed in form. Channelized systems consist of channels incised either upwards into glacier ice (Röthlisberger, 1972; Hooke et al., 1990) or downwards into bedrock (Nye, 1973). These channels form efficient networks with the capacity to drain large amounts of meltwater rapidly. Flow through distributed systems may be via meltwater films (Weertman, 1972), permeable subglacial sediment (e.g. Stone, 1993), linked cavities located on the lee side of bedrock bumps (Walder, 1986; Kamb, 1987) or `canals' above and within unconsolidated sediments (Walder and Fowler, 1994). Distributed systems drain extensive areas of the glacier bed at flow rates 1-2 orders of magnitude lower than

those typical of channelized systems.

Both channelized and distributed drainage systems may co-exist beneath a glacier (e.g. Humphrey et al., 1986; Willis et al., 1990; Fountain, 1992). Nienow (1993) proposed that at Haut Glacier d'Arolla, where the two drainage systems apparently co-exist, the channelized system may extend by headward growth during the summer melt season at the expense of the distributed system. The rate of headward growth appeared to be controlled by the retreat of the transient snowline. Seasonal evolution of the drainage system configuration is thus implied.

Due to the physical inaccessibility of the subglacial environment, indirect methods have been employed to infer the configuration of subglacial drainage systems. These methods include theoretical discussions (e.g. Shreve, 1972), forefield mapping (Walder and Hallet, 1979; Hallet and Anderson, 1980; Sharp et al., 1989), salt and dye tracing (e.g. Stenborg, 1969; Fountain, 1993) and the interpretation of bulk meltwater quality characteristics (e.g. Collins, 1979; Tranter et al., 1993; Raymond et al., 1995). All these methods, however, have their limitations.

Although theoretical discussions are an important basis of any scientific research, they must ultimately be tested by empirical observation to determine whether the theory adequately describes the process that it is designed to describe.

Forefield mapping provides a good indication of the scale of the subglacial drainage pathways present under a particular glacier. However, relic drainage pathways are only likely to be preserved in bedrock, so forefield mapping may not be used at glaciers underlain by unconsolidated sediment and is limited to glaciers that have retreated from a previously more extensive position. It is also not known whether all the observed pathways were active at the same time. Finally, no information will be gained concerning the occurrence of channels incised upwards into glacier ice.

Salt and dye tracing experiments provide an indication of through flow velocities (by dividing travel distance by the time from injection to the time of peak concentration in the outflow stream) and the efficiency with which the water is evacuated (from the form of the measured concentration/time curve and values of dispersivity (a measure of the length of individual branches of a subglacial drainage system)). Put simply, a trace that produces high velocities, forms a single peak concentration curve and has low dispersivity values may be interpreted as representing flow through a channelised system. Conversely, low velocities, a broad, multiple peaked concentration curve and high dispersivity values are likely to be more representative of flow through a relatively complex drainage system characterised by many pathways and potential storage sites (i.e. a distributed system). However, the accuracy of calculated flow velocities is affected by factors such as dye adsorption onto sediment (lower dye concentrations are measured), non-detection (the tracer may be stored at the bed and subsequently released at concentrations below the sensitivity of the measuring device) and the use of inaccurate travel distances (use of the straight line distance between the injection point and the snout does not take the sinuosity of the pathways into account). In addition, salt and dye are commonly injected into active moulins which, by their nature, evacuate large amounts of water rapidly and are therefore most likely to be linked to some form of channelised drainage system, thus introducing a bias into the results.

Bulk meltwater quality characteristics such as electrical conductivity and suspended sediment concentration have been used to determine the configuration of subglacial drainage systems. This relies on the assertion that waters flowing through different drainage systems possess different meltwater quality characteristics. For example, water flowing through a channel at the bed is likely to be dilute (due to short residence times) with a high suspended sediment concentration (due to high water flow velocities). Conversely, water flowing through a distributed system is likely to be more concentrated (due to longer residence times) with a lower suspended sediment concentration (due to lower water flow velocities). However, bulk meltwaters are a mixture of both the fast and slow flow components. Determination of the varying proportions of the different

components of bulk meltwaters from electrical conductivity and suspended sediment concentration measurements is not a simple process. This has become especially apparent with the realisation that non-conservative mixing occurs when dilute and concentrated waters mix (Raiswell, 1984).

Borehole drilling affords direct access to the glacier bed at chosen point locations. This has allowed for the measurement of basal water pressure (e.g. Hodge, 1976; Engelhardt, 1978; Hantz and Lliboutry, 1983) and water quality (e.g. Stone and Clarke, 1996; Tranter et al., in press), the determination of subglacial sediment characteristics (e.g. Stone and Clarke, 1993; Fischer and Clarke, 1994), down-borehole dye tracing (Fountain, 1993) and down-borehole video imagery (e.g. Pohjola, 1993). Boreholes are becoming increasingly important tools in the study of subglacial drainage system configurations as they now provide the most direct means of observing basal parameters.

The ultimate aim of this thesis is to employ borehole WL and basal water quality measurements to build-up a comprehensive picture of the nature and evolution of the subglacial drainage system over a summer ablation period under a part of Haut Glacier d'Arolla, Switzerland. However, borehole-derived data also have limitations. It has recently been demonstrated that the existence of a borehole can influence the water pressure and water quality measured at the bed (Ketterling, 1995). This is especially true in boreholes which remain open during the summer as changes in subglacial water pressure are registered as changes in borehole WL (this is not the case in boreholes that freeze shut near the base). This demands a flux of water into and out of the borehole over time which can be supplied by any combination of basal, englacial and supraglacial sources. Complex patterns of water circulation may thus develop within the borehole. Sensors placed at the bed may therefore record the character of the water leaving the base of the borehole, rather than the character of the water which would have been draining through the subglacial system had the borehole not existed.

Thus, although boreholes afford direct access to the glacier bed, borehole-derived measurements must be used with caution. Water sources and circulation patterns within a borehole (i.e. the 'plumbing' of the borehole) must first be determined before WLs and basal water quality measurements from that borehole are used to make any inferences about the configuration of the subglacial drainage system (Ketterling, 1995). This will be carried-out with additional information from EC profiling, down-borehole salt tracing and down-borehole video imagery (the description and methods of which will be presented in the following chapters). Once the plumbing of each borehole has been understood, WL and basal water quality measurements can be interpreted with a greater degree of confidence. This will allow for a systematic and detailed description of the nature and evolution of the subglacial drainage system and the discussion of possible explanations for the inferences made. No other study to date has combined such a wide variety of borehole-derived data to determine the temporal and spatial configuration of a subglacial drainage system. This work provides a unique opportunity of observing both the large scale seasonal evolution of the subglacial drainage system as well as its behaviour on diurnal timescales.

## 1.2 FIELD SITE:

Haut Glacier d'Arolla is located at the head of the Val d'Hérens, Valais, Switzerland (Figure 1.1). It has an area of 6.3km$^2$, spans an elevation range of 2560 to ~3500m.a.s.l, and is believed to be warm-based. Observations in subglacial cavities (Hubbard, 1992), and by borehole video (Copland et al., in press), together with interpretations of borehole WL measurements (Hubbard et al., 1995) suggest that this glacier is underlain at least partly by unconsolidated sediments.

During the summers of 1992, 1993 and 1995, 70 boreholes were drilled close to the eastern margin of the ablation area of the glacier, some 1.5km from the terminus (Figure 1.1). All the boreholes were drilled within an area of ~260m E/W by ~120m N/S (Figure 1.2a,b and c). Boreholes were identified by the year they were drilled followed by the number assigned during that year (e.g. 92/3 represents borehole number 3 drilled in 1992). Boreholes were drilled using high pressure, hot water (see Appendix I for drilling procedure), and varied in depth from 23m at the margin (93/38) to 144m towards the glacier centre line (93/46).

The location of the borehole array was chosen on the basis of previous dye tracing interpretations and theoretical reconstructions of the subglacial drainage system (Sharp et al., 1993) which predicted that a major drainage channel would develop beneath this part of the glacier during the melt season.

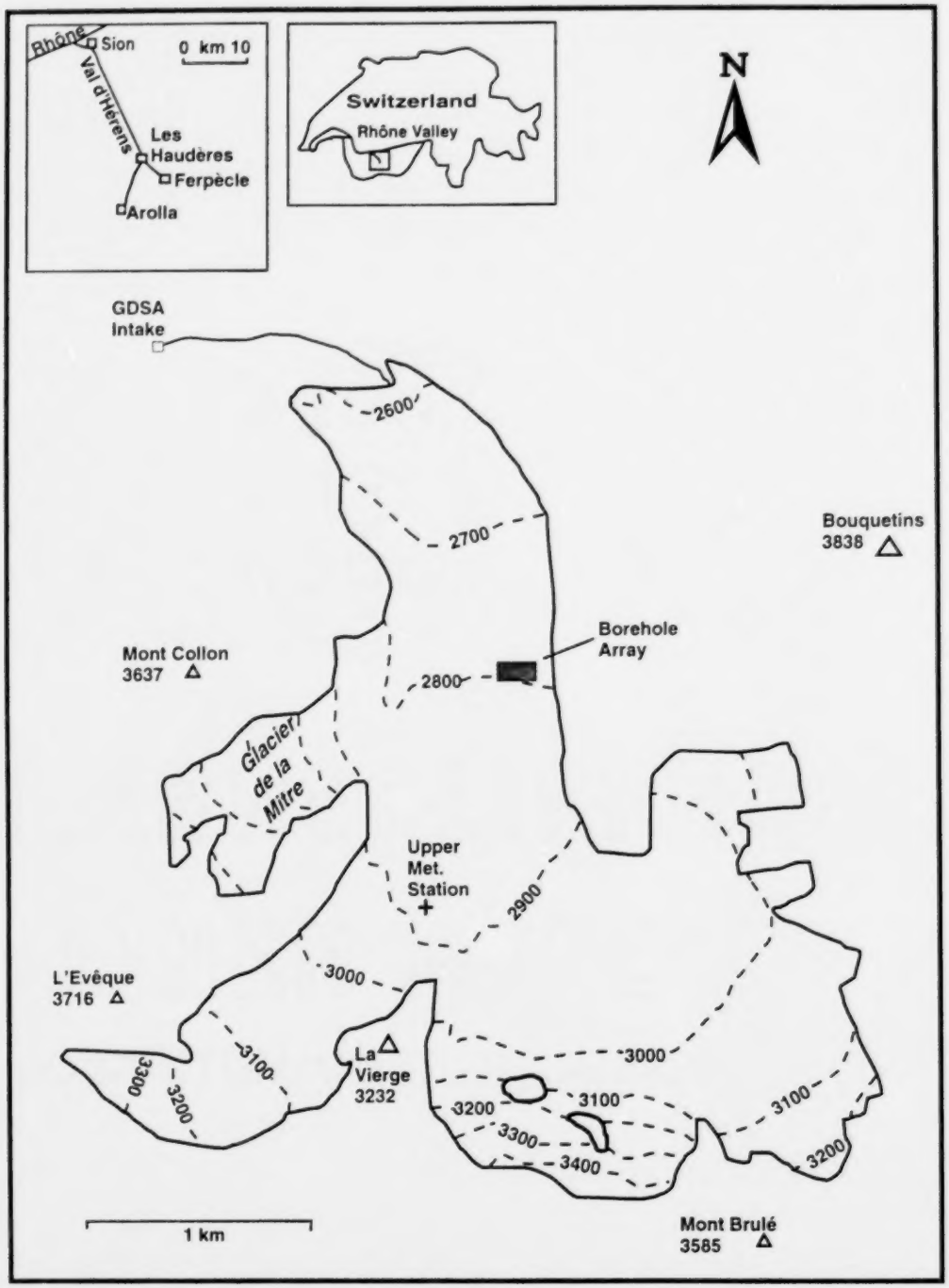


Figure 1.1: Haut Glacier d'Arolla showing the location of the borehole array, GDSA intake and upper meteorological station.

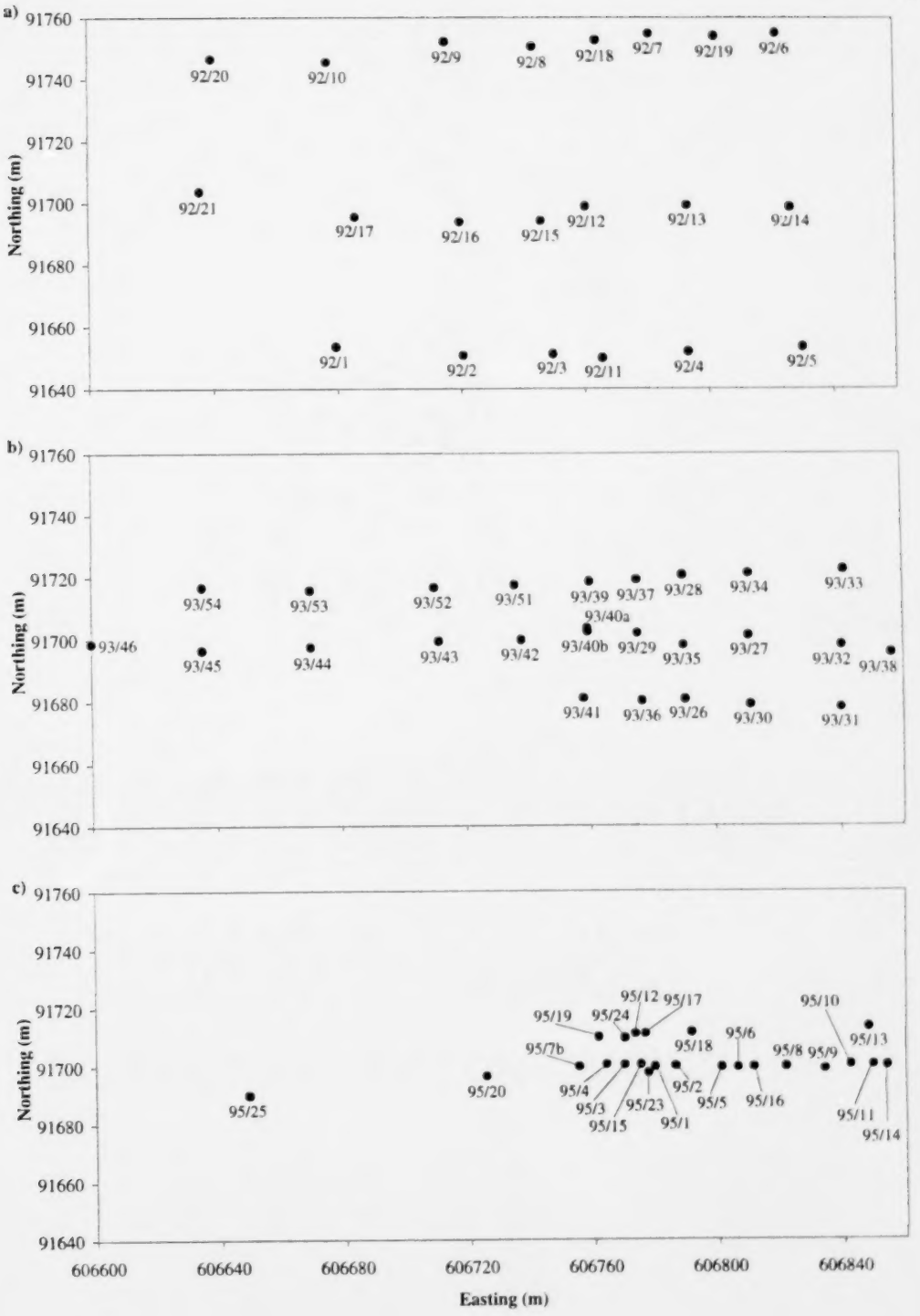


Figure 1.2: Borehole arrays for a) 1992, b) 1993 and c) 1995.

## 1.3 THESIS OUTLINE:

The study is divided into four sections:

**CHAPTER 2:** Interpretation of intra- and inter-annual distribution of borehole WL behaviour:

The primary objective is to construct a general picture of the nature of the subglacial drainage system that existed beneath the borehole array in the three observation seasons. This will be undertaken by interpreting the WL behaviour exhibited by each of the boreholes. A simple classification scheme will be employed that categorises borehole WL behaviour to simplify analysis. Once the WL behaviours are classified and their spatial distribution mapped, questions that will be addressed are:

a) What types of WL behaviour can be identified?

b) What information do the classified WL behaviours offer concerning basal water pressure conditions?

c) What is the spatial distribution of the WL behaviours?

d) What information does the spatial distribution of WL behaviours offer concerning the nature of the subglacial drainage system?

e) Does the distribution of the WL behaviours vary between the years? If so, why?

f) Are there any seasonal trends in WL behaviour?

**CHAPTER 3:** Determination of borehole plumbing for the interpretation of basal water quality measurements:

Before borehole WL and basal water quality measurements are analysed to provide a detailed description and explanation of the nature and evolution of the subglacial drainage system, the water sources and circulation patterns within each borehole must be determined. This will allow for the more accurate interpretation of the WL and basal water quality measurements.

Seven types of data (described in detail in Chapter 3) are used to determine the plumbing of each borehole both within the glacier ice and at the glacier bed.

a) Drilling records

b) Manual and continuous in-situ WL measurements

c) Continuous in-situ electrical conductivity measurements

d) Continuous in-situ turbidity measurements

e) Electrical conductivity profiling

f) Salt tracing

g) Down-borehole video imagery

After analysis of these data, categories of borehole plumbing will be identified and examples of each category presented. Examples of how WL and water quality records can be interpreted once water sources and circulation patterns have been determined will be presented.

**CHAPTER 4:** Determination of the nature and evolution of the subglacial drainage system:

Once the plumbing of each borehole is understood, a detailed interpretation of WL and basal water quality measurements can be undertaken to provide a comprehensive view of the nature and evolution of the subglacial drainage system over a summer ablation season. Both large scale seasonal evolution of the drainage system and small scale diurnal patterns in the WL and water quality measurements can be identified.

**CHAPTER 5:** Conclusion:

Interpretations from the previous three chapters will be integrated to demonstrate how a comprehensive description and explanation of the nature and evolution of a subglacial drainage system can be developed from the combination of a range of borehole-derived data.

# CHAPTER 2: INTRA- AND INTER-ANNUAL DISTRIBUTION OF BOREHOLE WATER LEVEL BEHAVIOUR

## 2.1 INTRODUCTION:

In boreholes that remain open during the summer observation season, changes in subglacial water pressure are registered as changes in borehole water level (WL) (e.g. Engelhardt, 1978; Fountain, 1994; Hubbard et al., 1995). As a result, analyses of borehole WL fluctuations are used to infer subglacial hydraulic conditions. Boreholes can be classed as `unconnected' or `connected' depending on the status of the WL. In unconnected boreholes, the WL generally remains stable at the glacier surface and the borehole is thought not to be connected to the subglacial drainage system. Connected boreholes generally exhibit fluctuating WLs, which indicate that the borehole has connected to a drainage system that experiences water pressure fluctuations. The initial WL decrease can occur in three ways: before the bed is reached whilst drilling, immediately as the bed is reached or several hours to several days after drilling. In the first case, an englacial channel is inferred to have been intercepted (e.g. Engelhardt, 1978; Fountain, 1994). In the latter two cases, the borehole drains due to the overpressurization at the bed created by the borehole water column and a connection to the subglacial drainage system is inferred. This connection may be either directly into a drainage pathway such as a channel, or indirectly to a drainage pathway at some distance from the borehole base via some sort of hydraulic link.

Minimum (base) daily WLs and the amplitude of daily WL fluctuations exhibited by an array of boreholes have been used to infer the characteristics of subglacial drainage systems (e.g. Fountain, 1994; Hubbard et al., 1995; Smart, 1996). This use of borehole WL behaviour is based upon the principles of water flow within and under a glacier (Shreve, 1972; Röthlisberger, 1972).

Shreve (1972) demonstrated that the direction of water flow within and at the base of a glacier should be normal to hydraulic equipotential contours, where hydraulic potential ($\Phi$) is given by:

$$\Phi = \rho i g(h-h_b) + \rho w g h_b \qquad (2.1)$$

and $\rho w$ and $\rho i$ are the densities of water and ice respectively, g is the acceleration due to gravity, and h and $h_b$ are the elevations of the glacier surface and of a point within or at the bed of a glacier, respectively. The first term on the right is therefore the pressure imposed on the water by the weight of the overlying ice, and the second term is the potential elevation of the water due to its height above a datum such as sea level. Equipotentials within a glacier dip upglacier (Figure 2.1a), and water flow at the bed is normal to the equipotential contours created by the intersection of these equipotentials with the bed (Figure 2.1b). Water flow at the bed is thus not necessarily in the direction of the maximum slope of the bed. Shreve thus assumes that water in subglacial channels is always at the ice overburden pressure (IOP) and that the presence of channels has no effect on the direction of water flow at the bed.

Röthlisberger's (1972) treatment of water flow assumes that channel size depends on the balance between two opposing forces: closure by deformation (if the IOP exceeds the water pressure within the channel) and enlargement via melting (produced by the frictional heat of flowing water and sensible heat transfer between flowing water and the surrounding ice). The size of a channel adjusts to changes in the amount of surface meltwater input by these processes. For any significant discharge, the water pressure in a channel will be less than IOP because melt offsets closure and prevents the water pressure from rising to IOP. This has a significant effect on the direction of water flow in areas adjacent to a channel as the low channel pressures create a 'valley' in the equipotential surfaces and divert water flow at the bed towards the channel (Figure 2.1c). However, on short timescales (e.g. diurnal) adjustment of channel size to increasing discharge is not instantaneous as the channel behaves essentially like a rigid pipe.

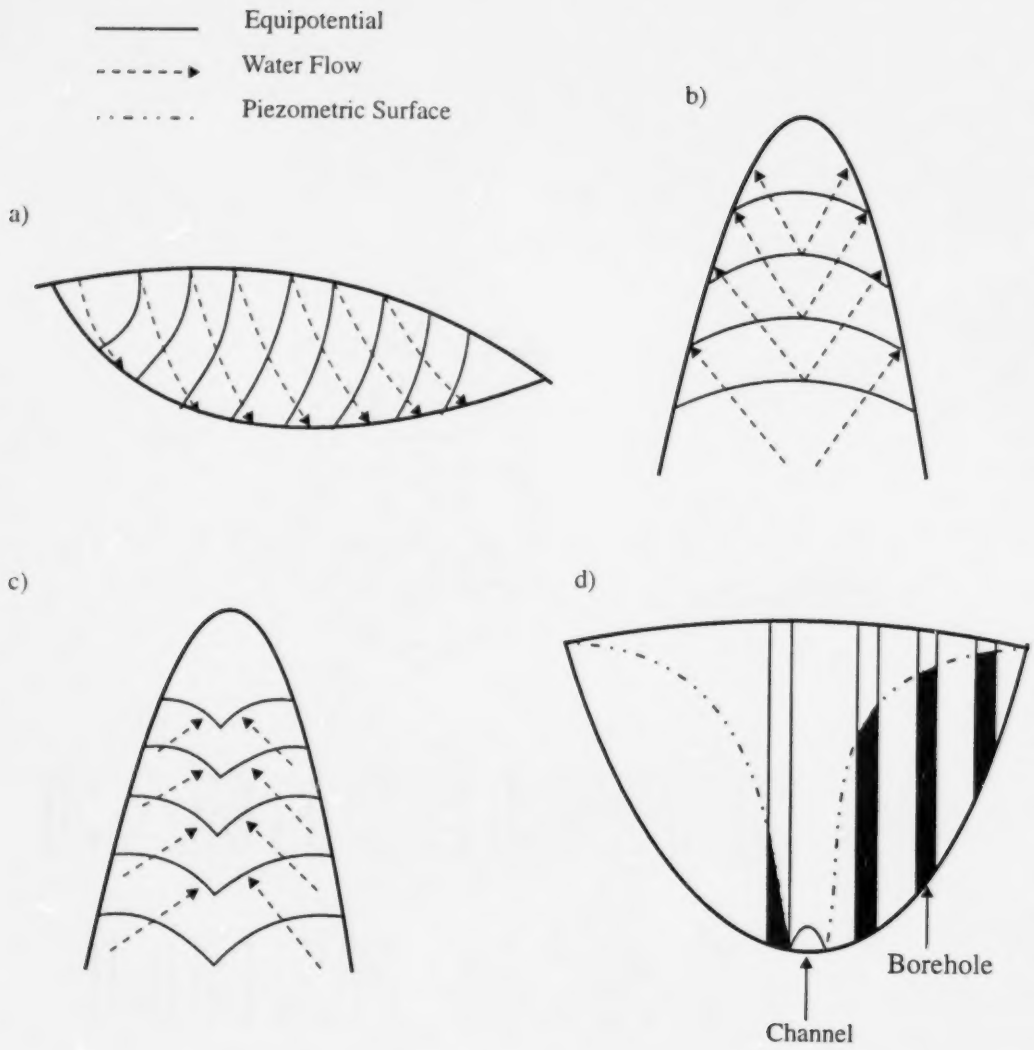


Figure 2.1: a) Longitudinal cross-section through an idealised glacier showing Shreve's equipotential surfaces, b) Plan view of an idealised glacier showing Shreve's equipotential contours and consequent water flow at the bed, c) Plan view of an idealised glacier showing Röthlisberger's 'valley' equipotential surfaces and consequent water flow at the bed, and d) Cross-section through an idealised glacier showing the effect of a channel at a pressure less than IOP on the piezometric surface and borehole water levels.

This is because heat transfer from water to ice is not an instantaneous process, so melt enlargement lags the rising discharge, while creep closure is too slow to shut down the channel as discharge decreases. Water pressure therefore rises with increases in daily discharge, producing discharge-related diurnal cycles in water pressure (e.g. Iken and Bindschadler, 1986; Fountain, 1994; Paterson, 1994).

If a cross-section through an idealised glacier is taken, the presence of a channel at low pressure exerts a `draw-down' effect on the piezometric surface on either side of the channel (Figure 2.1d) due to the establishment of a hydraulic gradient between the channel and surrounding areas of the bed. If boreholes were drilled on either side of the channel, their WLs would represent this piezometric surface (Figure 2.1d) with increasing base WLs occurring away from the channel (e.g. Fountain, 1994).

If the channel is unable to enlarge instantaneously to accommodate an increase in discharge, the velocity of water flow in the channel must rise to compensate. In a full pipe, this can only happen if the pressure gradient increases. As the water pressure at the snout is fixed at atmospheric pressure, water pressure must rise at all locations upstream of the snout. If the water pressure in the channel rises above that in surrounding areas of the bed, a hydraulic gradient away from the channel is established and lateral transfer of water can occur. Daily water pressure variations in the channel are therefore propagated into the surrounding bed, causing an increase in borehole WL. As channel pressure falls overnight the hydraulic gradient is redirected towards the channel, thus causing water to flow from the surrounding bed back to the channel, allowing borehole WLs to fall. The area within which daily WL fluctuations are observed has been termed a variable pressure axis (VPA) (Hubbard et. al, 1995).

The amplitude of the borehole WL increase will diminish with increasing distance from the channel due to a combination of three factors: a) the pressure wave diffuses with distance from its origin, b) full WL adjustment requires longer than allowed by the daily water pressure forcing (Alley, 1996), and c) subglacial sediment with a low hydraulic

conductivity resists the propagation of the pressure wave and reduces its amplitude with increasing distance from its origin (Fountain, 1994; Hubbard et al., 1995).

Therefore, boreholes exhibiting large diurnal WL fluctuations superimposed on low base WLs are thought to be located close to a major channel which becomes increasingly pressurized on a daily basis by daily meltwater inputs. Conversely, boreholes exhibiting high base WLs and low diurnal WL fluctuation amplitudes are thought to represent areas of the bed which are located further from a channel and are less efficiently drained, but are still affected by the presence of the channel. The latter borehole WL behaviour may indicate the presence of a distributed system. Boreholes that remain full and demonstrate no perceptible WL fluctuations (i.e. unconnected) are also likely to be located in a distributed drainage system, but are located too far from the channel to be affected by its daily pressurisation. Unconnected boreholes may also represent areas of the bed which are hydraulically inactive.

Smart (1996) devised a simple classification scheme based on minimum daily WL and diurnal WL fluctuation amplitude, which describes the main characteristics of borehole WL behaviour. He used this scheme to compare WL behaviours between summers and between different areas of a glacier and to infer the configuration of the subglacial drainage system. Quantitative comparisons of the observed WL behaviours were made using a nearest neighbour statistic which allowed Smart to determine whether there was significant clustering of boreholes of a given type a) in space, and b) in space between different years.

The aim of this chapter is to describe and compare the pattern of borehole WL behaviour observed on Haut Glacier d'Arolla in 1992, 1993 and 1995 in order to construct a general picture of the configuration of the subglacial drainage system within the borehole array. This will be achieved using a revised form of the borehole WL classification scheme devised by Smart (1996).

## 2.2 WATER LEVEL MEASUREMENTS:

Borehole WL measurements were made in two ways: either manually or automatically.

### 2.2.1 Manual WL measurements:

Manual WL measurements were made using EC profilers which were used to measure both the EC profile of borehole water columns (see Chapter 3) and record the WL of the boreholes. The profilers (see Appendix II) were lowered down the borehole until the WL was reached (if the borehole was not full) and this depth was recorded manually. It was clear when the profiler reached the WL as air readings were zero whilst water readings were $>0.5\mu S\ cm^{-1}$. This method was used in 1992, 1993 and 1995. Manual WL measurements were taken only at irregular intervals during the day (often between 09:00 and 20:00) and mostly in boreholes that were not being monitored automatically.

### 2.2.2 Automatic in-situ WL measurements:

In-situ WL sensors (see Appendix III) were suspended within a few decimetres of the borehole base. Measurements were logged as means of 30 readings every 10 minutes using Campbell Scientific CR-10 dataloggers. WL measurements are accurate to within 0.5m of water head. Twelve in-situ WL sensors were deployed in the 1993 summer ablation season and 5 in 1995 (Table 2.2). In-situ sensors were deployed only at the end of the 1992 field season and thus do not provide relevant data for the period during which borehole WL behaviour was observed.

## 2.3 CLASSIFICATION OF WATER LEVEL BEHAVIOUR:

Boreholes were initially classified as either connected or unconnected. Connected boreholes were further classified on the basis of their base WL and daily WL fluctuation amplitude. Base WL is defined as the minimum level attained on a daily basis and is termed DRY (drained), LOW (<50% of IOP), or HIGH (>50% of IOP) (where 50% of IOP is an arbitrary threshold). Diurnal WL fluctuation amplitude is taken as the difference between the base WL and the daily maximum WL and is classified as ZERO (no diurnal signal), LOW (rose by <50% of IOP), or HIGH (rose by >50% of IOP). The classes of WL behaviour are represented by a series of symbols (Table 2.1).

Many borehole WL studies (e.g. Hantz and Lliboutry, 1983; Iken and Bindschadler, 1986; Fountain, 1994) have observed long-term trends in WL behaviour as base WLs and the amplitude and frequency of WL fluctuations increased or decreased throughout the observation season in many connected boreholes. These trends were attributed to a combination of factors including: advection of the borehole base over bedrock bumps, changing connectivity associated with the growth and closure of linking passageways at the bed, growth or closure of the borehole, and variations in the transmissivity of the subglacial sediment layer. This non-stationary behaviour poses a problem for classification of borehole WL behaviours as boreholes may fall into different categories at different stages of the observation period. To overcome this problem, Smart (1996) chose a narrow time window of 2-3 days near the end of the observation season when the maximum number of boreholes was available for classification and when non-stationary WL behaviour was minimal. The limitation of this approach is that only the end-of-season WL behaviour is analysed. This excludes the possibility of analysing changes in WL behaviour over the observation season. These changes may be an indication of subglacial drainage evolution and should be discussed. This issue will be discussed further in Section 2.7.

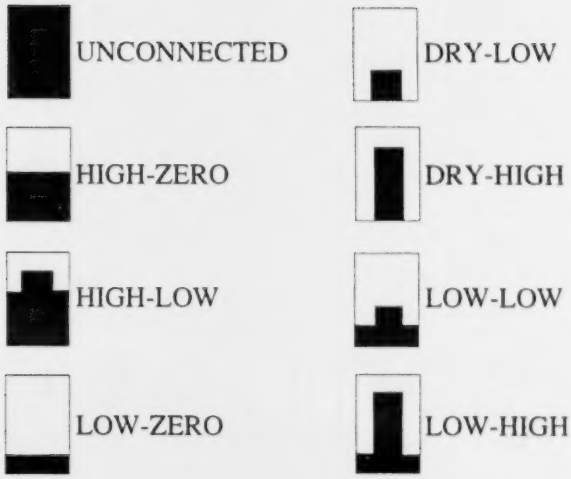


Table 2.1: Symbols for classified WL behaviour.

On Haut Glacier d'Arolla, 56 of the 59 boreholes with WL data were classified on the basis of their WL behaviour within an arbitrarily chosen 5 day period near the end of each observation season (JD 257-261 in 1992; JD 229-233 in 1993; JD 226-230 in 1995) (Table 2.2). The remaining 3 boreholes (93/26,93/40a,95/1) were monitored only during the early part of the observation season as they became constricted, prohibiting further WL measurements. It was thus not possible to determine whether any long-term changes in WL behaviour occurred and these boreholes were therefore not classified.

| Classification | 1992 (257-261) | 1993 (229-233) | 1995 (226-230) | Total |
|---|---|---|---|---|
| UNCONNECTED | 2,4,5,6,7,8,9, 10,15,16,17,18, 19,20 | 31,33,38,44,45, 46,52,53,54 | 5,6,8,9,25 | 28 |
| HIGH-ZERO | 11 | | 16,20 | 3 |
| HIGH-LOW | 1,3,14 | **42,40b,43,51** | 7b | 8 |
| LOW-LOW | 12 | 39 | **2,15,17,18** | 6 |
| LOW-ZERO | | | **4**,24 | 1 |
| LOW-HIGH | | 32,**36,37,41** | | 4 |
| DRY-LOW | 13 | | | 1 |
| DRY-HIGH | | **29,30,34,35** | | 4 |
| Total | 20 | 22 | 14 | 56 |

Table 2.2: Classification of borehole WL behaviours for a five day period in the 1992, 1993 and 1995 observation seasons. Borehole numbers in bold indicate boreholes with in-situ WL records (40a also had in-situ WL data, but measurements ceased before the classification period).

Boreholes can be classified using either manual or in-situ WL measurements. However, classifications based on manual measurements may be less reliable than those based on in-situ measurements as manual measurements may not capture the full range of the daily WL variation. Boreholes with in-situ measurements are thus highlighted in bold in Table 2.2.

The distribution of the classified boreholes is presented in Figure 2.2. All boreholes located to the west of this array (92/10,92/17,92/20,93/44,93/45,93/46,93/53,93/54,95/25) were classified as UNCONNECTED (except 92/1 which was HIGH-LOW).

No statistical analysis was undertaken on the distribution of Haut Glacier d'Arolla boreholes as the choice of borehole locations was not random. In 1992, a large, evenly-spaced array was drilled covering an area of ~19,000$m^2$, with distances between boreholes of ~20m E/W and 70m N/S, with the aim of locating the channel inferred to exist in the area by Sharp et al. (1993). In 1993, boreholes were drilled in the area where WL fluctuations were observed in 1992. The array was thus smaller in area (~11,000$m^2$), with distances between boreholes of 15-20m E/W and 20-25m N/S. In 1995, boreholes were primarily drilled for inclinometry purposes. Boreholes were thus initially drilled in a transect across the glacier from the eastern margin to the centre line. Not until later in the season were more holes drilled within the area of observed WL fluctuations. Boreholes were thus closely spaced (5-10m E/W and ~10m N/S) and covered an area of only ~4000$m^2$.

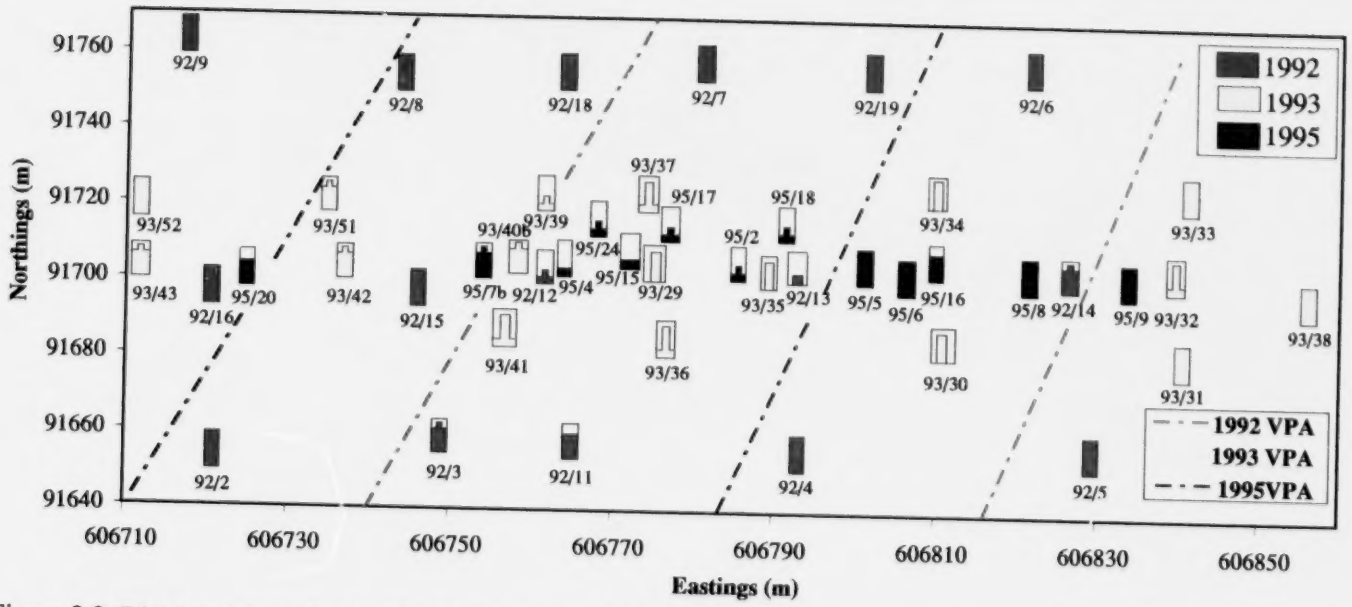


Figure 2.2: Distribution of all classified boreholes in 1992, 1993 and 1995. All boreholes to the west of the array are unconnected.

## 2.4 SPATIAL DISTRIBUTION OF CLASSIFIED WATER LEVEL BEHAVIOUR:

### 2.4.1 ANNUAL DISTRIBUTION OF CLASSIFIED WL BEHAVIOUR (Figure 2.2):

1992: A NE-SW trending axis of connected boreholes existed within a main body of UNCONNECTED holes. This axis was not detected in the northern borehole transect. A core zone exhibiting DRY and LOW base WLs (92/13 and 92/12) passed into a transitional zone of HIGH base WLs (92/14, 92/3, 92/11) which was enclosed by an UNCONNECTED zone. 92/1 (20m west of 92/2, off Figure 2.2) was a HIGH-LOW outlier in the UNCONNECTED zone. Only LOW amplitude WL fluctuations were observed.

1993: A NE-SW trending axis in which connected boreholes exhibited DRY-HIGH WL behaviour was present in the core of the borehole array. A progression of WL behaviour was observed with higher base WLs and lower WL fluctuations occurring away from the central core of DRY-HIGH holes. The eastern margin of the array consisted of UNCONNECTED holes.

1995: A NE-SW trending axis of LOW-LOW and LOW-ZERO boreholes existed within an outer zone of mainly UNCONNECTED boreholes. HIGH-LOW (95/7b) and HIGH-ZERO (95/20) holes separated the central boreholes from UNCONNECTED holes to the west. 95/20 is therefore taken to represent the western limit of the connected zone. 95/16 was an anomalous HIGH-ZERO hole within an otherwise UNCONNECTED zone to the east of the central boreholes.

**2.4.2 INTER-ANNUAL COMPARISONS OF WL BEHAVIOUR PATTERNS** (Figure 2.2):

2.4.2.1 *Width of connected zone:* The width of the connected zone can be measured as the distance between the unconnected boreholes located either side of the connected holes. As there is a gap between these two sets of holes, the boundaries between the unconnected and connected zones are subjective. The width of the connected zone in the 3 years was approximately 80m (±5m) in 1992, 120m (±10m) in 1993, and 70m (±5m) in 1995.

2.4.2.2 *WL behaviour in the connected zone:* 1993 exhibited the lowest base WLs and the highest WL fluctuation amplitudes (up to ~80m). Only low WL fluctuations were exhibited in 1992 and 1995 (~10-15m in 1992; ~1-30m in 1995).

## 2.5 POSSIBLE REASONS FOR THE OBSERVED DISTRIBUTION OF BOREHOLE WL BEHAVIOUR:

The late-season borehole WL behaviours observed in 1992, 1993 and 1995 demonstrate the presence of a VPA bounded on either side by an area of high, stable water pressure. The borehole WL behaviour and the width of the VPA measured in 1993 suggest that a well developed channel characterised by strong daily pressure cycles existed at the bed in the centre of the VPA during the 1993 5 day classification period. This channel appears to have been surrounded by a distributed drainage system as base WLs increased and WL fluctuation amplitudes decreased away from the inferred channel. WL behaviour in 1992 and 1995 was different to that in 1993 in three main ways:

a) DRY boreholes occurred only in 1993 and not in 1992 (except 92/13) and 1995;
b) There were no HIGH WL fluctuations in 1992 and 1995 as there were in 1993; and
c) The VPA was wider in 1993 than in 1992 and 1995.

In the light of these differences in WL behaviour, the question to be asked is why was 1993 so different from 1992 and 1995? These differences were most likely caused by different meltwater input regimes to the glacier in each year. The daily input and flow of meltwater within and beneath a glacier is the major process of channel formation as it is the frictional heat created by flowing water and the sensible heat transfer between the flowing water and the surrounding ice that melts the channel walls and enlarges the channel. Consequently, the amount of daily meltwater input determines whether a channel becomes pressurised or not and what magnitude of pressurization occurs. However, channel pressurization also depends on channel size, which is dependent on antecedent meltwater input history. These factors ultimately have an effect on the WL behaviour observed. The magnitude of daily meltwater input (and indirectly, channel size) to a particular part of a glacier is likely to be dependent on two main factors: meteorological conditions and snowline position.

### 2.5.1 Meteorological Conditions:

Air temperature has an obvious positive relationship with melt rates (Braithwaite, 1981). As air temperature increases, melt rates and thus meltwater inputs increase. However, in order for melt rates to remain consistently high, air temperature must also remain consistently positive. This is due to the retarding effect of sub-zero temperatures on melt rates. If the air temperature remains above zero, surface melting will always occur to some degree, but if sub-zero air temperatures occur, the meltwater on the glacier surface will re-freeze. Cooling of the surface will occur from longwave radiation losses and conduction from the ice to the cooler overlying atmosphere. The temperature of the ice surface then has to be brought back to zero before melt can resume. The onset of melt is therefore retarded.

Periods of snowfall during the melt season will also retard the melting of ice as snow has a higher albedo than glacier ice. Thus, incoming solar radiation is reflected to a greater degree by snow than ice and the energy available for melting is reduced. In addition,

meltwater inputs to a glacier are damped by storage within the snowpack. Finally, if the snowpack has been removed, periods of rainfall may enhance surface melting and in themselves represent an input of water to a glacier's hydrological system.

### 2.5.2 Snowline Position:

Snow on the glacier surface acts as a storage site for meltwater and thus damps the diurnal variability in inputs of meltwater to the subglacial drainage system. This is well demonstrated by the large slush fields that cover the glacier during the early parts of the ablation season. Snow cover may also plug moulin entrances, inhibiting meltwater input to the subglacial drainage system. As the snowline retreats, low albedo, impermeable ice surfaces are exposed which produce rapid runoff and strongly peaked diurnal meltwater inputs to moulins and crevasses which are likely to be linked to the subglacial drainage system. The onset of peaked diurnal meltwater inputs as the snowline retreats is thought to be significant in destabilising the distributed system at the bed and initiating channel development and rapid channel enlargement at Haut Glacier d'Arolla (Nienow, 1993; Nienow et al., submitted). Nienow proposed that the channelised system at Haut Glacier d'Arolla expanded upglacier during the summer melt season at a rate similar to the rate of snowline retreat, as this determined when peaked meltwater input cycles commenced.

## 2.6 DISCUSSION:

The influence of meltwater inputs on the WL behaviour observed in each year will be discussed and reasons for why the observed differences occurred will be suggested.

Meteorological and discharge data for 1993, 1992 and 1995 (Figures 2.3, 2.4 and 2.5) were supplied by Grande Dixence S.A. (GDSA), a hydro-electric company that captures water from Haut Glacier d'Arolla. The meteorological data were measured at Bricola weather station located 8km N.N.E from Haut Glacier d'Arolla. Discharge was measured at the GDSA intake structure located ~1km from the glacier terminus (Figure 1.1).

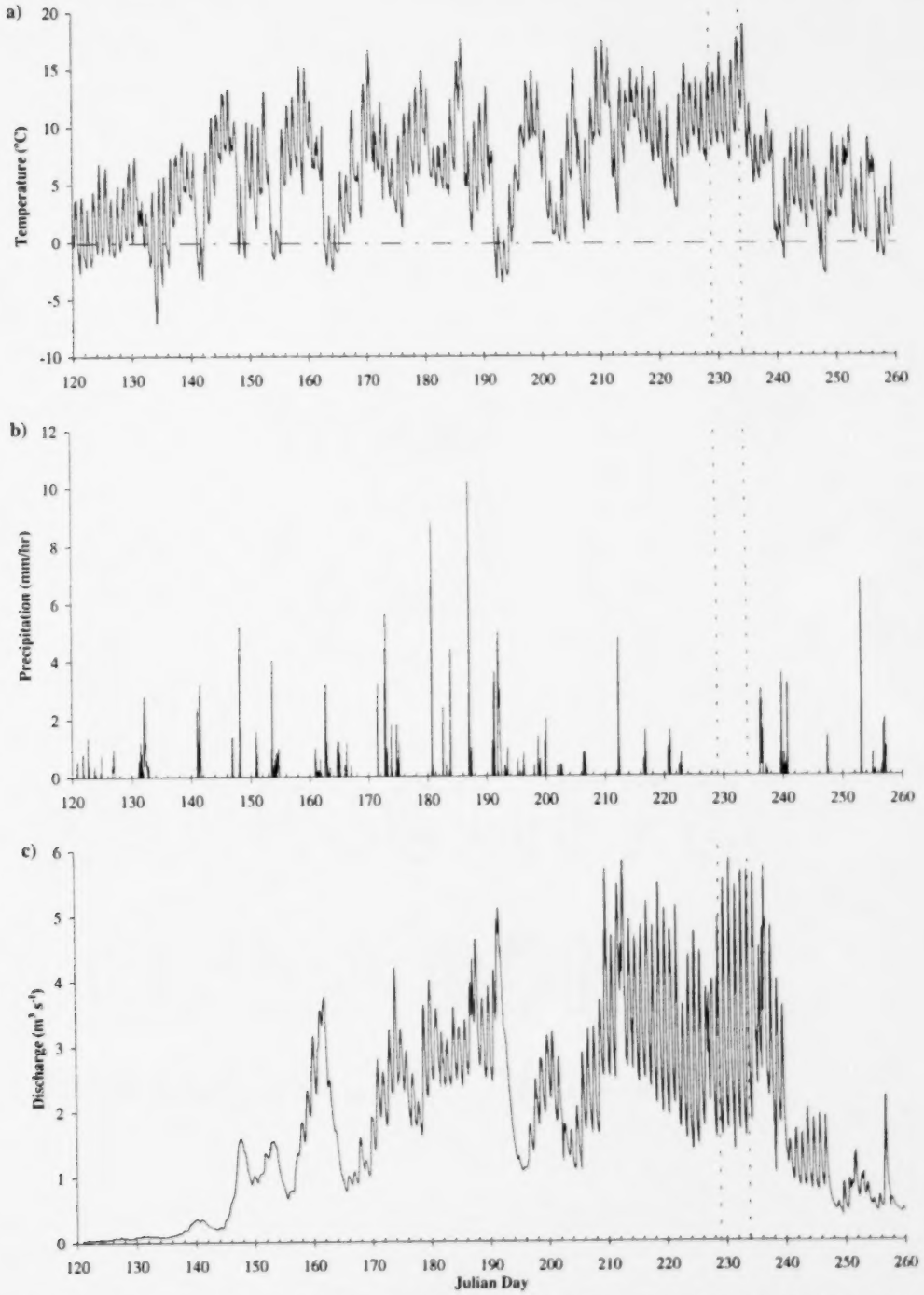


Figure 2.3: 1993 a) temperature, b) precipitation, and c) discharge. Dashed lines represent 5 day classification period. See text for data sources.

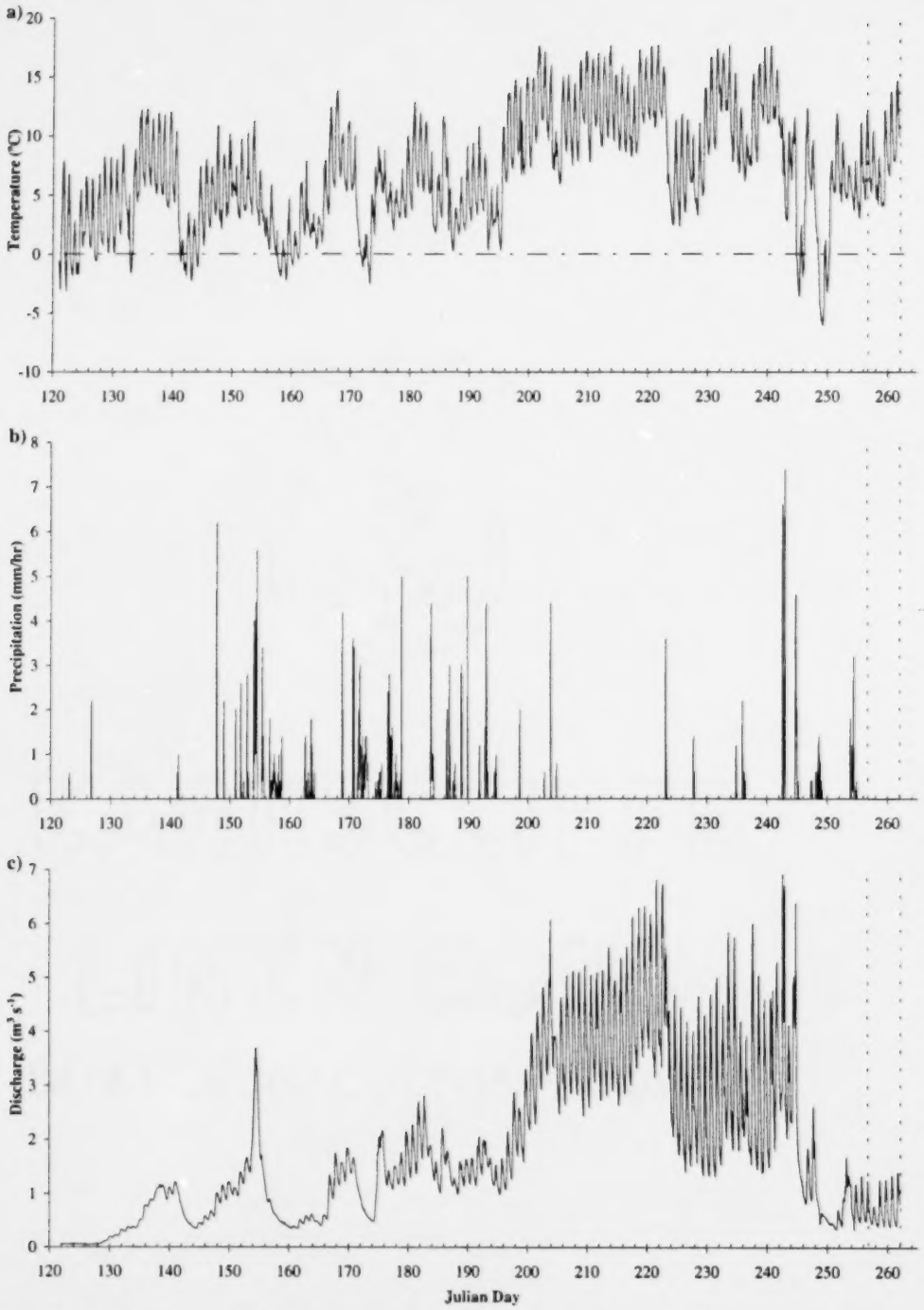


Figure 2.4: 1992 a) temperature, b) precipitation, and c) discharge. Dashed lines represent 5 day classification period. See text for data sources.

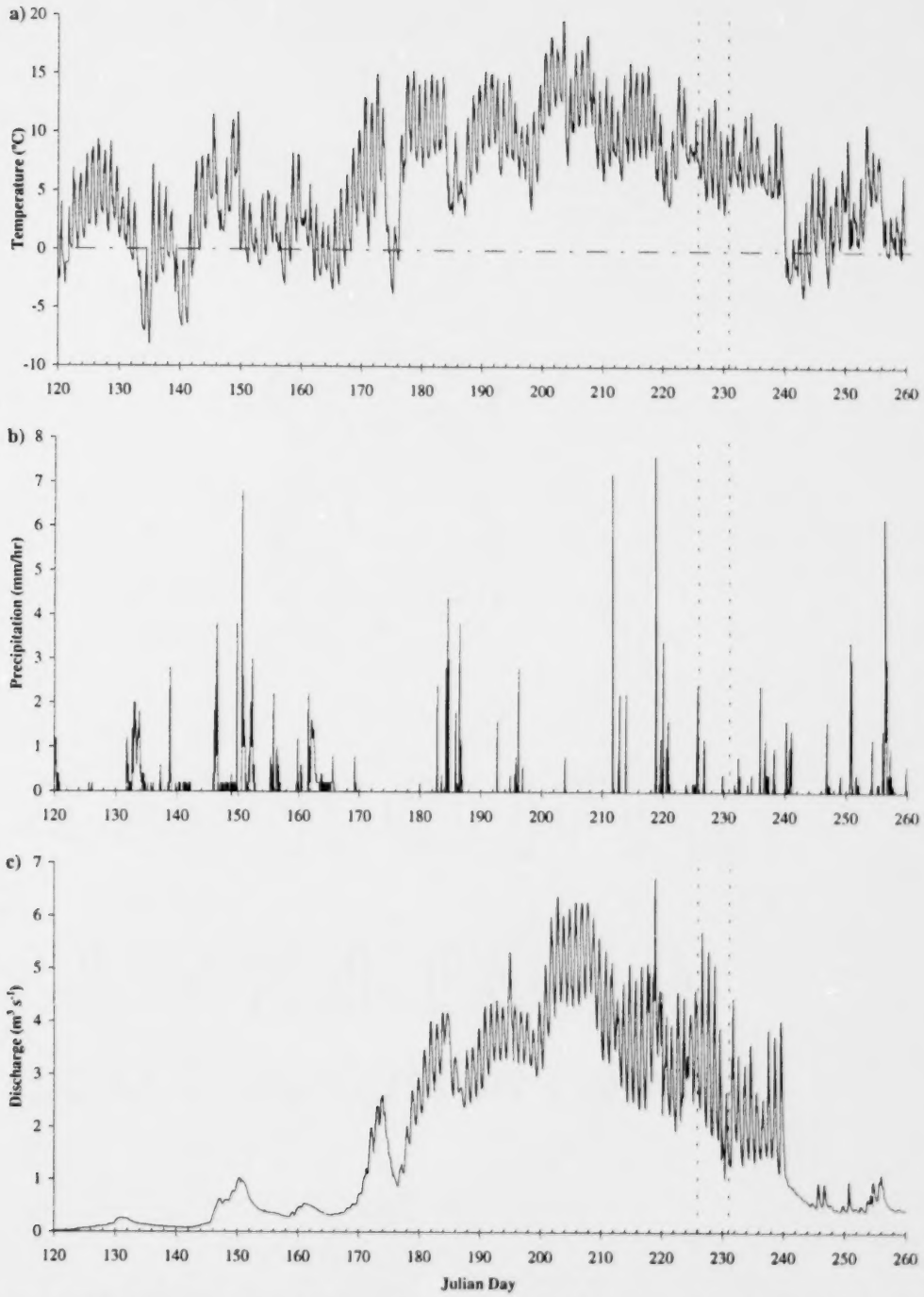


Figure 2.5: 1995 a) temperature, b) precipitation, and c) discharge. Dashed lines represent 5 day classification period. See text for data sources.

Snowline positions were taken from observations made during regular ablation surveys at a series of permanent stakes drilled in a transect up the centreline of the glacier. In these surveys, the glacier surface was described as consisting of either 'snow' or 'ice'.

**2.6.1 1993:**

The 5 day window period in 1993 (JD 229-233) occurred during the warmest period of the summer (Figure 2.3a) when the highest discharges associated with the highest diurnal discharge fluctuations were recorded (Figure 2.3c) and when snow covered only the upper 1km of the glacier. Daily meltwater inputs were thus likely to have been peaked and high. If a subglacial channel existed beneath the borehole array during the 5 day classification period, these conditions were likely to have been favourable for strong, daily channel pressurisation resulting in the propagation of a pressure wave away from the channel into the surrounding areas of the bed. The WL behaviour exhibited in the 5 day window period in 1993 suggests that such a channel did exist and that it was bounded by a distributed system. DRY base WLs and HIGH WL fluctuations in 93/29, 93/35 and 93/34 demonstrate that a channel located close to these holes became strongly pressurised during the day by high, peaked meltwater inputs, but returned to atmospheric pressure overnight when these meltwater inputs ceased. WL fluctuations observed in holes distant from these central holes show that channel pressurisation produced a hydraulic gradient away from the channel towards the surrounding areas of the bed, thus enabling the propagation of a pressure wave away from the channel. The decrease in WL fluctuation amplitude with distance from the central holes demonstrates the diffusion of the pressure wave with distance from its origin. Increasing base WLs away from the central DRY-HIGH holes (e.g. 93/41 and 93/42) represent the increase in the piezometric surface away from the channel (Section 2.1). As base WLs in the central holes were DRY and base WLs increased in the surrounding distributed system, a hydraulic gradient towards the channel from the surrounding areas of the bed must have developed, allowing the distributed system to drain overnight. Hydraulic gradients are therefore inferred to have reversed between the channel and the surrounding distributed system on a daily basis.

The relatively large width of the VPA in 1993 may be associated with the period of time over which the inferred channel was able to develop before the 5 day classification period. The 1993 ablation survey showed that snow had retreated from the borehole array by JD 200 and that no further snowfall occurred between then and the end of the summer observation period on JD 233. Air temperatures remained consistently above zero from JD 204 onwards (Figure 2.3a). Thus, favourable conditions for the production of peaked daily meltwater input cycles existed from JD 204 until the end of the observation period. These cycles will have increased in amplitude as the snowline retreated over the summer, exposing larger areas of low albedo, impermeable ice. This is demonstrated by the development of peaked daily bulk discharge cycles (Figure 2.3c). If the suggestion that the development of a channelised drainage system at a point on the glacier is initiated as the snowline retreats from that point is correct (Nienow, 1993; Nienow et. al, submitted), then the development of a subglacial channelised system in the 1993 borehole array would have been initiated ~JD 204. This channelised system would thus have had ~25 days (JD 204-229) within which to develop before the 5 day classification period (JD 229-233). Sustained high discharge over this 25 day period (Figure 2.3c) will have been significant in promoting the development of this channelised system. High daily water pressure fluctuations driven by high, peaked discharge over the 25 day period are likely to have been propagated away from the channel to distal parts of the surrounding bed, thus explaining the observed width of the VPA.

**2.6.2 1992:**

The DRY base WL in 92/13 suggests the possible presence of a subglacial channel at atmospheric pressure. Increasing base WLs with increasing distance from 92/13 suggest that this channel was surrounded by a distributed system that was constantly pressurised. However, the presence of only LOW WL fluctuations demonstrates that this inferred channel could not be pressurised sufficiently by the meltwater inputs to promote HIGH WL fluctuations.

The 5 day classification period in 1992 (JD 257-261) occurred near the end of the summer ablation season and followed a period of cool temperatures (JD 245-250) when snowfall occurred (Figures 2.4 a and b). This likely resulted in the low discharge measured after JD 245 (Figure 2.4c). Conditions for peaked daily meltwater inputs were thus not favourable for significant channel pressurisation, and may thus explain the lack of HIGH WL fluctuations in 1992.

The size of the inferred channel during the 5 day classification period may also explain why no HIGH WL fluctuations were observed. A period of high, peaked discharge associated with high temperatures occurred between JD 205 (when the snowline retreated from the borehole array) and JD 223 (when snow had been removed from most of the glacier) (Figures 2.4a and c). These conditions are likely to have promoted the development and growth of a channelised system beneath Haut Glacier d'Arolla to efficiently evacuate large volumes of meltwater. This channelised system is likely to have begun to close by ice deformation after JD 245, when discharge decreased significantly and there was unlikely to have been sufficient meltwater to offset closure. As such closure is not instantaneous, the channel would have been too large to be significantly pressurised by the declining meltwater inputs. This may explain why a DRY base WL was observed (channel drained to atmospheric pressure overnight), why only LOW WL fluctuations occurred in the 5 day classification period, and why the VPA was narrower than that in 1993 (pressure fluctuations in the channel were not great enough to reach distant parts of the bed).

It is therefore proposed that the WL behaviour observed in the 1992 5 day classification period represents the existence of an 'oversized' channel which had evacuated past high levels of discharge, but was subjected to only low meltwater inputs during the 5 day classification period. This channel was located within a distributed drainage system. Had drilling been undertaken between ~JD 205 and JD 223, it is possible that WL behaviour similar to that in 1993 would have been observed due to consistent high air temperatures and resulting high, daily peaked discharge.

**2.6.3 1995:**

The WL behaviour observed in the 1995 5 day classification period (JD 226-230) demonstrates that if a channel did exist within the borehole array (as was inferred in 1992 and 1993), it was constantly pressurised as no DRY base WLs were observed. In addition, the pressure in this channel did not rise significantly on a daily basis as only LOW WL fluctuations were observed and the width of the VPA was narrow. LOW WL fluctuations may have been due to reduced or damped meltwater inputs to the inferred channel as the snowline was ~2.7km from the glacier snout during the 5 day classification period. As snow still covered much of the upper glacier catchment, peaked meltwater inputs would have been reduced and damped due to the high albedo and storage capacity of the snow. The 5 day classification period also occurred on the downward trend of the seasonal discharge curve (Figure 2.5c) which may also explain the lack of HIGH WL fluctuations in 1995.

The 1995 WL behaviour does not conclusively point to the presence of a channel located within the borehole array during the 5 day classification period. Another possible explanation for the observed WL behaviour is that boreholes with LOW base WLs represent areas of the bed which were able to accommodate most of the water that was originally in the boreholes after they were drilled. The LOW WL fluctuations may not necessarily have been driven by basally-derived inputs, but by daily supraglacial and/or englacial inputs which exceeded the rate of drainage from the boreholes during the day, and drained from the boreholes overnight when the inputs ceased. In boreholes that exhibited no WL fluctuations (95/4 and 95/15), the rate of melt input is likely to have been equal to the rate of output. Boreholes with LOW base WLs may therefore represent areas of the bed with a higher hydraulic conductivity than areas of the bed characterised by unconnected boreholes.

## 2.7 CHANGING BOREHOLE WATER LEVEL BEHAVIOUR OVER AN OBSERVATION SEASON:

The above discussion has attempted to demonstrate the character of the subglacial drainage system within the three observation years. However, as mentioned in Section 2.3, the classification of borehole WL behaviour in a five day period at the end of each season excludes the possibility of identifying changes in borehole WL behaviour over an observation season. Such changes may indicate evolution of the subglacial drainage system (e.g. Nienow, 1993; Fountain, 1994; Nienow et al., submitted).

The revised version of the Smart (1996) classification system was applied to all the borehole WL data in each year over the entire observation season. Of the 56 boreholes classified in the original 5 day classification period, 10 demonstrated changes in WL behaviour over the observation periods. Two of these were from 1992 (92/4 and 92/13), seven were from 1993 (93/29, 93/32, 93/34, 93/35, 93/36, 93/41, 93/43) and the other was from 1995 (95/2). As WL behaviour in 1993 changed more than in the other two observation years, and as 1993 is the focus of Chapter 4, the WL behaviour changes of the 1993 boreholes will be discussed here.

With the exception of 93/43, all the boreholes with changing WL behaviour demonstrated increases in WL fluctuation amplitude (Figure 2.6). 93/29 and 93/36 exhibited DRY-HIGH and DRY-LOW WL behaviour respectively, between JD 195 and JD 199. As the base WLs in the boreholes surrounding 93/29 and 93/36 were either LOW or HIGH over this period, it is likely that the DRY base WLs in 93/29 and 93/36 represent conditions in an isolated area of the bed. This area may have been a region of bed separation where a cavity filled during the day from daily supraglacial and/or englacial meltwater inputs to the boreholes and drained completely overnight when these inputs ceased.

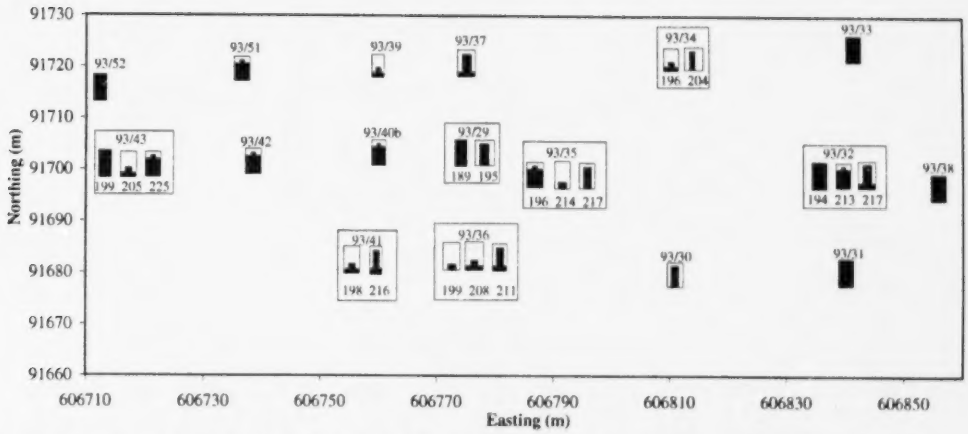


Figure 2.6: Distribution of classified boreholes in 1993 highlighting those holes that changed classification over the summer observation period (in boxes). The value below each classification symbol is the Julian day on which the WL behaviour changed on.

Between JD 204 and JD 217 there was a general trend towards decreasing base WLs and/or increasing WL fluctuation amplitudes in boreholes located towards the centre of the array. These changes in WL behaviour might indicate the gradual development of a channel in the centre of the borehole array. This would have resulted from water pressure in the areas of the bed surrounding the inferred channel being drawn-down by low water pressure in the channel (causing decreasing base WLs) and the channel becoming more significantly pressurised from increases in meltwater inputs that are inferred from increasing bulk discharge over this period (Figure 2.3c) (causing increasing WL fluctuation amplitudes). Increasing bulk discharge after ~JD 206 is likely to have resulted from the retreating snowline which was ~2.5km from the glacier snout on JD 214. As the snowline retreated, low albedo, impermeable ice surfaces were exposed which allowed rapid, peaked meltwater production and runoff. The period within which significant changes in WL behaviour occurred appears to have coincided with the removal of much of the snowpack from the glacier and a consequent increase in peaked bulk discharge. It is therefore proposed that the observed changes in WL behaviour, especially between JD 204 and JD 217, occurred in response to a common forcing (the onset of high, peaked meltwater inputs as the snowline retreated which promoted the gradual development of a channel) and not in response to random forcings on individual boreholes (e.g. a localised change in the hydraulic conductivity of the sediment at the base of a borehole or varying amounts of local supraglacial and/or englacial meltwater inputs to individual boreholes).

93/43 demonstrated slightly different behaviour. This borehole connected on JD 205 and exhibited LOW-LOW WL behaviour until JD 225 when its base WL rose to HIGH. Thus, a connection event was followed by a disconnection. This may have been caused by a number of factors such as a reduction in the hydraulic conductivity of sediment near the base of the borehole or the advection of the borehole base onto a bedrock bump.

The evolution of the subglacial drainage system in 1993 will be discussed in greater detail in Chapter 4.

## 2.8 SUMMARY:

The use of the borehole WL behaviour classification system has allowed the general pattern of WL behaviour within the borehole array to be analysed. In all three observation years a central zone of connected boreholes was located within a wider area of generally unconnected or high standing boreholes. Daily WL fluctuations in the connected area were greatest in 1993 as was the VPA width. The WL behaviour in the 5 day window period of 1993 suggests the presence of a well developed channel located within a more extensive distributed system. The daily pressurisation of the channel (indicated by the WL fluctuations) was detected to a reduced degree with increasing distance from the channel (indicated by decreasing WL fluctuation amplitudes away from the channel). In 1992, it was inferred that a channel did exist at the centre of the VPA, but that this channel was too large to be significantly pressurised by the decreasing meltwater inputs during the window period. This accounted for the LOW WL fluctuations observed, the DRY and LOW base WLs in the central holes and the narrow VPA width. The presence of a channel within the 1995 borehole array was not conclusively demonstrated. If a channel did exist, meltwater inputs during the window period may not have been great enough to significantly pressurise the inferred channel to register HIGH amplitude WL fluctuations due to the snow cover which persisted in the upper glacier catchment. Another suggestion was that the distribution of the WL behaviour represented areas of the bed with different values of hydraulic conductivity and that WL fluctuations were driven by supraglacial and/or englacial inputs.

The classification system has also been used to highlight changing borehole WL behaviour over an observation season. It was suggested that the observed changes in WL behaviour (which occurred over a 13 day period) represented the gradual growth and development of a subglacial channel within the borehole array. The development of the inferred channel was thought to have been initiated by the retreat of the snowline which allowed high, peaked meltwater inputs to the subglacial drainage system.

Despite the utility of a simple classification system for categorising a highly variable WL data set, two main limitations are encountered. Firstly, the classification system totally masks short-term events (e.g. the influence of rainfall on the WL curve) and it does not allow for the identification of WL trends within the categories. The WL fluctuation amplitude is either ZERO, LOW or HIGH and changing amplitudes within these categories cannot be identified. These short-term events and trends may be just as significant in describing the nature and evolution of the drainage system as the general WL behaviour. Secondly, the WL data are taken at face value. No account is taken of whether the borehole is actually connected to the bed or not. From observations at the surface, WL fluctuations are just as likely to be induced by daily meltwater inputs to the top of the borehole as by inputs from the base of the borehole and no account is taken of englacial influences. Without information concerning the water sources and circulation patterns within the observed boreholes, the interpretation of WL behaviour is problematic and may be unreliable. These factors will be addressed in the following chapters.

# CHAPTER 3: DETERMINATION OF BOREHOLE PLUMBING FOR THE INTERPRETATION OF BASAL WATER QUALITY MEASUREMENTS

## 3.1 INTRODUCTION:

Measurements of EC and turbidity (Tu) recorded by in-situ probes positioned at the base of boreholes, have been used to interpret the character of subglacial drainage systems (Stone et al., 1993; Hubbard et al., 1995; Stone and Clarke, 1996). EC was used to infer the source of water: low EC representing solute-poor melt, higher EC representing water that had remained at the bed for longer periods of time acquiring solute (Brown et al., 1994). Variations in Tu were thought to result from the fluvial entrainment and transport of sediment particles due to increasing basal water flow velocities either near the probe or at some distance away from the probe. By combining EC and Tu measurements, inferences about basal water velocity, subglacial water provenance, the hydraulic conductivity of basal sediments and changes in the drainage system morphology were made and used to describe the character of subglacial drainage systems (e.g. Stone et al., 1993; Hubbard et al., 1995; Stone and Clarke, 1996).

The thermal regime of the glacier in which the boreholes are drilled determines the reliability of the in-situ water quality records as indicators of *true* basal water quality and thus their use for characterising subglacial drainage systems. Boreholes drilled in predominantly cold glaciers seal rapidly by water freezing and rarely encounter englacial drainage structures (e.g. Trapridge Glacier: Stone et al., 1993; Stone and Clarke, 1996). Such conditions are ideal for measuring basal water quality as the presence of the borehole imposes a negligible influence on the water quality measured at its base. However, measurements of basal water quality from the base of boreholes drilled in warm-based glaciers (e.g. Haut Glacier d'Arolla: Hubbard et al., 1995) are likely to be less representative of *true* basal water quality conditions as these boreholes remain open throughout the summer and are thus prone to englacial and supraglacial influences.

A significant number of boreholes that have been drilled in warm-based glaciers intercepted one or more englacial connections (detected by the sudden drop of the drill tip or of the borehole water level during drilling) (e.g. Engelhardt, 1978; Hantz and Lliboutry, 1983; Iken and Bindschadler, 1986; Fountain, 1994). The existence of englacial connections has also been inferred by down-borehole salt tracing (Hooke et al., 1988). Such observations can now be verified using down-borehole video imagery which allows for the direct identification of englacial inputs and outputs (englacial channels) and storage locations (englacial voids) (Pohjola, 1994; Harper and Humphrey, 1995; Copland et al., in press). Direct supraglacial inputs to the tops of boreholes have also been observed (e.g. Engelhardt, 1978). WL variations and water circulation within `open' boreholes are thus likely to be significantly influenced by englacial and supraglacial inputs and outputs.

An `open' borehole can thus store both basally and supra/englacially derived water if basal pressures are great enough to force water into the borehole and/or impede drainage from it. In-situ probes at the base of `open' boreholes may therefore not be continually monitoring changes in basal water quality, but rather the characteristics of water entering and exiting the base of the boreholes, which may be basally and/or supra/englacially derived. In-situ water quality measurements may also reflect water exiting the borehole mixing with water flowing past the base of the borehole. In-situ water quality measurements in `open' boreholes may therefore rarely represent *true* basal water quality conditions.

As a result, it is clearly necessary to determine the source and circulation of water within each borehole (i.e. determine borehole plumbing) before attempting to interpret in-situ water quality measurements. This is the objective of the present chapter. A number of data collection techniques used to identify the sources and circulation of water within boreholes will be presented. After analysis of these data, a classification of borehole plumbing will be suggested and applied to all of the boreholes drilled on Haut Glacier d'Arolla. Finally, examples of each borehole plumbing category will be discussed.

## 3.2 DATA SOURCES:

Seven types of data allow the determination of borehole plumbing. These can be viewed in a hierarchical fashion as each data source supplements the inferences made by the previous one. Thus, a borehole that has data from all seven sources will be associated with more accurate and reliable interpretations than a borehole with data from only one source. The seven data sources are: drilling records, continuous in-situ and manual WLs, continuous in-situ EC measurements, continuous in-situ Tu measurements, EC profiling, salt tracing and borehole video imagery.

### 3.2.1 Drilling Records:

Records are kept concerning the status of the borehole WL during drilling. If the WL drops before the bed is reached, the depth at which the drill tip lies is recorded (Table 3.1). If the borehole proceeds to refill from the continuous input of drill fluid (supraglacial water), it is inferred that an englacial void of finite volume has been intercepted. If the borehole does not refill, the interception of an englacial channel is inferred. Subsequent to drilling, records are kept of the time and duration of borehole reaming (unblocking of borehole constrictions with the drill to allow measuring instruments to be lowered to the base of a borehole) as this represents an artificial input of supraglacial water to a borehole. Some anomalous WL, and water quality behaviour may be explained by this artificial introduction of water into the borehole, therefore reaming records aid the interpretation of the WL and water quality measurements.

| BOREHOLE NUMBER | DRILLING RECORDS |
|---|---|
| 93/26 | Connected at bed - dry |
| 93/27 | Connected at 32m bs - stopped drilling |
| 93/28 | Stopped at 82m ab(rocks) - not at bed |
| 93/30 | Connected at 35m bs and at bed |
| 93/36 | Connected at bed - dry |
| 93/40a | Connected 31m ab-WL dropped to 30m ab |
| 93/41 | Connected 5m ab (WL↓to 15m ab) |
| 93/42 | Connected at 33,57 and 96 m ab |
| 93/44 | Void at 50m ab, re-filled |
| 95/7b | Connected at 34m ab |
| 95/8 | Connected at 20.5m ab |

Table 3.1: Borehole drilling records. Depths are given as metres above the bed (m ab) and metres below the surface (m bs).

### 3.2.2 Continuous in-situ and manual WLs:

As discussed in Chapter 2, initial analysis of WL data provides an indication of whether a borehole is connected to the basal drainage system (drop in WL) and of the proximity of the borehole to the source of WL forcing (amplitude of WL fluctuation). Boreholes with continuous in-situ WL measurements have more reliable WL data than boreholes with manual WL measurements as measurements are taken continuously throughout the observation season (unless technical difficulties arise) rather than at irregular times during

the day (see section 2.2 for methods of in-situ and manual WL measurements). In order to determine the source of the water that drives WL variations, both types of WL measurements must be supplemented by the following types of data.

### 3.2.3 Continuous in-situ EC measurements:

EC is proportional to the concentration of ions in solution and can be used as a surrogate for total dissolved solids (TDS). Although the conductivity of solutions is affected by factors such as temperature, ionic composition, pH and sediment load (Fenn, 1987), measurements of EC in this study are used solely to provide an indication of the TDS of the sampled water.

Sharp (1991) discussed five factors that primarily govern the extent of solute acquisition by glacial meltwaters: the chemistry of the source waters, the availability of protons, the duration of contact between meltwaters and weatherable rock material, the grain size, shape and mineralogical properties of particulate rock material in the subglacial environment, and the ratio between meltwater volume and the surface area of rock material available for weathering. Consequently, different types of drainage system may be characterised in terms of characteristic values of the above properties. As detailed water chemistry analysis is not the focus of this study, EC values will be taken as an indication of the relative contact times between meltwaters and weatherable rock material. Thus, dilute water represents water that has spent little time in contact with weatherable rock material and is therefore likely to represent recently produced meltwater. More concentrated water is thought to have spent a longer period of time in contact with weatherable rock material and may therefore represent water that has been stored at the bed for a period of time. The remaining four factors discussed by Sharp (1991) are recognised, but are not the focus of this study. Measured EC of meltwaters can therefore be used as an indication of the source of the water; recently derived-surface melt characterised by low EC versus basally-derived water characterised by higher EC.

EC measurements may also vary due to the mixing of waters characterised by different conductivities. This is exemplified by an inverse relationship between bulk discharge and EC (Fenn, 1987; from Tsidjiore Nouve, Switzerland). When discharge was low, high EC (~50μS $cm^{-1}$) represented the overnight drainage of stored water, whilst rising discharge was associated with a decrease in EC (~15μS $cm^{-1}$) due to the evacuation of the daily melt. The mixing of stored water and supraglacial meltwater was demonstrated as the EC during the day did not descend to values characterised by supraglacial meltwaters (<10μS $cm^{-1}$). This mixing process must also be considered when interpreting EC measurements.

In 1993 and 1995, EC was recorded continuously by in-situ automated sensors placed within a few decimetres of the bed (see Appendix III for sensor construction and calibration details). Measurements were logged as means of 30 readings every 10 minutes using Campbell Scientific CR-10 data loggers and EC values are presented as measured in water at c. 0°C. In-situ measurements were taken in 13 boreholes in 1993 and in 5 boreholes in 1995 (Table 3.2). From this point, EC measurements recorded by in-situ sensors will be referred to as 'in-situ EC'.

| SENSOR | 1993 | 1995 |
|---|---|---|
| EC | 27, 29, 30, 34, 35, 36, 37, 40a, 40b, 41, 42, 43, 51 | 2, 4, 15, 17, 18 |
| Tu | | N/A |

Table 3.2: Boreholes monitored by in-situ EC and Tu sensors in 1993 and 1995.

A frequency histogram of in-situ EC measured over the three years of observation exhibits four EC modes (designated Modes 1, 2, 3 and 4) at 0-10, 11-40, 41-80 and 81-150μS $cm^{-1}$ (Figure 3.1). The first three modes are similar to the three EC modes observed on Haut Glacier d'Arolla in 1992 by Tranter et al. (in press). This study inferred that Mode 1 waters represented dilute supraglacial ice melt and drill fluid; Mode 2 waters represented subglacial channel water as they were slightly less concentrated in the major ions than bulk glacial runoff; and Mode 3 waters were derived from flow in a distributed system where residence times at the bed were of the order of a few months or less. Mode 4 waters which were not detected in 1992, may represent water that had spent considerable time at the bed in storage or in a distributed system. However, it must be kept in mind that the definitions of these modal EC groups are crude, as no account has been taken of the process of mixing as a means of producing these groups. As no chemical analysis has been undertaken, the importance of this process cannot be quantified. Thus, by applying these modal EC categories, measured in-situ EC has the potential to act as a crude natural tracer of water source.

### 3.2.4 Continuous in-situ Tu measurements:

Turbidity results from the fluvial entrainment and transport of sediment particles (Stone and Clarke, 1996) which may be caused by:

a) increasing flow velocities exerting a shear stress on sediment at the ice-bed interface. Particles are dislodged when the shear stress is great enough and these particles may be transported as suspended sediment if they are small enough.

b) direct mechanical action of rapidly sliding ice (e.g. during mini-surges; Humphrey et al., 1986).

c) exposure of new areas of the bed to turbulent flow when high water pressure within a channel may cause ice-bed separation (Walder and Fowler, 1994).

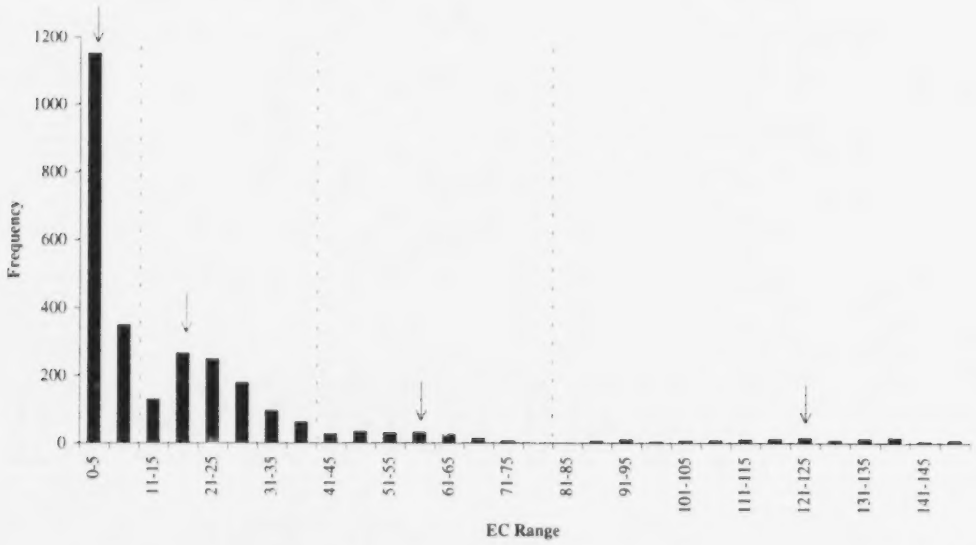


Figure 3.1: Frequency histogram of in-situ EC measured in 1992, 1993 and 1995. Arrows indicate modal EC ranges.

Stone and Clarke (1996) used Tu pulses measured at the base of one borehole (initiated by the sudden drainage of another borehole) to determine the velocity of flow between boreholes during the drainage event. This could be calculated as the distance between the two boreholes was known. Hubbard et al. (1995) interpreted the arrival of Tu pulses measured in boreholes located at increasing distances from an inferred channel as demonstrating water being forced across the bed laterally from the channel as the water pressure increased within the channel. Tu pulses can thus be used as natural tracers of flow at the bed.

As with EC, Tu was measured continuously in 13 boreholes in 1993 (Table 3.2) by automated in-situ sensors placed within a few decimetres of the bed (see Appendix III for construction and calibration details). Measurements were also logged as means of 30 readings every 10 minutes using Campbell Scientific CR-10 data loggers. Tu is presented as relative turbidity (Tu[r]), defined as:

$$Tu[r] = (Tu[c]-Tu[s])/Tu[c] \qquad (3.1)$$

where Tu[c] and Tu[s] are the turbidity signals recorded in clear water and the sample, respectively. Clear water therefore has a Tu[r] of 0 and highly turbid water a Tu[r] of 1. From this point, Tu[r] measured by in-situ sensors will be referred to as 'in-situ Tu'.

### 3.2.5 EC Profiling:

The modal EC categories discussed above can also be used to identify the source and circulation of water within a borehole. The latter is only possible if the borehole water column exhibits an EC *stratification* where more than one mode of water exists. In such a case, waters of different modes are separated by a *condocline*. Patterns of water circulation within a borehole can be deduced by monitoring the movement (if any) of the EC stratification.

EC profiling was conducted in 1992, 1993 and 1995 (see Appendix II for construction and calibration details of EC profilers). The EC profiler was lowered down the borehole until the WL was reached (if the borehole was not full) and this depth was recorded. It was clear when the profiler reached the WL as air readings were zero whilst water readings were >0.5μS $cm^{-1}$. EC readings were taken just below the WL and subsequently at 5m intervals until the bed was reached. EC profilers were also used to monitor WLs in boreholes that were not monitored by in-situ pressure sensors.

Of the 70 boreholes drilled in 1992, 1993 and 1995, 59 were profiled. Four major EC stratification categories have been identified in these 59 boreholes:

a) **Type 1:** Mode 1 water only. Exhibits no EC stratification.
b) **Type 1/2:** Mode 1 water overlying Mode 2 water.
c) **Type 1⇒1/2:** Mode 2 water enters the base of a Mode 1 water column on a diurnal basis.
d) **Type 1/2/3:** Mode 1 water overlies Mode 2 water which overlies Mode 3 water.

These four categories represent 54 of the 59 boreholes profiled. The remaining 5 boreholes exhibit anomalous EC stratifications (1/2/4⇒1/3/4, 2/3/2, 1⇒1/2⇒1/2/3, 2/3⇒1/2/3 and 2⇒1/2 (where the arrows indicate a change in the stratification type during the observation season)). By combining the manual and in-situ WL records with the EC profiling data, a general idea of the plumbing of each borehole can be gained. Three main borehole plumbing types are identified:

a) **Unconnected:** the borehole remains full and no movement in the EC stratification (if present) is observed.
b) **Compound:** WL variations are observed and movement of the EC stratification occurs (especially near the bed). Inputs and outputs may be from any combination of supraglacial, englacial or basal sources.

c) **Englacially connected:** WL variations are observed, but there is no movement in the basal EC stratification indicating that englacial and/or supraglacial inputs and outputs are driving the WL variations .

### 3.2.6 Borehole Salt Tracing:

Dissolved salt can be used as an artificial tracer of water flow within a borehole water column (Hooke et al., 1988). Its use is especially advantageous as the EC values produced can be much greater than the highest EC values of natural borehole waters if sufficient salt is used. This enables tracing in boreholes that possess no EC stratification and clearer monitoring of flow in those that do, allowing for the identification of possible englacial and basal inputs and outputs.

To conduct a salt trace, a 1cm diameter plastic hose was taped to 100m of the EC profiler cable so that the hose outlet was directly above the sensor. This attachment was necessary to weight the hose sufficiently for it to reach depths of up to 100m bs. The hose and cable were lowered to the desired injection depth and secured. 1kg of table salt was dissolved in a 14 gallon bucket of supraglacial water and poured down a funnel into the hose. The saline solution was flushed down the hose with fresh meltwater. Profiles were subsequently logged at c. 20-30 minute intervals with readings taken every m bs. The additional weight of the hose physically prevented a shorter time interval between profiles. Salt traces were undertaken in boreholes 93/37 and 93/41, the results of which will be discussed in section 3.4.4.

### 3.2.7 Borehole video imagery:

In 1995 a GeoVision Micro™ colour borehole video camera (see Appendix IV for further details) was used to record the internal properties of 11 boreholes. A view of the internal properties of the boreholes was afforded by a small colour monitor whilst the camera was being lowered down the borehole and the image was recorded simultaneously on a video

cassette which allowed for more detailed inspection of interesting features. Written logs of the borehole properties were produced after repeated inspection of the video recordings.

The video logs provided useful information on three aspects of the internal properties of the boreholes. These were:

a) **Internal structure of borehole walls:** identified englacial channels (both passive and active) and voids.
b) **Water quality:** indicated whether the water was clear or turbid.
c) **Bed conditions:** demonstrated the nature of the bed.

Table 3.3 presents statistics on relevant features observed on the video logs. Borehole video imagery allows for the verification and/or refinement of interpretations made from the data sources discussed above as direct observations of the internal properties of the boreholes are afforded. The addition of borehole video imagery as a data source for interpreting borehole plumbing can thus significantly increase the reliability of such interpretations.

| Borehole Feature | Frequency |
|---|---|
| Video reached bed | 6 |
| See bed | 4 |
| No. of englacial voids | 16 (in 7 boreholes) |
| No.of englacial channels | 5 (2 possibly active) |
| See water quality stratification | 7 |

Table 3.3: Features seen in video logs from 11 boreholes drilled in 1995.

## 3.3 CLASSIFICATION OF BOREHOLE PLUMBING:

All the data gathered were compiled and analysed to determine the water sources and patterns of water circulation in each borehole drilled over the three summers. Four categories of borehole plumbing are identified and one category with anomalous behaviour is also included (Table 3.4). These categories have expanded on the ones identified by the EC profiling discussed above. The five categories are:

1) **Unconnected:** the borehole remains full throughout the observation season. Two types of unconnected borehole are recognised:

a) **Unstratified:** no EC stratification is present.
b) **Stratified:** EC stratification within the borehole water column is observed.

The unconnected boreholes are differentiated in terms of their EC stratification because it is possible that basal EC may indicate the bed type; whether it is a hard bed (EC may remain low and stable) or one composed of unconsolidated sediment (EC may increase over time due to the acquisition of solute from suspended sediment disturbed when the drill hit the bed).

2) **Passively connected:** a drop in the borehole WL is recorded during drilling, but the borehole re-fills and remains full throughout the season. This behaviour indicates the presence of an englacial void of finite volume. No connection to the subglacial drainage system via the bed is inferred despite the lowering of the WL.

3) **Englacially connected:** WL variations occur, but EC stratification at the bed remains stable. This suggests that water enters and exits the borehole via an englacial channel located above the condocline. Supraglacial inputs may also contribute to the rise in the WL.

4) **Actively connected:** the WL falls when the bed is reached during drilling or after the borehole has been completed. WL and EC stratification variations (especially at the bed) are observed either on a daily basis or over a period of several days. This indicates that the borehole has a basal connection. Englacial inputs and outputs and supraglacial inputs often have an additional influence on the WL and the EC stratification.

5) **Anomalous behaviour**: three instances of borehole behaviour that do not fall into the above categories have been identified. These will be discussed in the following section.

The following section will present examples of boreholes in each of these categories and explain how the classifications were reached.

| CATEGORY | YEAR | BOREHOLE NUMBER | TOTAL |
|---|---|---|---|
| UNCONNECTED | 1992 | 2,6,8,9,10,16,17,20 | 11 |
| (UNSTRATIFIED) | 1993 | 31,53 | |
| | 1995 | 6 | |
| UNCONNECTED | 1992 | 7,15,18,19 | 12 |
| (STRATIFIED) | 1993 | 33,38,45,46,52,54 | |
| | 1995 | 9,25 | |
| PASSIVELY | 1992 | 4,11 | 8 |
| CONNECTED | 1993 | 44 | |
| | 1995 | 5,7b,8,20,24 | |
| ENGLACIALLY | 1992 | 1,3 | 7 |
| CONNECTED | 1993 | 35,39,42 | |
| | 1995 | 2,15 | |
| ACTIVELY | 1992 | 12,13,14 | 18 |
| CONNECTED | 1993 | 26,29,30,32,34,36, 37,40a,40b,41,43,51 | |
| | 1995 | 1,4,18 | |
| ANOMALOUS | 1992 | 5 | 3 |
| | 1995 | 16,17 | |

Table 3.4: Final classification of borehole plumbing based on all available data sources.

## 3.4 EXAMPLES OF BOREHOLE PLUMBING CATEGORIES:

### 3.4.1 Unconnected:

3.4.1.1 *Unstratified:* **92/2:** EC profiles taken over a period of 20 days illustrate that the WL remained at the surface throughout and the water column consisted of Mode 1 water only. This borehole was thus filled with the supraglacial water used for drilling. Low basal EC of 3μS $cm^{-1}$ suggests that the bed was bedrock at this location. If unconsolidated sediment had been present, it is likely that drilling would have disturbed the sediment and the basal EC would have increased with time due to solute acquisition.

3.4.1.2 *Stratified:* **92/7:** EC profiles (Figure 3.2) demonstrate that a consistent layer of Mode 2 water existed in the lower 25m of this borehole and that this was overlain by a stable layer of Mode 1 water. This EC stratification may indicate that the bed at this point consisted of unconsolidated sediment. Sediment may have been put into suspension by drilling disturbances, allowing the water at the base of the borehole to acquire solute.

### 3.4.2 Englacially connected:

3.4.2.1 **93/39:** A 5m layer of Mode 4 water remained stable at the base of the borehole whilst the daily WL increase consisted of Mode 1 water (Figure 3.3). Overnight, the Mode 1 water drained to ~15m ab without affecting the Mode 4 water at the base of the borehole. This suggests that there was no basal connection and that the Mode 1 water drained and possibly entered via an englacial channel ~15m ab. Supraglacial inputs were also likely to be a major source of water for the daily WL rise.

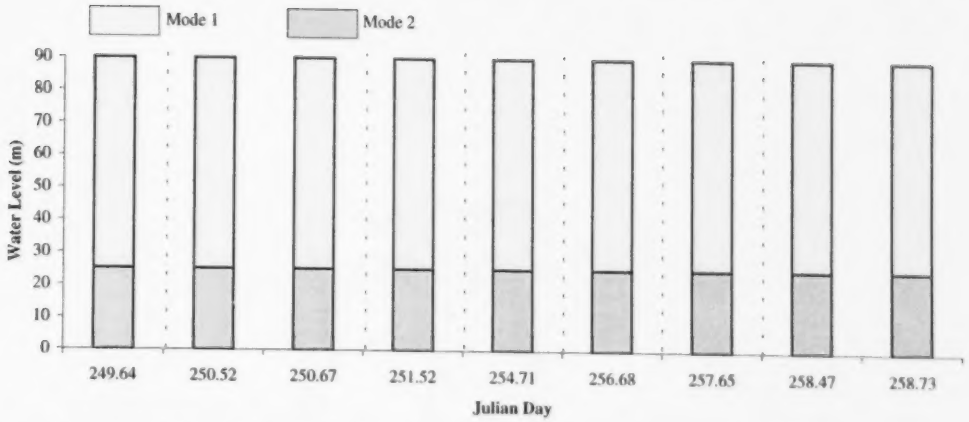


Figure 3.2: 92/7 EC profiles. Borehole depth = 90m.

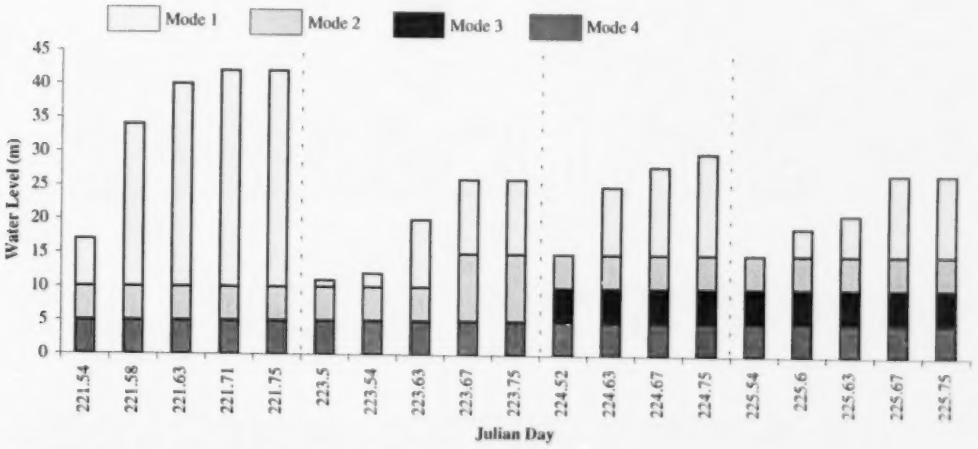


Figure 3.3: 93/39 EC profiles. Borehole depth = 100m.

3.4.2.2 **95/2:** This borehole drained to a depth of 32m ab two days after drilling was completed on JD 210. EC stratification recorded below 32m ab before and after the borehole drained was identical. This suggests that drainage occurred via an englacial channel located 32m ab and not via the base of the borehole.

In-situ WL and EC probes were installed at the base of 95/2 6 days after it had drained (Figure 3.4). Basal EC rose steadily from ~18-28μS $cm^{-1}$ over a period of 10 days, suggesting that no basal flow was occurring and that solute acquisition was the cause of the increase in EC. The WL increases (produced by Mode 1 water) were sporadic and coincided either with high temperature days (JD 222 and 227), rainfall (JD 225) or periods of reaming (JD 228). The water drained back to 32m ab overnight (except on JD 227 and 228). This again suggests the presence of an englacial channel.

Video imagery identified a round englacial channel of ~2cm diameter at 36.8m ab. The Tu of the water was significantly greater below the level of this channel. This corresponds with the EC profiling data which show a stable layer of Mode 2 water below this level (Figure 3.4) (Note: the difference in WL between manual WL measurements and the video log is due to the use of different instruments to measure depth below the ice surface. Such differences will occur throughout this chapter). WL variations are therefore inferred to be derived from englacial and/or supraglacial sources with no significant flow of water occurring at the bed.

**3.4.3 Passively connected:**

**95/8:** Drilling records state that this borehole drained during drilling when the drill tip was 27m bs. The borehole re-filled as drilling continued and remained full for the rest of the season. This implies that an englacial void of finite volume was intercepted, the borehole draining until the void was filled and then re-filling with the continual additions of drill fluid. The video logs support this interpretation as a narrow, longitudinal void ~60cm high and 7cm wide was observed at a depth of 26.8m bs. This feature is likely to

be a partially closed remnant crevasse. The boundary between clear and turbid water revealed by the video logs corresponds well with the condocline between Mode 1 and Mode 2 water measured by EC profiling (Figure 3.5). The stable water quality boundaries suggest that no perceptible water flow was occurring at the bed which may possibly consist of unconsolidated sediment due to the high Tu of the basal water.

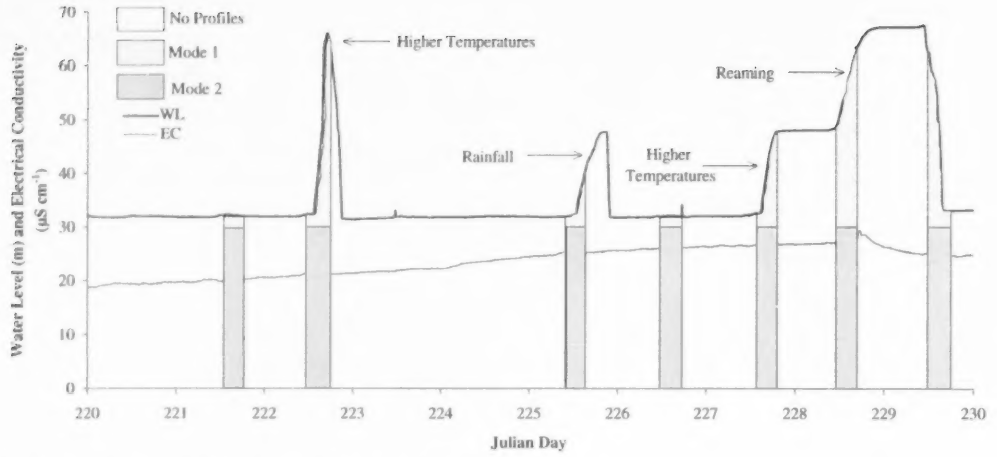


Figure 3.4: 95/2 in-situ WL and EC and EC profiles. Borehole depth = 96.5m.

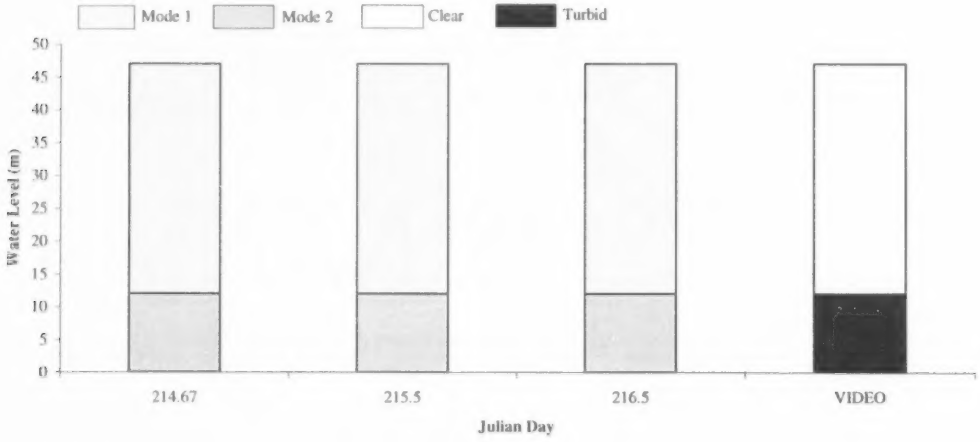


Figure 3.5: 95/8 EC profiling and video log measurements. Borehole depth = 47.5m.

**3.4.4 Actively connected:**

3.4.4.1 **93/37:** This borehole drained on the night that it was drilled and subsequently exhibited daily, high amplitude WL fluctuations (80-90m) and in-situ EC cycles (~3-20μS $cm^{-1}$) (Figure 3.6a and b). EC profiling data (Figure 3.6a) demonstrate that a plug of Mode 2 water entered the base of the borehole in the early afternoon followed by Mode 1 water. The rate at which the Mode 2 layer rose up the borehole was equal to the rate of WL increase. This suggests that the borehole was fed primarily from the bed. This interpretation is supported by the results of a salt trace (Figure 3.7). The layer of dissolved salt (introduced at 7m ab before the WL began to rise) rose up the borehole as a coherent layer (despite disruptions in the lower 40m) at the same rate as the WL increase. This salt layer was clearly forced up by significantly lower EC water entering the base of the borehole. The Tu signal (Figure 3.6b) was complex, though peaks did occur during periods of rapidly rising and falling WL. This demonstrates the flow of water at the base of the borehole. Consequently, it is concluded that 93/37 was fed primarily from the bed.

Based upon this interpretation, the EC profiling data can be used to interpret the in-situ EC cycles. The in-situ EC decreased from ~20-3μS $cm^{-1}$ on the rising WL limb and returned to ~20μS $cm^{-1}$ on the falling limb (Figure 3.6b). EC profiling data illustrate that this EC cycle represents Mode 2 water being forced up the borehole by Mode 1 water as the WL rose. As the WL fell, the Mode 1 water drained from the base of the borehole followed by the Mode 2 water (Figure 3.6a). The water draining from the borehole was also likely to have been mixing with water flowing past the base of the borehole at the bed. The in-situ EC signal therefore only reflected *true* basal water quality as the WL rose. Measurements made as the borehole drained simply reflected the composition of the water that had been stored in the borehole during the day. Measurements of *true* basal conditions would next be made after the borehole had drained completely.

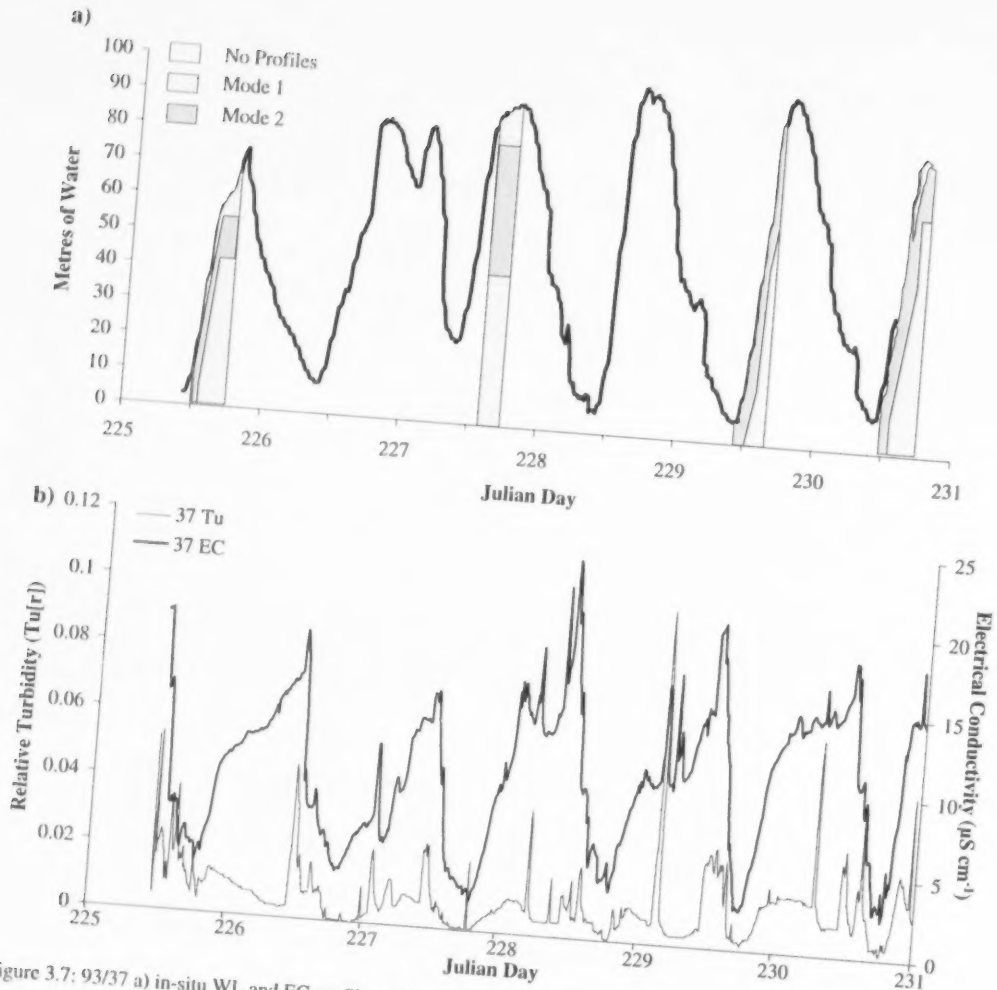


Figure 3.7: 93/37 a) in-situ WL and EC profiles and b) in-situ EC and Tu.

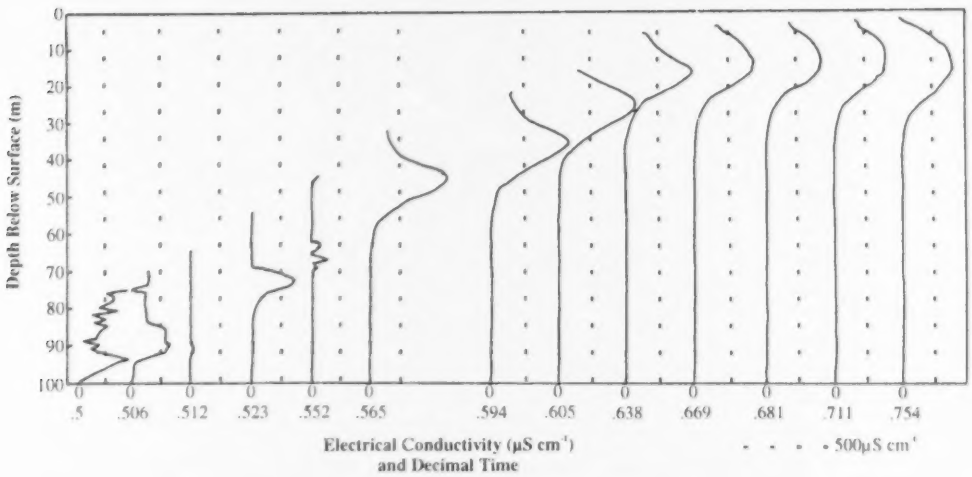


Figure 3.7: 93/37 Salt trace profiles conducted on JD 232.

3.4.4.2 **93/41:** This borehole connected 5m ab during drilling and the WL drained to 15m ab. Subsequently, daily WL fluctuations occurred throughout the observation period (Figure 3.8a). The in-situ EC and Tu records (Figure 3.8b) exhibited semi-diurnal cycles (except on JD 222 and 223 for Tu) which occurred on both the rising and falling limbs of the WL cycle. EC profiles (Figure 3.8a) aid the initial interpretation of these in-situ records. The borehole initially filled with supraglacial and/or englacial inputs. Subsequently, a sharp, ephemeral peak of Mode 2 water entered and exited the borehole under rising WL conditions. The flow of water at the base of the borehole that generated this input of Mode 2 water was represented by the first Tu peak in the semi-diurnal cycle. The subsequent downflux of this Mode 2 water was likely the result of supraglacial and englacial additions to the water column which forced the Mode 2 water out of the base of the borehole.

A salt trace conducted on JD 231 and accompanying in-situ EC and Tu data (Figure 3.9a and b) contribute further to this interpretation. Salt water was injected 20m ab at JD 231.552 when the WL was 39m ab and the natural spike of Mode 2 water had already been registered at the bed (**i**). Profiles 1 to 13 illustrate the movement of the salt water up the borehole.

i) *Profile 1:* ~4000μS $cm^{-1}$ water (**A**) was capped by lower EC 'noise' (**B**) possibly induced by the failure to adequately flush the salt water from the hose before the hose was removed from the borehole (Ketterling, 1995).

ii) *Profile 2:* **A** was forced up the water column by lower EC water below. **B** became a coherent unit of ~750μS $cm^{-1}$ probably due to mixing by the profiler.

iii) *Profiles 3 and 4:* **A** disappeared from the water column. **B** became a well defined peak of ~500μS $cm^{-1}$ and rose up the borehole. It is suggested that an englacial channel existed ~30m ab. As **A** rose past 30m ab it exited the borehole via this englacial channel.

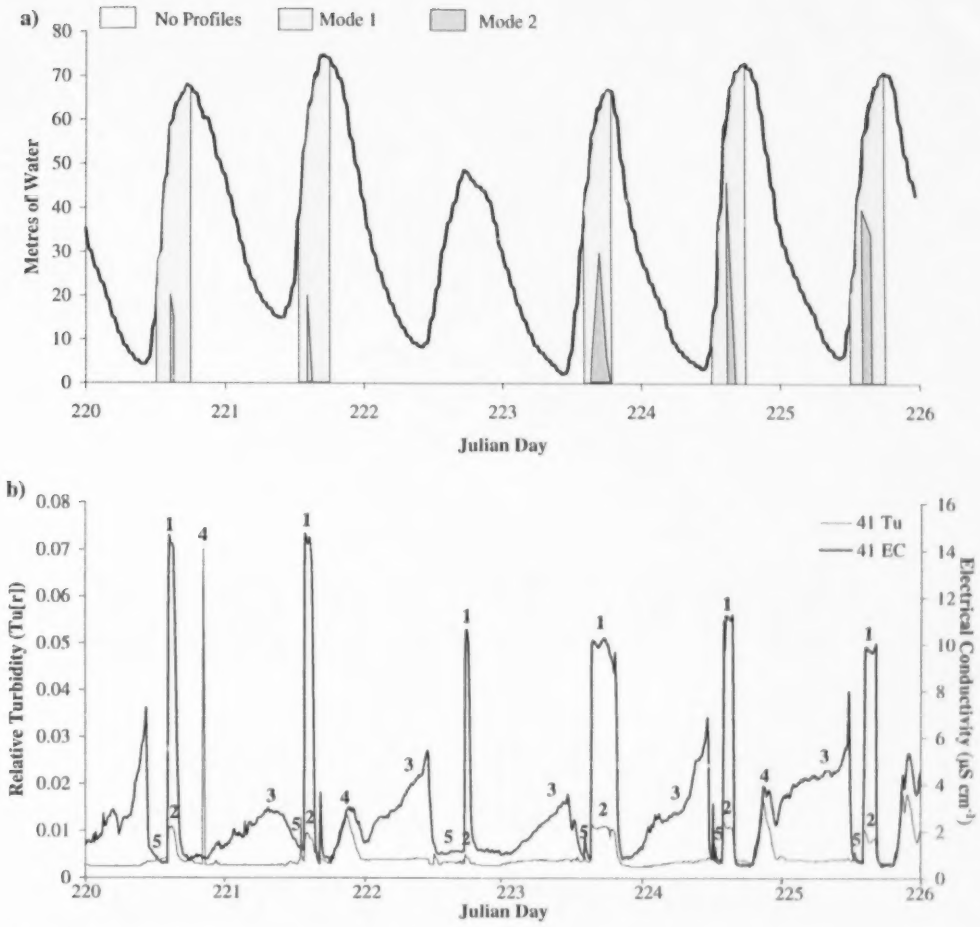


Figure 3.8: H41 a) in-situ WL and EC profiles and b) in-situ EC and Tu.

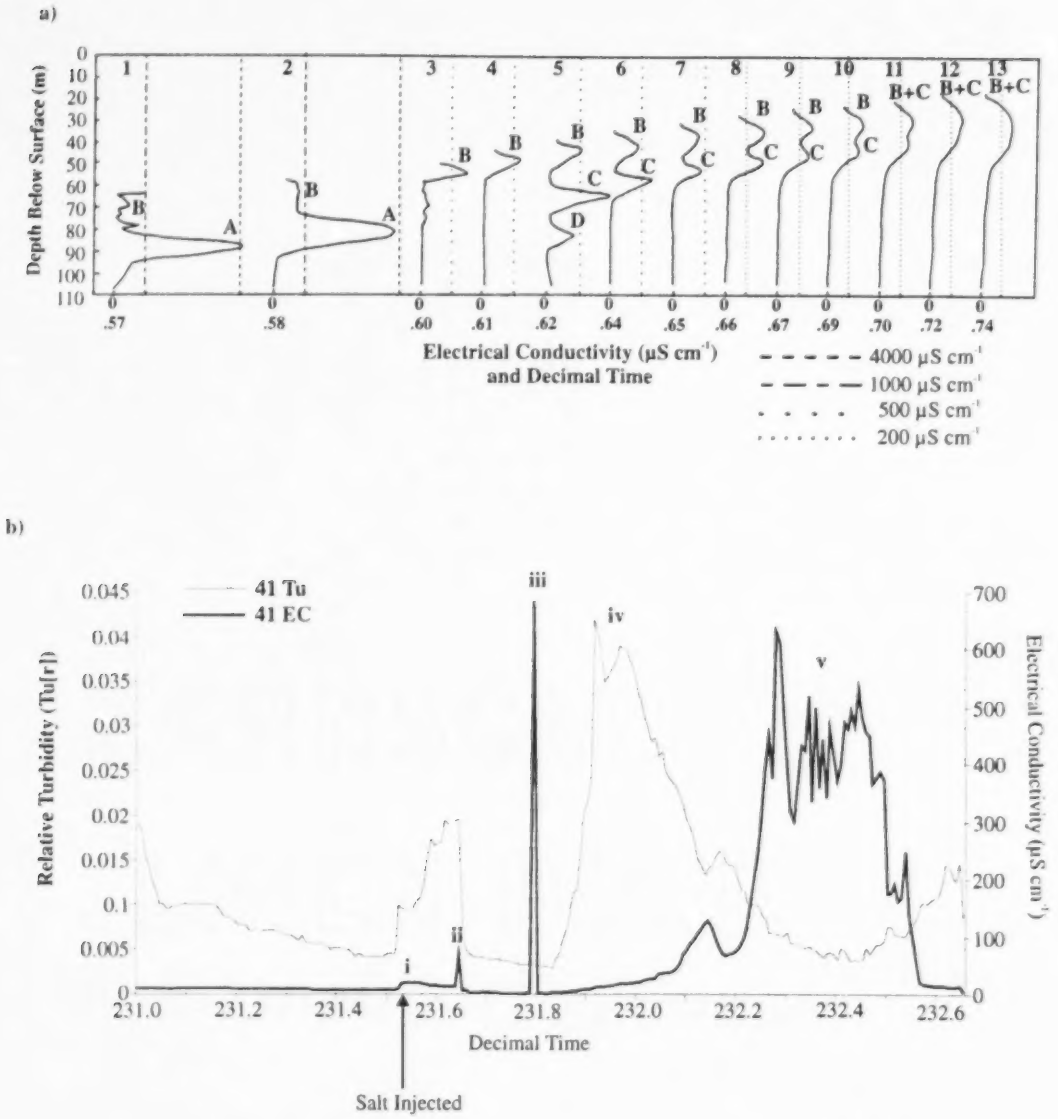


Figure 3.9: a) 93/41 salt trace profiles conducted on JD 231, b) 93/41 in-situ EC and Tu measurements for JD 231-232.

iv) *Profiles 5 and 6:* two slugs of salt water (**C** and **D**) appeared. These are thought to represent the reintroduction of **A** as water in the englacial channel backed-up due to increasing water pressures at the bed. **A** had therefore not been entirely evacuated from the englacial channel. Once **A** was reintroduced, the continued englacial inflow split the salt layer into **C** and **D**, forcing **C** up and **D** down the borehole. A spike of 68μS $cm^{-1}$ registered at the bed at 231.625 (**ii**) suggests that only a small proportion of **D** left the base of the borehole as **D** was initially measured as ~500μS $cm^{-1}$. The englacial channel intercepted at 5m ab during drilling may have drained much of **D**.

v) *Profiles 7-13:* **B** and **C** rose up the borehole and eventually merged due to diffusion and mixing by profiling disturbance. The WL started to fall between profiles 12 and 13.

vi) *Post-profiling observations:* At JD 231.76 (35 minutes after the WL started to fall) a second salt trace was undertaken in 93/41 to demonstrate the outflux of water from the base of the borehole as the WL fell. Four minutes after the salt was injected at 20m ab, an ephemeral peak of 684μS $cm^{-1}$ was registered by the in-situ sensor (**iii**), thus confirming the rapid outflow of water via the base of the borehole. Following this, the second Tu peak of the semi-diurnal cycle occurred as the borehole drained (**iv**) and **B+C** were eventually recorded leaving the base of the borehole between 232.18 and 232.52 as the water drained overnight (**v**).

Interpretations from the salt trace experiment demonstrate the complex nature of water circulation within 93/41 and the controlling influence of englacial inputs and outputs on this circulation. Although water was introduced to the borehole via the base during the day, englacial outputs and inputs acted as a sink and source for some of this water. The re-introduction of water from the englacial input at 30m ab forced water back out of the base of the borehole even under conditions of rising WL. Water that drained from the base of the borehole overnight was thus unlikely to be exactly the same water that entered via the base during the day.

With the improved knowledge of water circulation within 93/41, the in-situ EC and Tu records (Figure 3.8b) can be interpreted more accurately. The high, ephemeral EC peak (**1**) represents basal water rapidly entering and exiting the borehole, the downflux imposed by the activation of the englacial input ~30m ab being responsible for the rapid exit of the Mode 2 water. The flow of water at the base of the borehole is demonstrated by the coincident Tu peak (**2**). The lower EC `shoulder' (**3**) represents the dilution of relatively concentrated basal water flowing past the base of the borehole by the outflow of relatively dilute englacial water from the borehole as the WL fell. Tu peaks that occurred during the initial period of falling WL and rising EC (**4**) again demonstrate flow at the base of the borehole as rapid outflow stirred up basal water into the base of the borehole. Low EC values that separate the lower EC `shoulder' and the high EC peak (**5**) represent supraglacial inputs reaching the bed in the late morning at the onset of the daily melt cycle.

A problem with this interpretation is highlighted by EC profiles recorded on JD 224 and 225 as Mode 2 water rose above the level of the inferred englacial channel at 30m ab. In such a case, the activation of the englacial input (which is inferred to force the Mode 2 water out of the borehole base) should have split the column of Mode 2 water at 30m ab. This would have left an isolated layer of Mode 2 water above the level of the englacial input. Such an isolated layer of Mode 2 water was not detected in the JD 224 and 225 profiles. This could be explained by the dilution of the uppermost portion of Mode 2 water from the rising input of englacial water that was exemplified by the rise of salt slug **C** in the salt trace.

According to this interpretation, *true* basal water quality is recorded only during the initial input of basal water to the base of the borehole. The remaining measurements represent the flow of basal and englacial water out of the borehole base and subsequent mixing of this water with water flowing across the bed.

3.4.4.3 **92/14:** The daily WL variations exhibited by this borehole mainly consisted of Mode 1 water (Figure 3.10). EC profiling revealed that an ephemeral layer of Mode 2 water entered the base of the borehole on a daily basis. Had this Mode 2 water not been recorded, the WL variations might have been interpreted to have originated solely from supraglacial and/or englacial inputs. The entry of the Mode 2 water indicates that basal inputs and outputs were at least partially responsible for the WL fluctuations.

### 3.4.5 Anomalous behaviour:

3.4.5.1 **92/5:** This borehole remained full for the entire observation season. EC profiles illustrate that for a period of 15 days after the borehole was completed, the water column exhibited a stable EC stratification with a 10m layer of Mode 2 water overlain by Mode 1 water (Figure 3.11). However, subsequent EC profiles show that the water column consisted mainly of Mode 2 water capped by only 5m of Mode 1 water. This demonstrates that Mode 2 water must have been forced up from the bed. As the borehole was already full, no change in WL could be observed and no artesian flow was recorded. The flow of water out of the borehole top was probably accommodated by the surface weathering crust of the glacier or by gradual outflow over the surface, both of which would have been imperceptible. Had no EC profiling been undertaken, this borehole would have been classified as unconnected, when in reality a basal connection had developed.

3.4.5.2 **95/16:** This borehole drained to a depth of 23m ab 30 minutes after drilling was completed. EC profiles illustrate that the WL remained at this level for the next two weeks and that the water column consisted of Mode 1 water throughout. With these data it appears that the borehole drained to an englacial void after drilling and would therefore have been classified as passively connected. However, observations from the borehole video log suggest otherwise. First, the logs show that a significant amount of supraglacial water was pouring down the sides of the borehole walls. Second, two englacial channels were observed at 32.1 and 26.3m ab. These appeared to be active channels feeding the borehole with water.

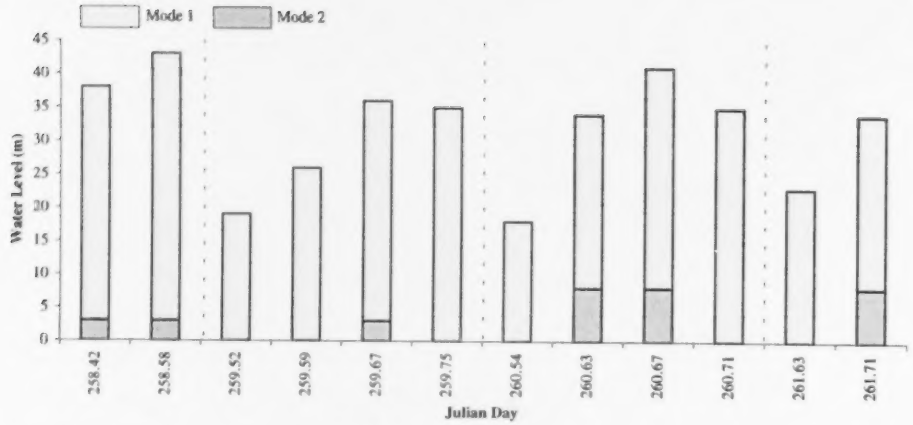


Figure 3.10: 92/14 EC profiles. Borehole depth = 48m.

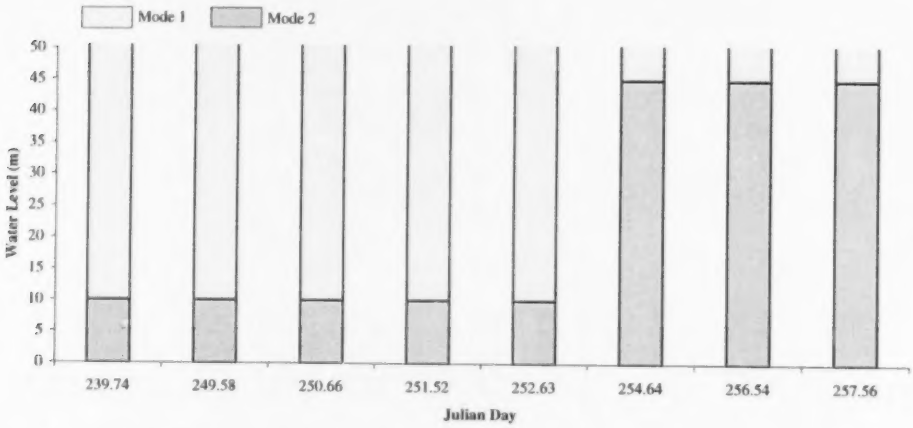


Figure 3.11: 92/5 EC profiles. Borehole depth = 50m.

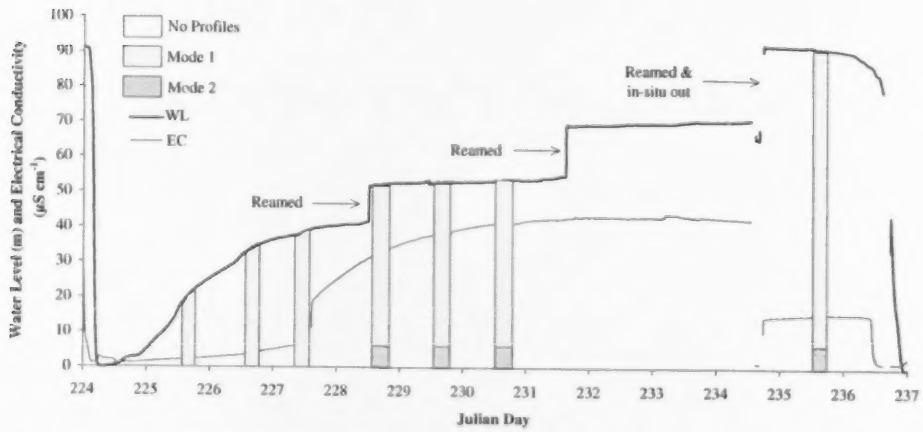


Figure 3.12: 95/17 in-situ WL and EC and EC profiles. Borehole depth = 91.5m.

Had the borehole been passively connected to an englacial void, a daily increase in WL should have occurred due to the observed inputs of supra- and englacial water. The fact that no WL increase was registered implies that there must have been an englacial or basal output. This output must have continually adjusted to the input volume such that the outputs and inputs were equal and no change in WL was recorded. This borehole was therefore not passively connected, but either englacially or actively connected. As no EC stratification existed in the water column and the video log showed that the water column was clear throughout, it is not possible to determine in which of these categories this borehole should be placed.

3.4.5.3 **95/17:** This borehole drained to the bed the day after it was drilled and then filled slowly for 5 days until reaming on JD 223 eventually re-filled it. Drainage to the bed occurred early on JD 224 flushing high EC water out of the base of the borehole (Figure 3.12). This would indicate that a connection had been made with the basal drainage system, but the borehole re-filled over the next 12 days with supraglacial water and reaming additions. EC profiles illustrate that after JD 228 the basal EC stratification remained stable whilst in-situ EC increased slowly (except on JD 227) possibly due to solute acquisition. The step in in-situ EC on JD 227 and the subsequent introduction of a 5m layer of Mode 2 water to the base of the water column suggests that a basal inflow occurred on JD 227. 95/17 filled by JD 234 and finally drained to the bed again on JD 236. This behaviour indicates sporadic basal connections due to overpressurization at the bed followed by the rapid closure of the connection after drainage.

## 3.5 DISTRIBUTION OF THE CLASSIFIED BOREHOLES:

By mapping the distribution of these categories (Figure 3.13) a clustering of actively connected boreholes is clearly highlighted (Figure 3.13b). The centre of the VPA identified in Chapter 2 is at the centre of this cluster. The WL and water quality variations measured in these boreholes are likely to be a response to channel pressure fluctuations, but some of the WL and water quality measurements may be attributed to supraglacial and englacial inputs and outputs.

Unconnected boreholes generally surround the actively connected cluster (Figure 3.13a). These represent areas of the bed that are not efficiently drained by the subglacial drainage system and that are not influenced by pressure fluctuations within the VPA. The distribution of unconnected unstratified and stratified boreholes (Figure 3.13 c and d) does not demonstrate any particular pattern. This may indicate that a) the hypothesis that the EC at the base of an unconnected borehole could be used as an indication of bed type is wrong, or b) the composition of the bed is heterogeneous at a scale small enough to be detected by the spacing of the boreholes drilled.

Five of the seven englacially connected boreholes lie within the centre of the VPA (Figure 3.13e). This appears to support the contention that the location of channels at the glacier bed is likely to correlate closely with the location of channels on the glacier surface (Sharp et al., 1993). This could explain why moulins fed by surface streams tended to be clustered along reconstructed lines of major subglacial pathways. Englacial channels are obviously needed to transmit meltwater to the bed, and are thus likely to be most common in the vicinity of both supraglacial and subglacial channelised systems.

Passively connected boreholes are located at the margins of the VPA (Figure 3.13f) and may demonstrate areas where relict crevasses or englacial channels exist.

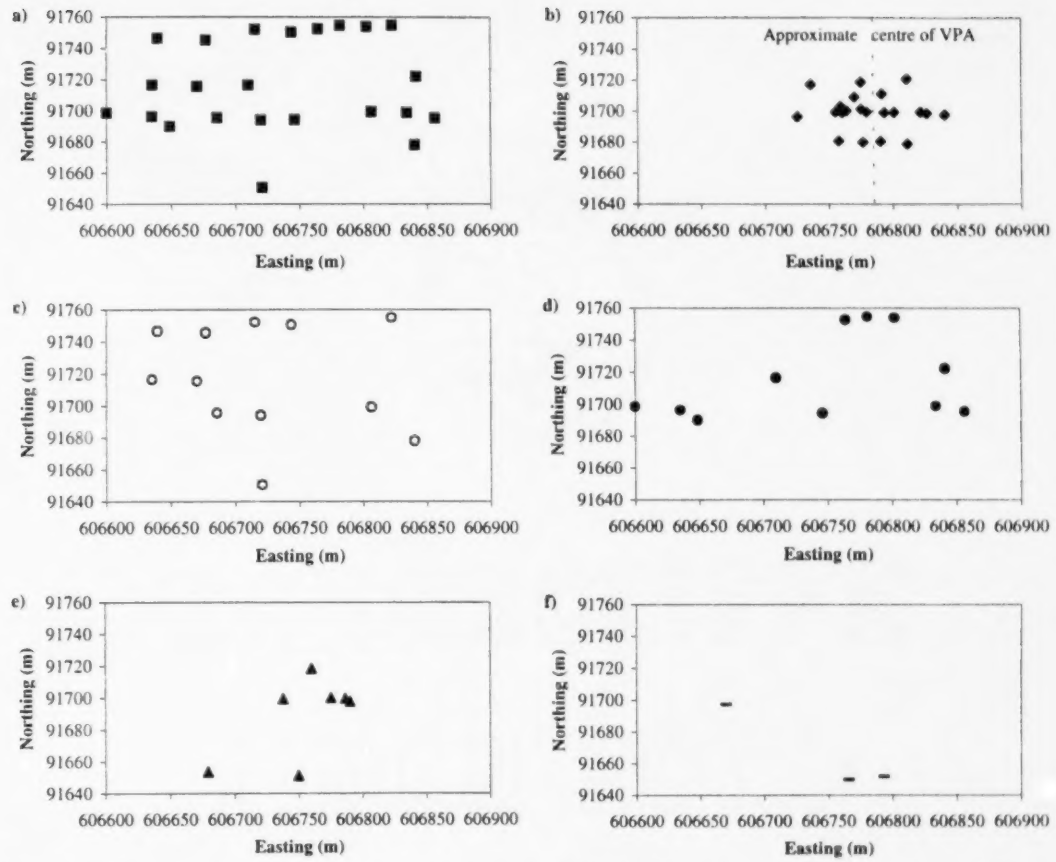


Figure 3.13: Distribution of classified boreholes; a) unconnected, b) actively connected, c) unconnected unstratified, d) unconnected stratified, e) englacially connected, and f) passively connected.

## 3.6 SUMMARY:

The need for determining the source and circulation of water within `open' boreholes prior to the interpretation of their in-situ water quality records has been demonstrated. A series of data sources has been presented which, if used in conjunction with each other, can provide a detailed interpretation of the plumbing of individual boreholes. A classification scheme of borehole plumbing has been devised which allows for the identification of boreholes that may require special attention when analysing their in-situ water quality records. If supra and/or englacial influences are dominant, in-situ water quality records may not necessarily measure the continuous characteristics of *true* basal water. Instead, the sensors may be measuring the quality of water draining from a borehole (under conditions of both rising and falling WL), and the mixing of this water with water flowing across the bed past the base of the borehole.

It is proposed that the classification and analysis of borehole water sources and circulation should be an integral part of any study of `open' borehole WL and water quality behaviour if accurate interpretations are to be made.

# CHAPTER 4: SEASONAL RE-ORGANISATION OF SUBGLACIAL DRAINAGE INFERRED FROM MEASUREMENTS IN BOREHOLES

## 4.1 INTRODUCTION:

Chapters 2 and 3 were concerned with identifying the late season subglacial drainage configuration in the borehole array from the distribution of borehole WL behaviour and with ways of using drilling records, EC profiling, salt tracing and borehole video imagery to determine the water source and patterns of water circulation within boreholes so that in-situ water quality measurements can be interpreted with confidence. This chapter will use the understanding gained from the previous chapters to describe and explain the seasonal re-organisation of the subglacial drainage system within the 1993 borehole array.

As discussed in Chapter 2, Nienow (1993) inferred that a system of major drainage channels (characterised by rapid flow velocities and low dispersivities) developed within the lower 3.3 km of the 4.0 km long glacier during the 1989-1991 melt seasons. This system appeared to develop by headward growth at a rate controlled by the retreat of the transient snowline on the glacier surface, and replaced a distributed drainage system (characterised by low flow velocities and high dispersivities) as the main means of evacuating water from the lower part of the glacier. The distributed system was the principal means of drainage throughout the year in the upper 0.7 km of the glacier, and it appeared to survive in residual form in areas between major channels in the lower glacier during the melt season (Nienow et al., in press).

In mid-August 1993 (JD 228-234), Hubbard et al. (1995) identified a variable pressure axis (VPA) characterised by diurnal water pressure variations. These were inferred to be driven by diurnal variations in discharge within a channel located at the centre of this axis. Diurnal reversals in the direction of the hydraulic gradient between the channel and surrounding areas of the bed appeared to drive water out of the channel during the afternoon and back to it overnight. The resulting flows appeared to a) selectively remove

fine material from basal sediments in the area around the channel, with the result that the hydraulic conductivity of the basal sediment layer decreased exponentially with distance from the channel, and/or b) create micro-channel links between the main subglacial channel and surrounding areas of the bed which concentrated flow at the ice-sediment interface.

In this chapter, thirty one-day time series of in-situ WL, EC and Tu are used to determine how the subglacial drainage configuration described by Hubbard et al. (1995) developed during the 1993 melt season.

## 4.2 ANALYSIS OF IN-SITU RECORDS:

As all the discussion is focused on 1993 data, borehole numbers are given the prefix `H' instead of `93'. Interpretations are based on analyses of data from 7 boreholes: H29, H34, H35, H36, H40a, H41 and H42. These were located either side of the channel that was inferred to have existed at the centre of the VPA in August 1993 by Hubbard et al. (1995) (Figure 4.1); H29 and H35 being the closest boreholes to the channel (~5m away). All of these boreholes were classified as *actively connected* in Chapter 3 (except for H35 and H42 which were classified as *englacially connected*). H41 and H34 have the most continuous in-situ WL, EC and Tu records spanning the period July 22 to August 21 (JD 203-233), and they also have good EC profiling coverage. Note that in the H34 water quality records, measurements of EC and Tu are removed when the WL is recorded as zero. Records from H35 and H29 are used interchangeably to represent near-channel conditions since WL varied synchronously at the end of the observation period in these holes (Hubbard et al., 1995). The WL record for H35 is continuous, but water quality data are not used as the base of the borehole is thought to have been blind (see further discussion below). In-situ instruments were thus measuring the quality of stagnant water at the base of H35. The WL and water quality records for H29 are patchy, but are used instead of H35 whenever possible so that water quality behaviour can be examined.

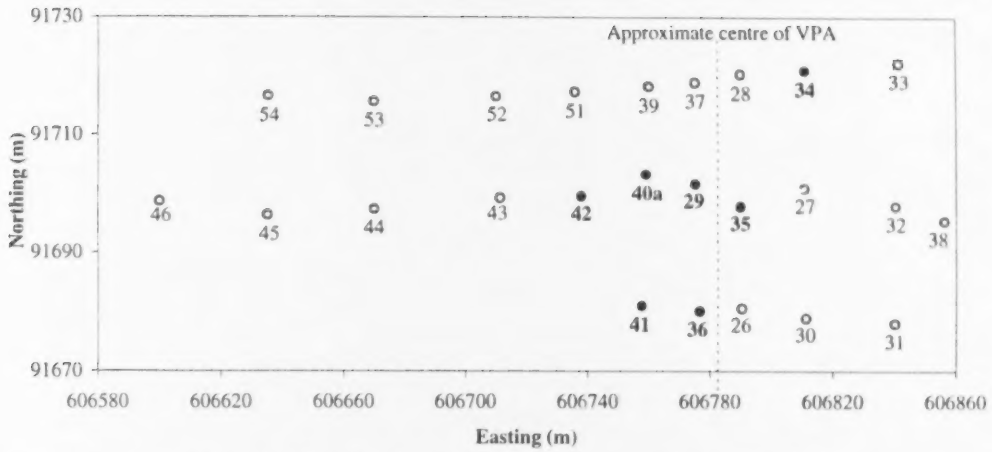


Figure 4.1: 1993 borehole array highlighting the location of the seven holes discussed in this chapter (in bold).

Only WL measurements for H36, H40a and H42 are included as insufficient profiling data are available to allow reliable interpretation of the in-situ water quality measurements. H40a WL measurements are only available from JD 203 to JD 220.

Calculations of the difference in WL between adjacent pairs of boreholes (head difference; HD) are used to infer the likely pattern of water flow at the glacier bed. A more accurate parameter for inferring the pattern of water flow at the bed is the hydraulic gradient as the direction of water flow is determined by the slope of the hydraulic potential surface. However, hydraulic gradients have not been calculated because: a) the shape and slope of all holes have not been measured by inclinometry, thus the position of the base of each borehole is uncertain, and b) the true form of the hydraulic potential surface cannot be reconstructed as there are no data available between the isolated borehole points. Although HD is not as reliable an indicator of the pattern of water flow at the bed as the hydraulic gradient as true reversals in water flow may not be seen, HD is used as a general indicator of the pattern of water flow at the bed in this chapter. Following discussions in Chapter 3, measurements of in-situ EC and Tu are used as indicators of the provenance of water and the flow of water at the base of boreholes, respectively. Meteorological and discharge data from JD 198 to JD 233 (Figure 4.2) are included for discussion purposes. These were measured at the upper meteorological station and the GDSA intake, respectively (Figure 1.1).

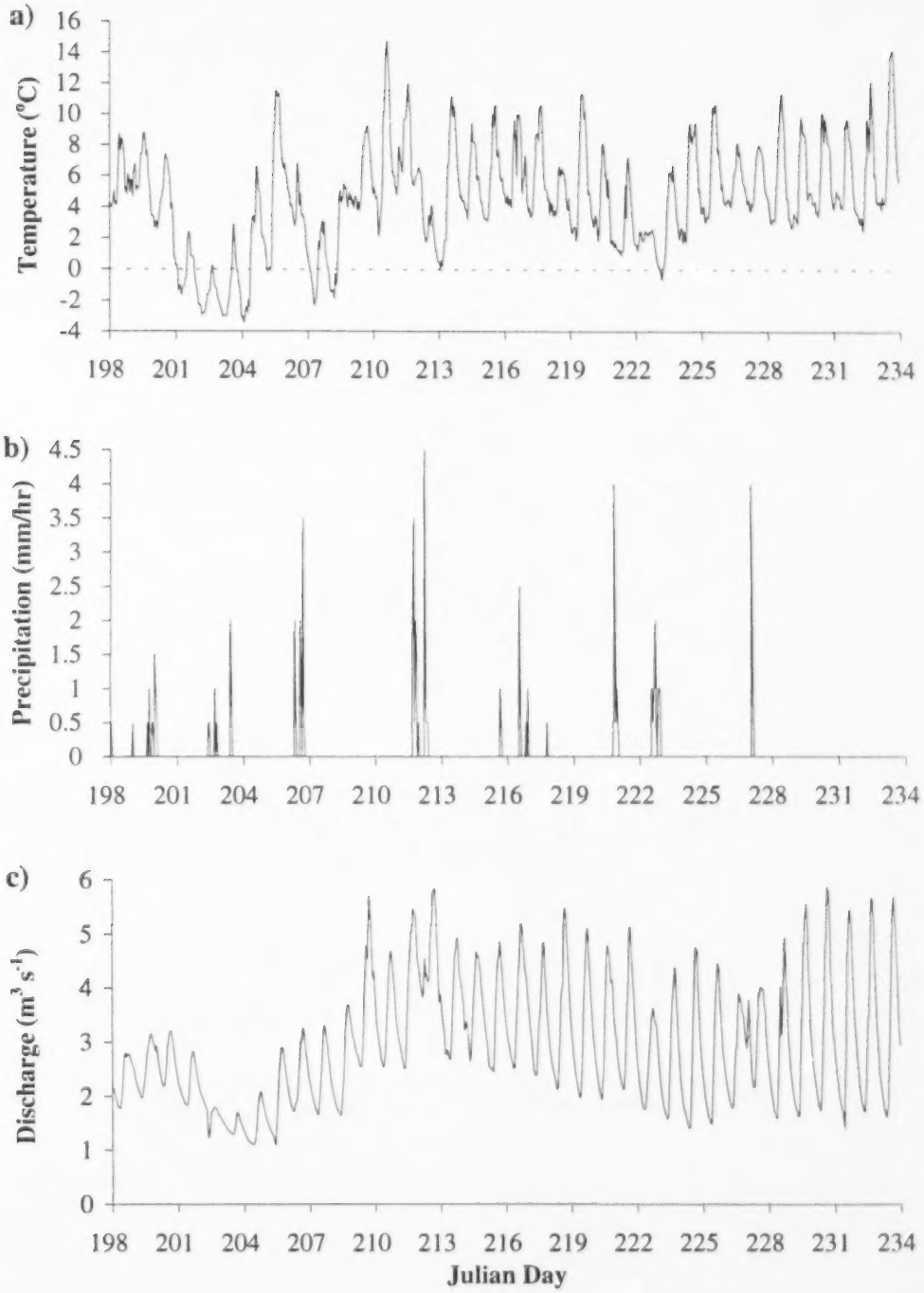


Figure 4.2: 1993 a) temperature, b) precipitation, and c) discharge from JD 198 to JD 233. See text for data sources.

In-situ records of WL, HD and water quality display significant changes over the study period. These changes involve:

a) the daily minimum or background levels of the data series (Figures 4.3-4.7);

b) the frequency and amplitude of fluctuations in the data series (Figure 4.8); and

c) the relative timing of fluctuations in the data series in different boreholes (Figure 4.9).

On the basis of identification of intervals of especially marked or rapid change in one or more data series, the measurement period was split into five sub-periods (JD 203-208; 209-214; 215-219; 220-224; 225-233), which were used as a framework for interpreting the evolution of the subglacial drainage system. In making this subdivision, particular emphasis was placed on records of WL and HD, since these parameters probably drive changes in basal water quality behaviour. Having established the subdivision, cross-correlation methods were used to quantify changes between sub-periods in (a) the degree of correlation, and (b) lead-lag relationships between different data series. Prior to analysis, the data series were detrended by calculating a 25 point running mean, subtracting this from the raw data, dividing the data into the relevant periods and then re-expressing them as standardised residuals from the running mean of each period. Analyses were performed using the statistical package *SPSS for Windows 6.1*. Maximum cross-correlation coefficients and associated lags were used to express the degree of coherence between different data series (Tables 4.1 and 4.2).

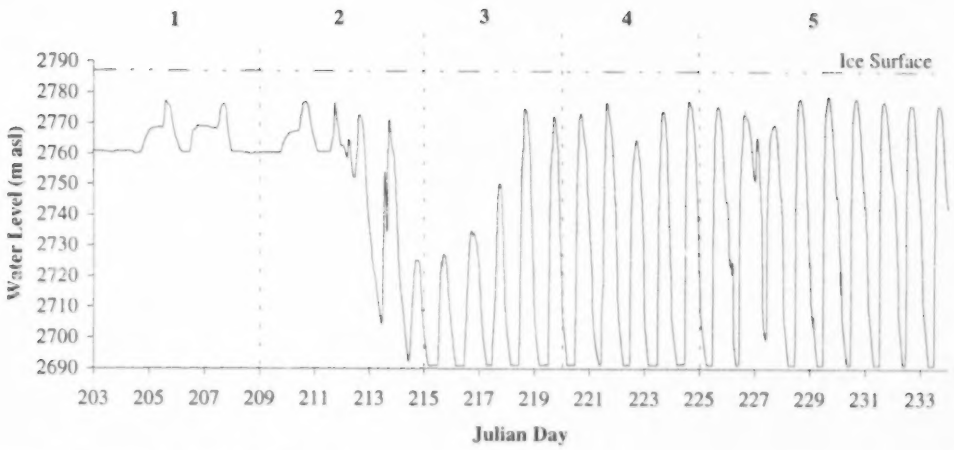


Figure 4.3: H35 WL from JD 203 to JD 233.

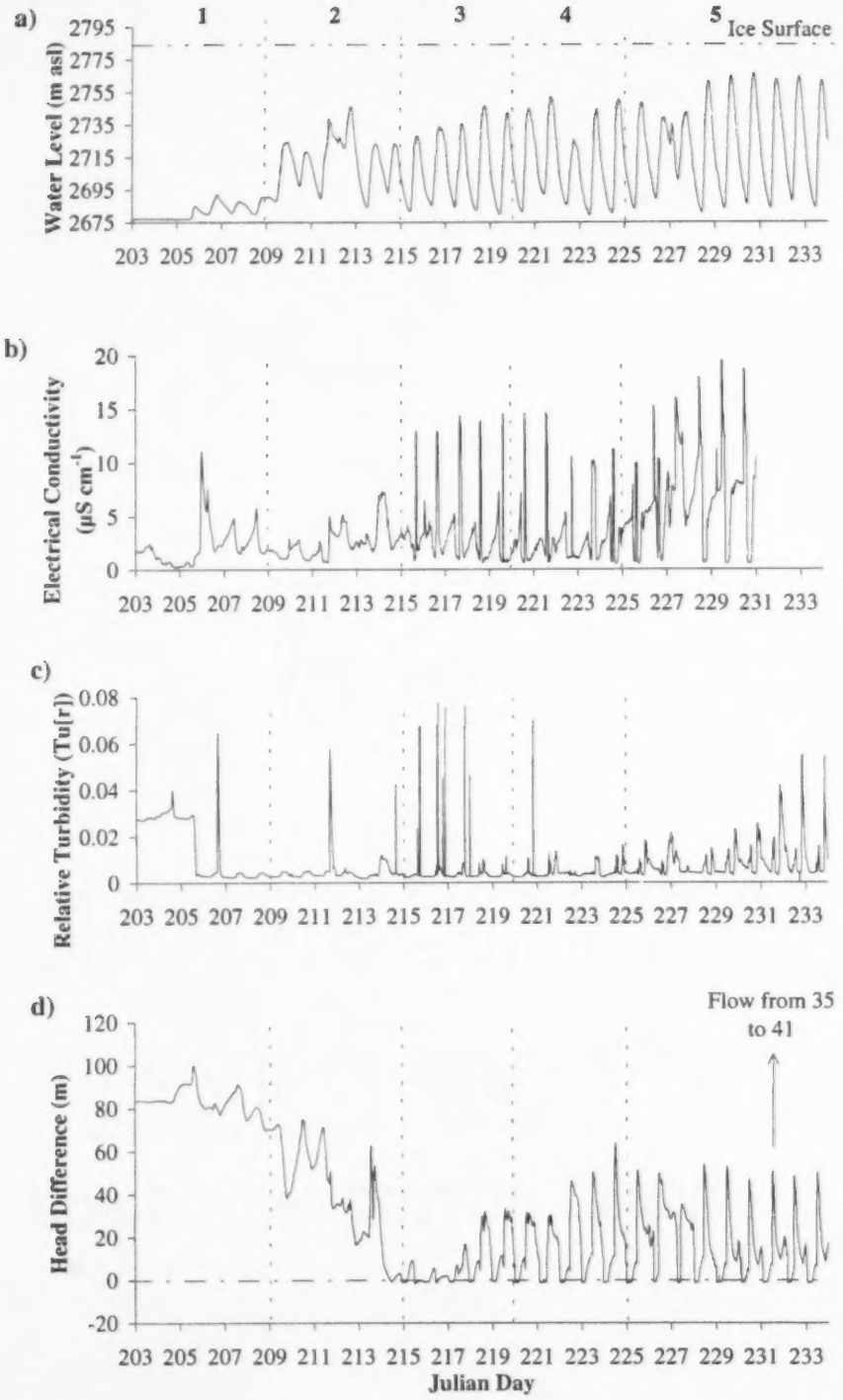


Figure 4.4: H41 measurements from JD 203 to JD 233; a) WL, b) in-situ EC, c) in-situ Tu, and d) H35-H41 HD.

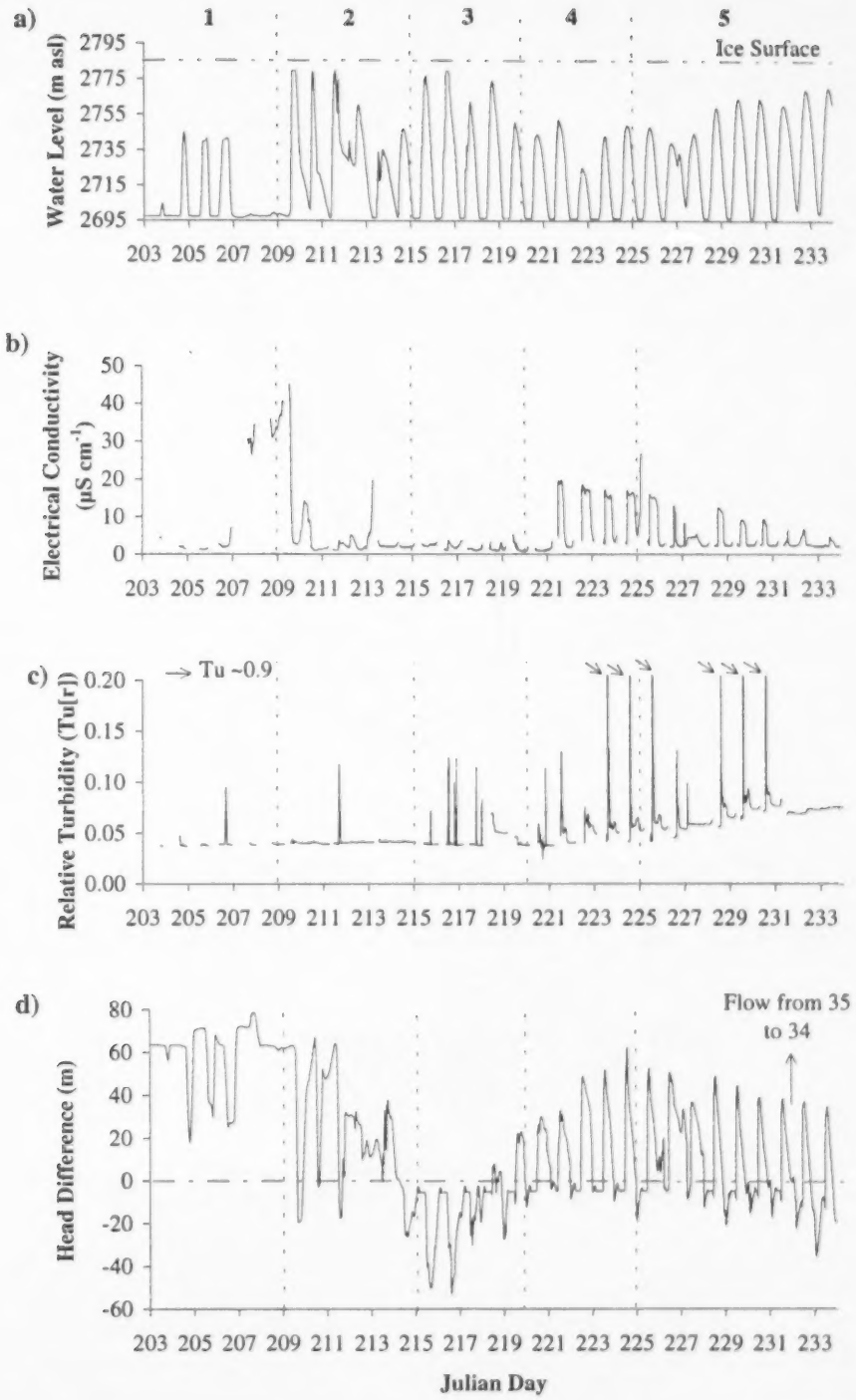


Figure 4.5: H34 measurements from JD 203 to JD 233; a) WL, b) in-situ EC, c) in-situ Tu, and d) H35-H34 HD. Note: EC and Tu values have been removed for dry WL readings.

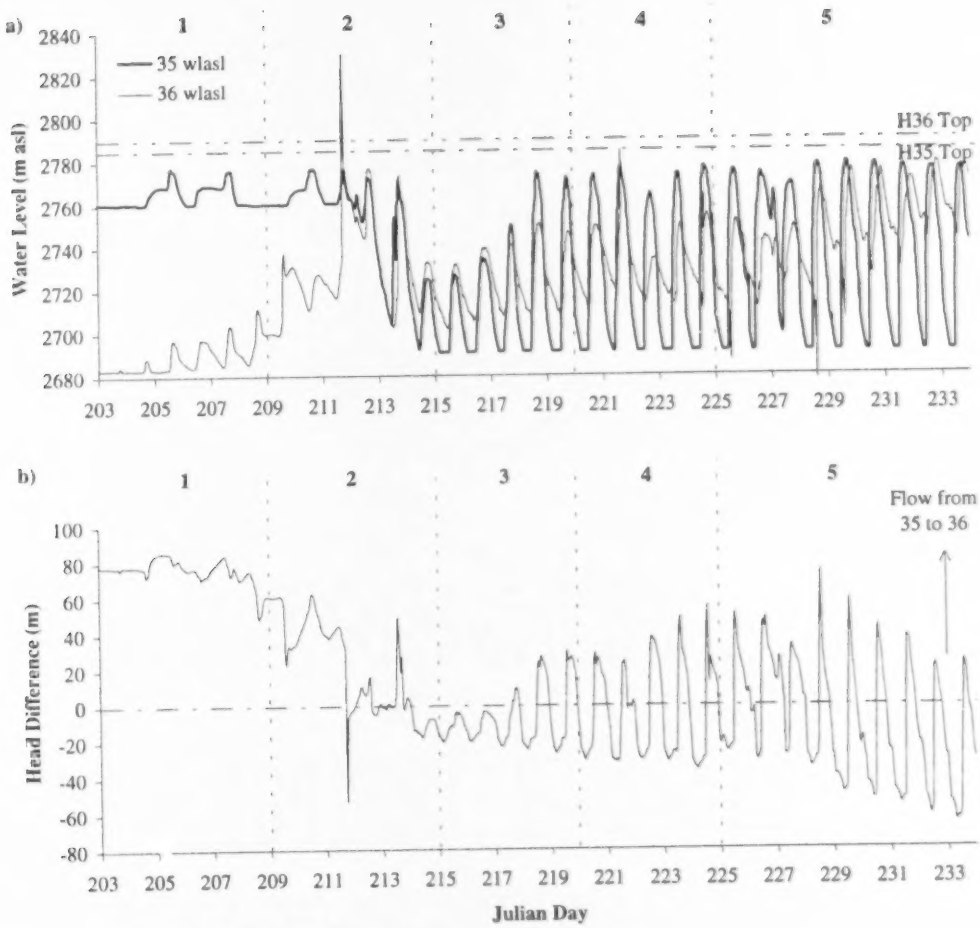


Figure 4.6: a) H35 and H36 WL and b) H35-H36 HD from JD 203 to JD 233.

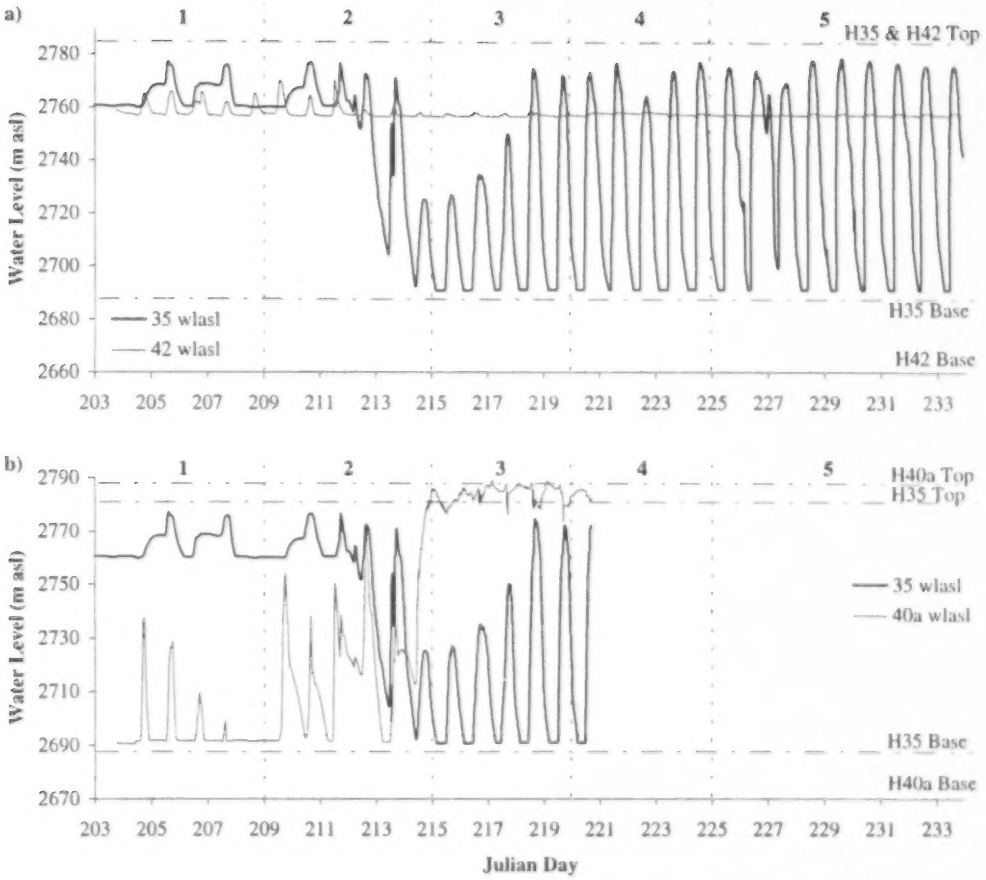


Figure 4.7: a) H35 and H42 WL from JD 203 to JD 233 and b) H35 and H40a WL from JD 203 to JD 220.

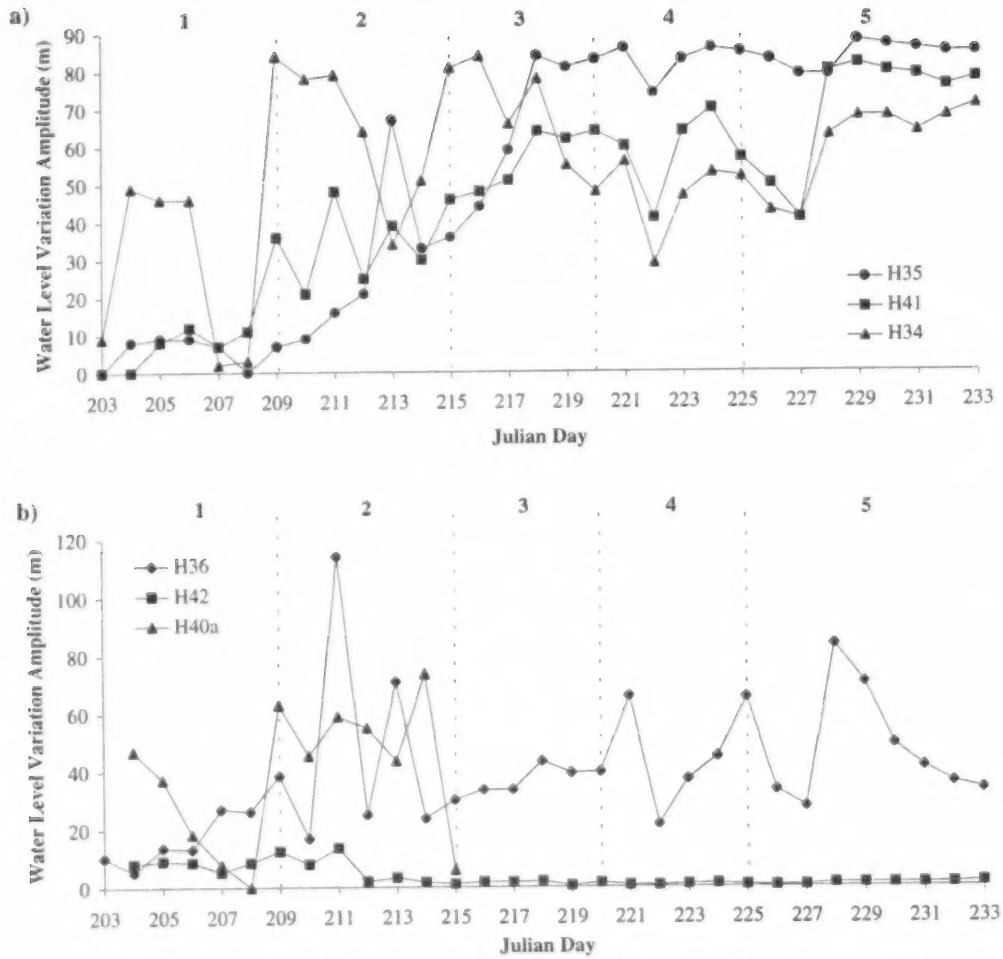


Figure 4.8: Water level variation amplitudes in a) H35, H41 and H34 and b) H36, H42 and H40a from JD 203 to JD 233.

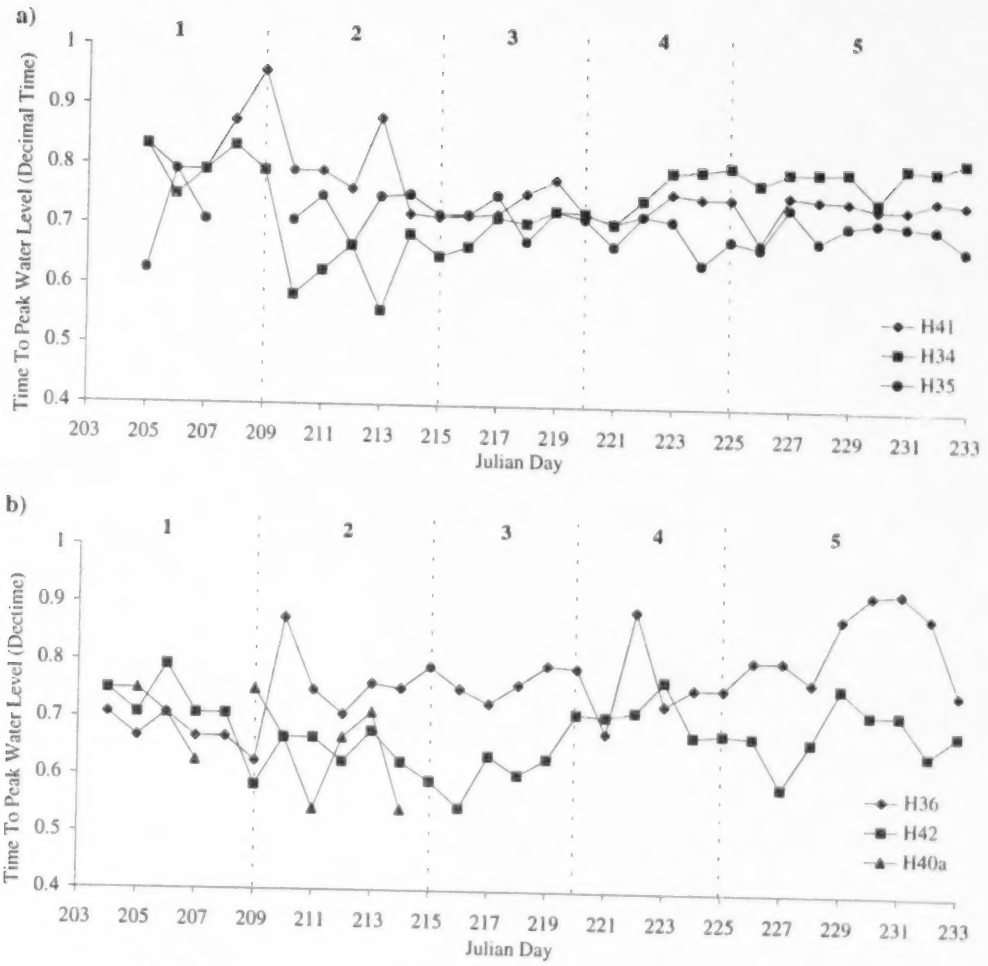


Figure 4.9: Time (in decimal fractions of a day) at which daily peak WL was reached in a) H35, H41 and H34, and b) H36, H42 and H40a from JD 203 to JD 233.

| | 1 | 2 | 3 | 4 | 5 |
|---|---|---|---|---|---|
| **H35/H41** | .64 (4) | .77 (1) | .97 (0) | .97 (1) | .97 (1) |
| **H35/H34** | .47 (-1) | .52 (-1) | .89 (0) | .95 (1) | .96 (2) |
| **H35/H36** | .66 (-1) | .70 (0) | .96 (0) | .89 (1) | .89 (1) |
| **H41/H34** | .60 (-4) | .79 (-2) | .95 (-1) | .97 (0) | .97 (1) |
| **H41/H36** | .86 (-4) | .80 (-1) | .99 (0) | .93 (0) | .90 (1) |
| **H34/H36** | .44 (-1) | .55 (3) | .94 (0) | .92 (0) | .86 (1) |
| **H36/H42** | .82 (0) | .55 (-5) | .75 (-3) | .66 (0) | .73 (-2) |
| **H35/H42** | .59 (-1) | .21 (-5) | .67 (-3) | .59 (2) | .73 (1) |
| **H41/H42** | .74 (-4) | .57 (-6) | .72 (-3) | .61 (1) | .80 (-1) |
| **H34/H42** | .71 (-1) | .65 (-3) | .80 (-3) | .56 (0) | .68 (-2) |
| **H35/H40a** | .36 (-2) | .62 (-1) | -.58 (-1) | - | - |
| **H41/H40a** | .40 (-4) | .85 (-3) | -.55 (-2) | - | - |
| **H34/H40a** | .79 (-2) | .84 (0) | -.60 (-2) | - | - |
| **H36/H40a** | .44 (0) | .62 (-2) | .57 (-16) | - | - |
| **H42/H40a** | .72 (-1) | .55 (3) | .47 (12) | - | - |

Table 4.1: Maximum cross-correlation coefficients and associated lags (hours) for pairs of borehole WL records for each of the five sub-periods of the 1993 melt season. See text for definition of sub-periods. Positive lags indicate that the first data series leads the second.

| PERIOD | T/H35 | T/H41 | T/H34 | T/H36 | T/H40a | T/H42 |
|---|---|---|---|---|---|---|
| 1 | .41 (-1) | .60 (6) | .58 (2) | .63 (1) | .61 (0) | .73 (1) |
| 2 | .65 (5) | .81 (6) | .72 (3) | .61 (1) | -.72 (-9) | .55 (-1) |
| 3 | .83 (3) | .91 (4) | .90 (3) | .88 (4) | -.63 (1) | -.64 (-13) |
| 4 | .90 (3) | .90 (4) | .91 (4) | .82 (4) | - | -.47 (-6) |
| 5 | .91 (3) | .93 (4) | .94 (5) | .82 (5) | - | .64 (2) |

Table 4.2: Maximum cross-correlation coefficients and associated lags (hours) for pairs of temperature and borehole WL records for each of the five sub-periods of the 1993 melt season. See text for definition of sub-periods. Positive lags indicate that temperature leads the WL it is correlated with.

Forcing-response plots (F-R plots) are used to analyse relationships and phase lags between pairs of borehole WL records by showing how WL variations in one borehole affects WL variations in an other (e.g. Murray and Clarke, 1995). Hourly WL measurements from pairs of holes were taken, one was designated as a forcing record and one as a response record. F-R plots were constructed for Period 1 (on JD 206; Figure 4.10) and Period 5 (on JD 229, except H40a on JD 218; Figure 4.11) to compare the different WL responses at the beginning and end of the summer observation season.

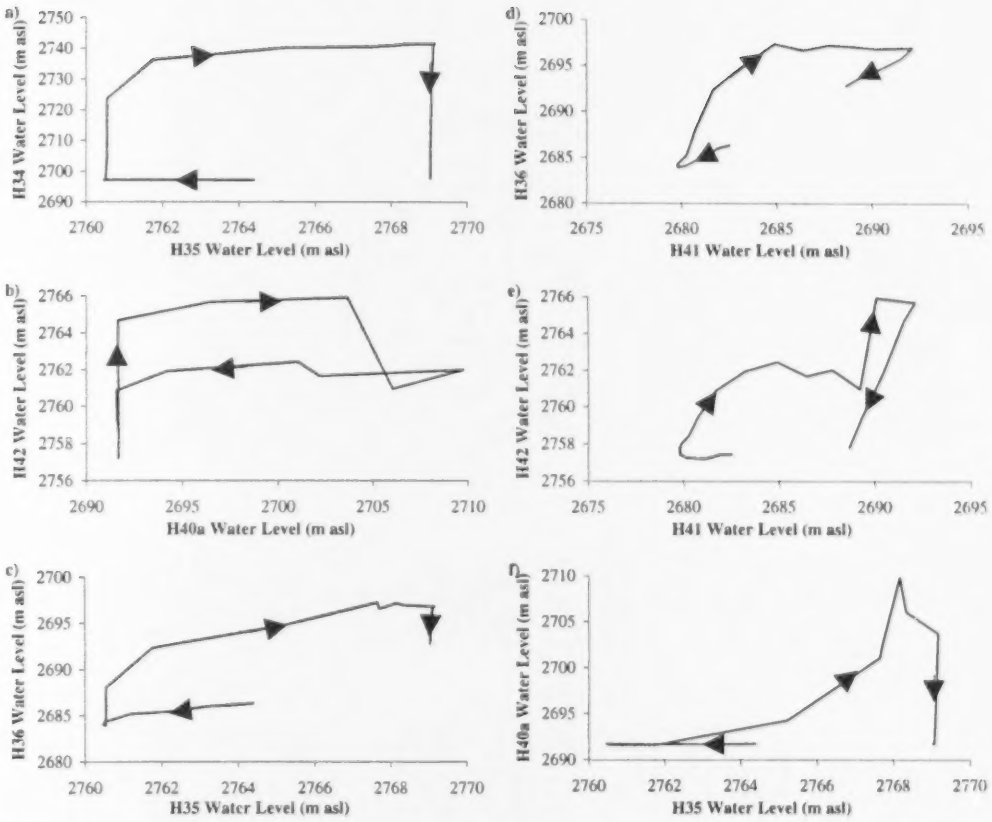


Figure 4.10: F-R plots for JD 206 in Period 1; a)H34 with H35, b) H42 with H40a, c) H36 with H35, d) H36 with H41, e) H42 with H41, and f) H40a with H34.

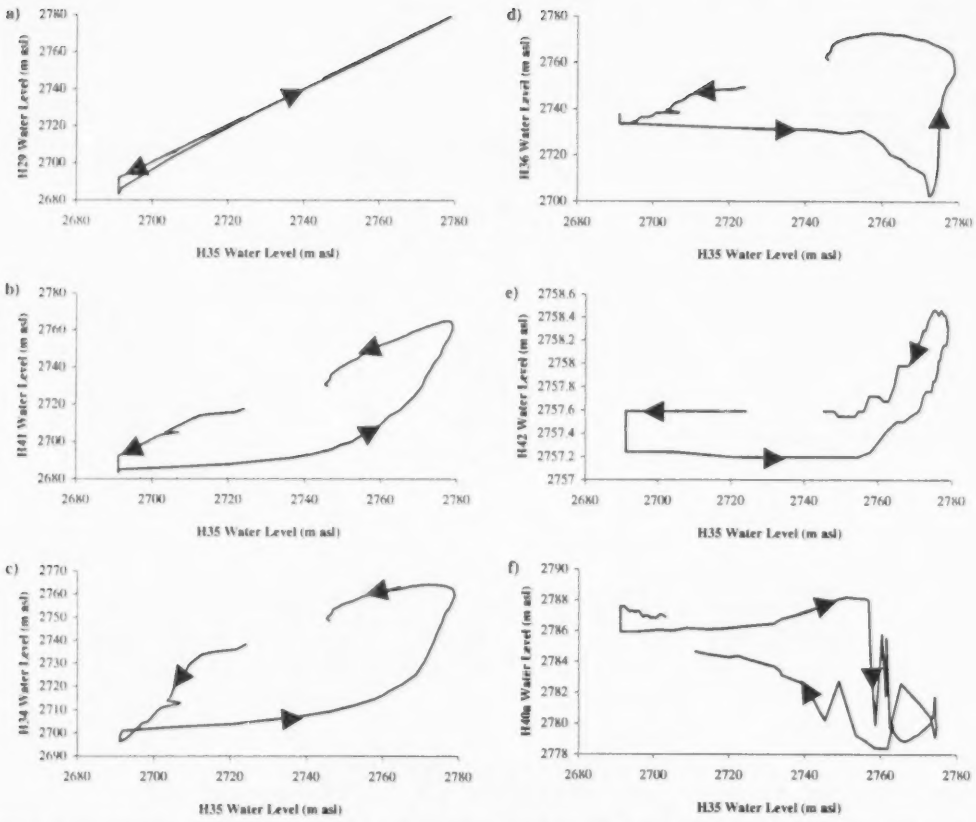


Figure 4.11: F-R plots on JD 229 in Period 5; a) H29 with H35, b) H41 with H35, c) H34 with H35, d) H36 with H35, e) H42 with H35, and f) H40a with H35 (on JD 218).

## 4.3 WATER LEVEL AND HEAD DIFFERENCE RECORDS:

As outlined above, the WL and HD records were sub-divided into 5 periods. The main features of the records in each period are described below.

***Period 1: JD 203-JD 208 (22-27 July):***

All the boreholes considered appear to have connected to the glacier's drainage system. This is indicated by a fall in WL during or after the end of drilling and by subsequent WL fluctuations. However, there is little evidence for coherent WL fluctuations (Table 4.1), and diurnal WL cycles were weakly developed and of low amplitude (Figure 4.8). H35 WL showed a two-day cycle (Figure 4.3). The time at which daily peak WL was reached by each borehole was inconsistent (Figure 4.9). HD records suggest basal water flow was always directed away from H35 towards H41, H34 and H36 (Figures 4.4d, 4.5d and 4.6b). WL behaviour was not strongly correlated with temperature (Table 4.2).

F-R plots for JD 206 (Figure 4.10) show that there was a clear phase lag between the pairs of WL records demonstrated by the hysteresis loop. The rectangular shape of the H42/H40a, H34/H35 and H36/H35 plots suggest that WLs in these holes were fluctuating independently rather than in response to some common forcing. For example, in the H34/H35 F-R plot (Figure 4.10a) the WL in one hole rose or fell while the WL in the other hole remained relatively constant. The positive slopes of Figures 4.10d,e and f may demonstrate that the WLs in these borehole pairings were slightly more dependent.

This period is characterised by incoherent WL behaviour in which WL fluctuations appear to have varied independently of each other.

***Period 2: JD 209-JD 214 (July 28- August 2):***

The main event in this period was a 70m fall in the base WL of H35 between JD 212 and JD 214 (Figure 4.3). During this event, the base WL in H35 dropped in three stages to successively lower base levels of 2750m, 2705m and 2690m.a.s.l. These successive base levels were separated by clear diurnal WL peaks. The event itself followed three days (JD 209-211) of generally increasing temperatures (Figure 4.2a) and thus surface melt, which resulted in increased background WLs in H41, H34 and H36 (Figures 4.4a, 4.5a and 4.6a) (indicating that the bed was being surcharged) and extremely high diurnal WL peaks in H34 and H40a (Figures 4.5a and 4.7b). This period culminated in a heavy rainfall event, during which 14mm of rain was recorded between JD 211.71 and JD 212.25 (Figure 4.2b). Water inputs from this rainstorm prevented WLs in H41, H34, H36 and H40a from falling to their normal base levels between JD 211 and JD 212, so these holes recorded a sustained period of high water pressures. This high pressure event seems to have been the trigger for the connection of H35 to the subglacial drainage system.

Following this connection event, a diurnal WL cycle gradually developed in H35 and more distinct diurnal WL cycles were apparent in H41, H34 and H36. The diurnal WL peak was reached first by H34, followed by H35, H41 and H36 (except on JD 214) (Figure 4.9). Peak cross-correlation coefficients (CCCs) between pairs of WL records were generally higher than in Period 1 (Table 4.1). Amplitudes of diurnal WL cycles were greater than in Period 1 (20-50m in H41, 30-80m in H34 and H35, 30-70m in H36; Figure 4.8). There was a dramatic reduction in HD between H35 and H41, H35 and H34, and H35 and H36 and there were short-lived reversals in the direction of HD between H35 and H34 and H35 and H36 (Figures 4.4d, 4.5d and 4.6b). WLs were more significantly correlated with temperature than in Period 1 (except H42) and temperature generally led the WLs (except H40a and H42) (Table 4.2).

WL behaviour in H42 and H40a after the connection event was different to that seen in H35, H41, H34 and H36. WL fluctuation amplitudes in H42 fell from between 2-13m to <2m (Figure 4.8b). In contrast, H40a appeared to disconnect on JD 214 as the hole filled almost to the surface (Figure 4.7b).

Period 2 was dominated by changes in the WL behaviour of all the boreholes observed. This appears to have been induced by meteorological conditions between JD 209 and JD 212. The changes in borehole WL behaviour suggest that a significant change in the configuration of the subglacial drainage system occurred during this period.

***Period 3: JD 215-JD 219 (August 3-7):***

Diurnal WL cycles increased in amplitude in H35, H41, H34 and H36 (Figure 4.8), and peak CCCs between WL records increased (except for H40a; Table 4.1). The order in which peak diurnal WL was reached changed over the period (Figure 4.9) with H35 leading H41, H34 and H36. By the end of the period, there were clear diurnal HD cycles between H35 and H41, H35 and H34, and H35 and H36 (Figures 4.4d, 4.5d and 4.6b). CCCs between temperature and WL continued to strengthen with temperature leading WLs by 3 to 4 hours (except H40a and H42) (Table 4.2).

WL behaviour in H42 and H40a continued to contrast with that observed in H35, H41, H34 and H36. WL fluctuations in H42 continued to be barely perceptible throughout this period (Figures 4.7a and 4.8b). H40a WL remained close to the surface and diurnal WL fluctuations were small (Figure 4.7c), but they were inversely correlated with WL fluctuations in H35, H41, H34 and H36 (Table 4.1). This negative correlation is also shown by the H40a/H35 F-R plot (Figure 4.11f).

Period 3 may be viewed as a period during which the subglacial drainage system re-adjusted to the events of Period 2. High and coherent WL fluctuations in H35, H41, H34 and H36 suggest that the WLs in these boreholes had started to be driven by a common

forcing. However, the WL behaviour exhibited by H40a and H42 does not conform with this interpretation and demonstrates that either the common forcing mechanism did not have the same effect on all the boreholes or that more than one forcing mechanism existed.

***Period 4: JD 220-JD 224 (August 8-12):***

Period 4 appears to have been one of stability as diurnal WL cycles displayed a relatively stable amplitude and time of peak WL in all the observed holes (except on JD 222 when sub-zero temperatures were measured; Figure 4.2a) (Figures 4.8 and 4.9). H35 registered the highest WL fluctuation amplitudes and was the fastest to reach peak WL of all the boreholes. WL cycles were very coherent between all the borehole pairings with lags between 0 and 1 hours (except for H35/H42) and CCCs remained high (except for CCCs with H42) (Table 4.1). Strong diurnal cycles in HD between H35 and H41, H35 and H34, and H35 and H36 occurred (Figure 4.4d, 4.5d and 4.6b).

***Period 5: JD 225-JD 233 (August 13-21):***

WL and HD behaviour in this period was very similar to that in Period 4 with a few exceptions. First, the base WL in H36 increased significantly over this period from ~30 to ~70m ab (Figure 4.6a). In addition, rapid drainage events in H36 started to occur on JD 224 and continued through this period, and a semi-diurnal WL signal emerged on JD 229. Second, H35-H41 and H35-H34 HD records show a clear semi-diurnal component (Figures 4.4d and 4.5d). CCCs between temperature and WL were the highest of all the periods with temperature leading WL by 2 to 5 hours (Table 4.2).

In general, CCCs for the WL records were the highest for all the periods, but no lags of zero hours were recorded as in Period 4 (Table 4.1). F-R plots for JD 229 (Figure 4.11a-e) demonstrate a variety of relationships between pairs of WL records. The H29/H35 plot (Figure 4.11a) shows no significant phase lag and demonstrates that the records are very

similar. This observation supports that by Hubbard et al. (1995) that H35 and H29 WL records are almost identical. Murray and Clarke (1995) observed the same pattern between two connected boreholes with synchronous WL behaviours (their Figure 6a). As Hubbard et al. (1995) demonstrated that WL variations in H29 and H35 represented near-channel water pressure variations, H35 was used as the forcing record for the F-R plots in this period. Plots of H41/H35 and H34/H35 (Figures 4.11b and c) show a phase lag and a positive slope. This suggests that WL variations were a response to a common forcing with differential lags. The hysteresis loop in the H34/H35 plot is more open than that in the H41/H35 plot as it took longer for H34 WL to respond to the forcing of the H35 WL. This is also exemplified by the CCC lags which are greater for H35/H34 than H35/H41 (Table 4.1). Finally, the H36/H35 and H42/H35 plots (Figures 4.11c and d) show a different response to H35 WL forcing. In both F-R plots, the WL in H36 and H42 did not respond to rising WL in H35 until a critical WL in H35 was reached, upon which H36 WL fell and then rose whilst H42 WL rose. The WL in both holes subsequently fell after H35 WL started to fall. This behaviour suggests the WL in H36 and H42 was forced by the H35 WL, but that a threshold WL in H35 was required before the WL in H36 and H42 responded. F-R plots for Period 5 are clearly different to those for Period 1 as the WL records for Period 5 are all shown to be driven by a common forcing despite lags between the forcing and the response.

***Summary***

There were marked changes in WL and HD behaviour over the 31 day observation period. This suggests that evolution of the subglacial drainage system within the borehole array occurred over the period. Before the WL behaviours changed in Period 2, WL fluctuations in each of the boreholes were inconsistent and varied independently. The event in Period 2 which caused the WL behaviours to change likely represented a re-organisation of the subglacial drainage system configuration. This re-organisation did not have the same effect on all the boreholes. In H35, H41, H34 and H36 WL fluctuations became larger, developed a clearer diurnal rhythm and were more coherent between the

boreholes. This suggests that the WL fluctuations were driven by a common forcing, which by Period 5, was likely to have been diurnal pressure variations in a channel located close to H35 (Hubbard et al., 1995). WL in H36 deviated from this pattern in Period 5 as base WL increased and sudden drainage events started to occur which appear to have been associated with the attainment of a threshold WL in H35. Following the dramatic fall in the base WL in H35 during Period 2, HD records developed a clear diurnal rhythm, with diurnal reversals in the direction of the HD (and presumably water flow) between H35 and H34, and H35 and H36 and changes in HD magnitude between H35 and H41, H35 and H34, and H35 and H36. Towards the end of the observation period, H35-H41 and H35-H34 HD records developed a semi-diurnal component of variation. A systematic sequence of diurnal WL peaking developed in Period 3 and generally persisted unchanged through Periods 4 and 5. Hubbard et al. (1995) suggest that this sequence is consistent with the propagation of a diurnal pressure wave away from the inferred location of a channel at the centre of the VPA.

However, WL behaviour in H40a and H42 after Period 2 did not conform to that observed in H35, H41, H34 and H36. WL behaviour in H40a was inversely correlated with that in the other holes and WL fluctuation amplitudes in H42 became almost imperceptible. It is therefore suggested that either the common mechanism that forced the WL behaviour in H35, H41, H34 and H36 did not affect all the borehole WLs in the same manner, or that more than one forcing mechanism existed.

## 4.4 IN-SITU WATER QUALITY RECORDS

Close inspection of EC and Tu records from H41 and H34 (Figures 4.4b,c and 4.5b,c) shows that, while the records from the two boreholes are quite different, both sets of records showed major changes which can be associated with the changes in WL and HD records discussed above. The nature of these changes is described in qualitative terms below, but discussion of their significance is deferred until later.

The in-situ EC record from H41 (Figure 4.4b) displayed relatively strong diurnal cycles in Periods 1 and 2 and these were replaced by a semi-diurnal cycle in Period 3. During this period the daily EC cycle showed a double peak, with an initial, smaller and more attenuated peak of ~5μS $cm^{-1}$ being followed by a larger, sharper peak of 10-15μS $cm^{-1}$. During Period 4, the semi-diurnal cycle weakened and the diurnal cycle became stronger as the two peaks merged. In Period 5, the EC record showed a long, attenuated shoulder at ~10μS $cm^{-1}$ followed by a sharp rise to ~15μS $cm^{-1}$ and then by a fall to <1μS $cm^{-1}$. Both the daily peak EC and the EC values of the attenuated shoulder rose progressively during Period 5. The in-situ Tu record from H41 (Figure 4.4c) showed a diurnal cycle that strengthened from Period 1 to 2 and weakened in Period 3, when an erratic Tu signal was superimposed on the daily cycle. A strong daily cycle re-emerged in Period 4, and was accompanied by a significant semi-diurnal cycle in Period 5, when the record clearly had a double-peaked character.

The in-situ EC record for H34 (Figure 4.5b) in Periods 1, 2 and 3 exhibited diurnal cycles which were relatively weak compared with those seen in Periods 4 and 5. The diurnal cycle was especially strong in Period 4, when EC rose to ~20μS $cm^{-1}$ for several hours each day. In Period 5, a small semi-diurnal cycle developed which manifested itself as a small EC peak preceding the main daily peak. Throughout Periods 4 and 5, the peak daily EC decreased from ~20 to ~5μS $cm^{-1}$, behaviour directly opposite to that observed in H41 over the same period. The H34 in-situ Tu record (Figure 4.5c) is quite complex. It showed little variation during Periods 1 and 2, except for clear peaks on JD 206 and

JD 211. Diurnal and semi-diurnal cycles were clearly developed in Period 3, but the record from Periods 4 and 5 is complicated by the superimposition of large peaks on what appear to be diurnal cycles. The occurrence of these peaks was clearly associated with a long-term rise in background Tu values.

Although Tu fluctuations were generally small during Period 2, Tu spikes were recorded in both H41 and H34 during the rainstorm late on JD 211 (Figures 4.4c and 4.5c). They record disturbance of subglacial sediments during the rainstorm. Whilst it is impossible to tell whether the disturbance resulted from increased rates of subglacial water flow, or from enhanced basal glacier motion, it seems likely that it helped to re-organise the subglacial drainage system in such a way that H35 became connected to it.

## 4.5 BOREHOLE ELECTRICAL CONDUCTIVITY PROFILING

In this section, the results of borehole EC profiling are linked to WL and HD records, in an attempt to explain the in-situ EC and Tu records from H34 and H41 in terms of patterns of water circulation within and between the boreholes.

### *Periods 1 and 2*

WLs during Period 1 and the early part of Period 2 seem to have been driven largely by englacial and supraglacial water inputs to the boreholes.

Prior to the marked drop between JD 212 and JD 214, WL in H35 varied with a two-day cycle. WL increased from a base level of 74m ab by 8m on the first day of each cycle, and by a further 9m on the second, before falling rapidly back to 74m ab (Figure 4.3). EC profiling data collected on JD 210 (Figure 4.12) show a 50m thick plug of water with EC $>2\mu S\ cm^{-1}$ at the base of the borehole, the thickness of which remained unchanged as WL varied. The WL changes were accommodated by variations in the thickness of a cap layer in which EC was $<2\mu S\ cm^{-1}$.

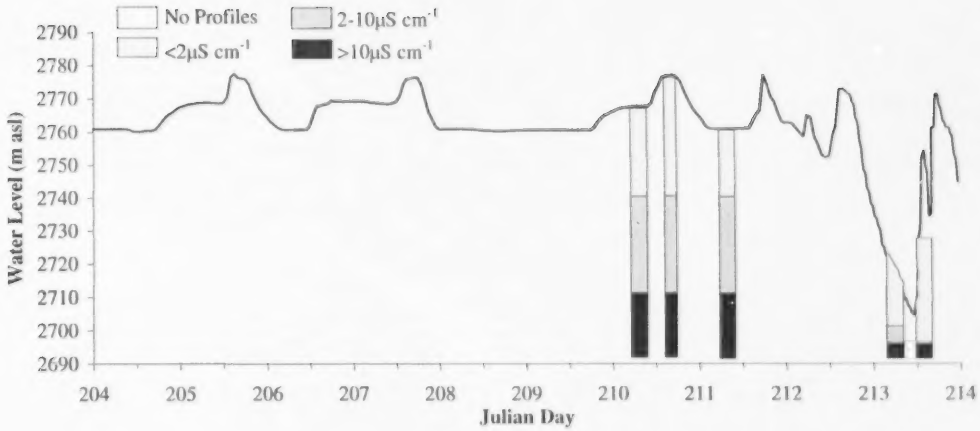


Figure 4.12: H35 WL and EC profiles from JD 204 to JD 214.

This layer was presumably fed by supraglacial inflow, and drained by episodic outflow through an englacial channel located 74m ab. It is suggested that when the WL in H35 reached a threshold level of 91m ab, a siphon was initiated in the englacial channel which drew water out of H35. When H35 drained to the level of the englacial channel, this siphon was switched off, allowing the WL to rise from supraglacial inputs until the siphon was re-initiated when the WL reached 91m ab. Such a process has also been described by Hooke et al. (1985).

EC profiling data suggest that the connection of H35 to the subglacial drainage system occurred via an englacial channel located close to the bed. Profiles measured at 09:59 and 12:27 on JD 213 (Figure 4.12) showed a 5m thick layer of water with EC of 20μS $cm^{-1}$ at the base of the borehole. At 09:59, this layer was overlain by 5m of 10μS $cm^{-1}$ water and 10m of 2μS $cm^{-1}$ water. By 12:27, the cap consisted of 30m of 1μS $cm^{-1}$ water, suggesting that the borehole WL had risen because of supraglacial/englacial inputs. These inputs seem to have forced the water of intervening EC out of the borehole walls, leaving the high EC layer undisturbed at the base of the hole. This implies that drainage of H35 occurred via an englacial connection located 5-10m above the glacier bed. By JD 215 the WL record appears to demonstrate that H35 was draining completely overnight (due to the stable `flat-line' readings; Figure 4.3), indicating that a basal connection to the subglacial drainage system had developed. However, upon closer inspection of the WL data, the apparent dry or `flat-line' WL signal is actually a value of 5m of water head. In addition, the H35 in-situ EC record demonstrates that EC increased steadily over the summer observation period. It is therefore concluded that the in-situ sensor was located at the bottom of a blind hole and that water was entering and exiting the hole from the inferred englacial connection located ~5m ab. The base WL in H35 was thus fixed by the height of this englacial channel.

EC profiles for H41 and H34 show that the water columns comprised entirely water with EC <1μS $cm^{-1}$. WL variations were accommodated entirely by waters with this characteristic, and were presumably driven by supraglacial/englacial inputs. Minimum

WLs recorded in both holes were at or just above the glacier bed, however, indicating that drainage occurred from the base of the boreholes. In-situ EC and Tu records from both boreholes did show changes which indicate drainage past the base of the boreholes (Figures 4.4b,c and 4.5b,c), but waters with basal characteristics did not rise into the boreholes. In H41, there were weak diurnal cycles in in-situ EC, which were inversely correlated with WL variations. This suggests that high EC basal water flowed past the base of the borehole along the bed, but that it was diluted by supraglacially/englacially-derived waters draining out of the base of the borehole. The rate of basal outflow presumably increased as borehole WL rose, resulting in greater dilution (and lower in-situ EC) when WL was higher. Occasional Tu peaks recorded at the base of H41 coincided with periods of rising WL, and may have resulted from disturbance initiated by an increasing rate of basal outflow. In H34, diurnal cycles in in-situ EC and Tu (Figures 4.5b and c) were extremely weak, but high EC (up to 50$\mu$S cm$^{-1}$) was recorded during the period JD 207-210, when the borehole was nearly dry. This again suggests that basal water flow past the base of the borehole was most readily detected when there was no drainage of supraglacially or englacially-derived waters from the base of the borehole.

These observations lead to the following conclusions about the nature of connections between the boreholes and the glacier's drainage system during Periods 1 and 2:

(a) Prior to JD 212 there was no connection between the base of H35 and any active subglacial system. H35 was, however, connected intermittently to some sort of drainage system via an englacial channel. When a threshold WL was reached, a siphon in the englacial channel was initiated which drew water out of H35 until the WL reached the level of the englacial channel. The siphon was consequently switched off and the WL rose from supraglacial inputs to the borehole until the threshold WL was attained and the siphon was re-initiated.

(b) Both H34 and H41 connected basally to a drainage system that was able to absorb the volume of water introduced to the boreholes during drilling. Water pressure in this system was probably close to atmospheric pressure because WL dropped to or close to the glacier bed in the absence of supraglacial/englacial inputs, and because basal water detected by in-situ sensors was never able to rise up the boreholes which may be an indication of limited water flux at the bed. These boreholes filled during the day as a result of water inputs from supraglacial/englacial sources, and they drained when these inputs ceased. The fall in in-situ EC as WL rose suggests that there was basal outflow even at times of rising WL, implying that WL rose because supraglacial/englacial inputs exceeded the drainage capacity of the subglacial system.

(c) The connection of H35 to the subglacial drainage system was triggered by an intense rainstorm on JD 211-212, which followed three days of high melt inputs to the glacier. This connection was via an englacial passageway located ~5m ab.

*Period 3*

Following the marked fall in H35 WL between JD 212 and JD 214, there were significant changes in the character of in-situ EC and Tu records. EC profiling demonstrates that these reflect marked changes in the way in which the boreholes were connected to the glacier's drainage system. Profiling data from JD 218 will be used to illustrate this point.

During Period 3, there is clear evidence for the inflow of basal water into H41 (Figure 4.13). During the diurnal WL peak on JD 218, the H35-H41 HD was always directed towards H41. During the initial part of the WL rise, in-situ EC fell and EC profiling showed that the water column consisted entirely of water with EC < 2μS $cm^{-1}$. This suggests that the initial rise was driven by supraglacial/englacial inputs to the borehole. After JD 218.55, however, in-situ EC and Tu rose sharply, and profiling showed that a column of water with EC >10μS $cm^{-1}$ rose 30m up the borehole.

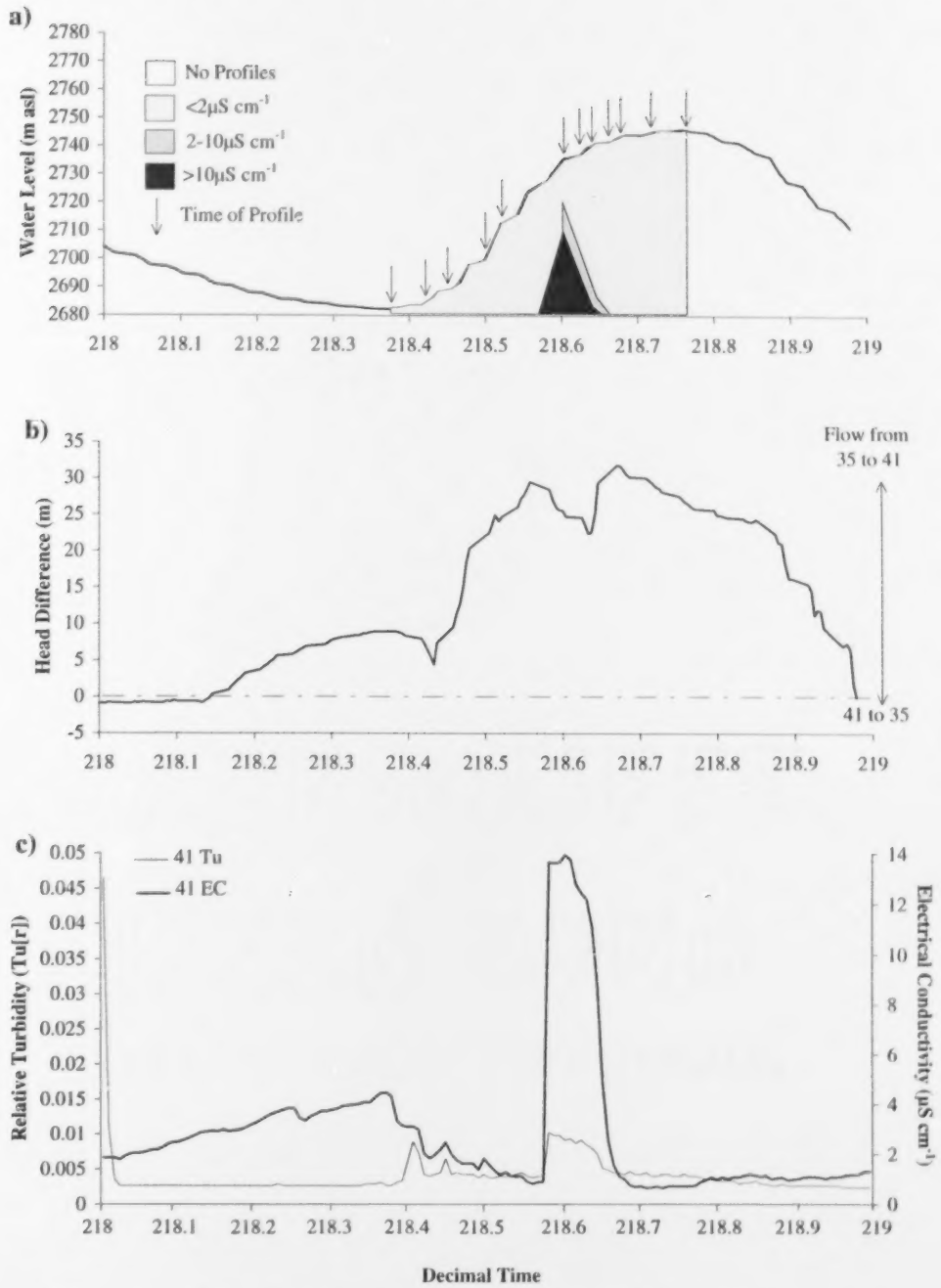


Figure 4.13: H41 a) WL and EC profiles, b) H35-H41 HD, and c) in-situ Tu and EC on JD 218.

During this period, WL rose only 20m, however, suggesting that some of the dilute water initially in the borehole was displaced into an englacial void or channel. After JD 218.63, the H35-H41 HD stopped rising, in-situ EC and Tu fell, and the column of high EC water disappeared from the borehole. WL continued to rise, however, suggesting that continued inputs of supraglacial/englacial water overpressured the borehole and initiated basal outflow. The magnitude of this outflow presumably decreased overnight as WL fell and H35-H41 HD decreased, allowing in-situ EC to rise slowly as the degree to which basal waters were diluted by the borehole outflow decreased. This example clearly demonstrates the utility of EC profiling data for the interpretation of in-situ records of basal water quality.

Whilst H41 clearly experienced basal water inputs in Period 3, WL fluctuations in H34 continued to be driven by variations in supraglacial and/or englacial inputs to the borehole. In-situ EC was low (the peaks at 218.1 and 218.47 being relatively insignificant) and profiling failed to register any waters with EC >2μS $cm^{-1}$ in the water column (Figure 4.14). In contrast to H41, there is no evidence for basal water inputs to H34 during this period.

These results suggest that in Period 3, H41was influenced by daily water pressure forcings in the subglacial drainage system which drove basal water across the bed and into H41. The records from H34 do not show this transport of basal water, suggesting that a conductive subglacial drainage system had yet to reach that area of the bed.

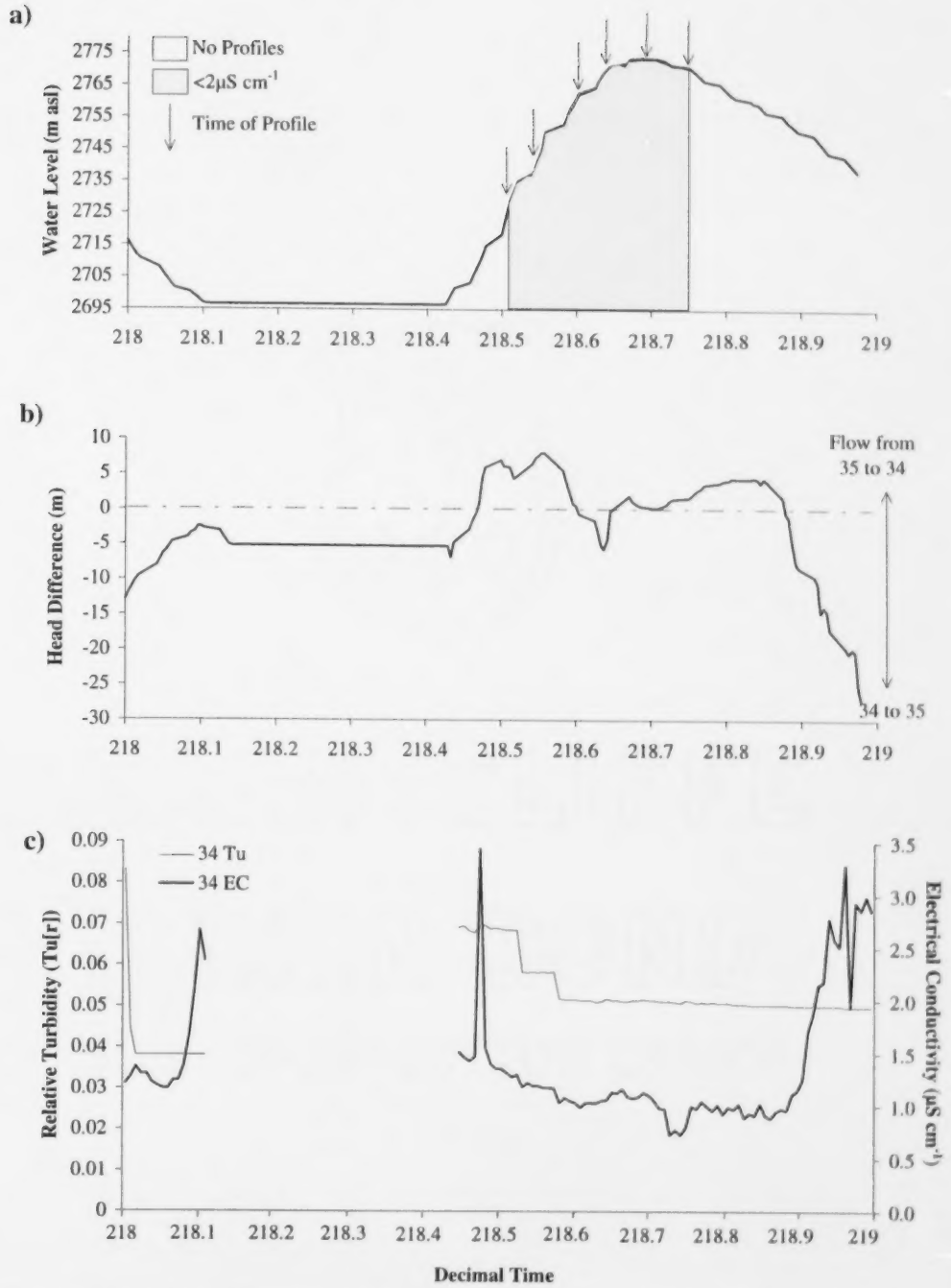


Figure 4.14: H34 a) WL and EC profiles, b) H35-H34 HD, and c) in-situ Tu and EC on JD 218.

***Period 4***

This period was characterised by clear, high amplitude diurnal WL cycles. The amplitude of these cycles was greatest in H35, and the sequence in which WL peaked stabilised. Borehole records for JD 224 are used to demonstrate how the drainage system functioned in this period and H29 measurements are substituted for H35 as water quality data are available for this hole.

Records from H29 show that the diurnal WL peak was associated with a large H29-H41 HD, and with low values of in-situ EC and Tu (Figure 4.15). HD was directed towards H41 throughout the WL peak, and the peak HD value (60m) was nearly double the peak in H35-H41 HD recorded on JD 218. The in-situ water quality data record the arrival of the diurnal melt wave at the glacier bed during the period of rising and peak WL, and the return of water with higher EC and Tu as WL fell and HD decreased.

During the period of WL rise in H41, H29-H41 HD was always directed towards H41. The initial WL rise was fed by supraglacial/englacial inputs, resulting in a dilute water column and reduction in in-situ EC (Figure 4.15). As in Period 3, however, basal water with high EC and Tu entered the borehole after JD 224.58, rising to a height of 40m ab (compared with only 30m ab on JD 218, when the peak HD from H35 was lower). By JD 224.63, this high EC water column had been split in two by more dilute water, leaving a 10m thick layer of water with EC >10μS $cm^{-1}$ 40m ab and continued high in-situ EC. Subsequently, in-situ EC fell to <2μS $cm^{-1}$ by JD 224.67, at which time there was no high EC water in the borehole. As discussed in Section 3.4.4.2 this behaviour suggests that H41 intercepted an englacial channel ~30m ab. This appears to have fed dilute water into the borehole and split the rising column of high EC water. Initiation of this input seems to have triggered basal outflow, driving high EC water from the base of the borehole while supraglacial inputs may have forced the upper layer of high EC water out of the englacial channel. The pattern of water circulation within H41 on JD 224 seems to have been more complex than on JD 218.

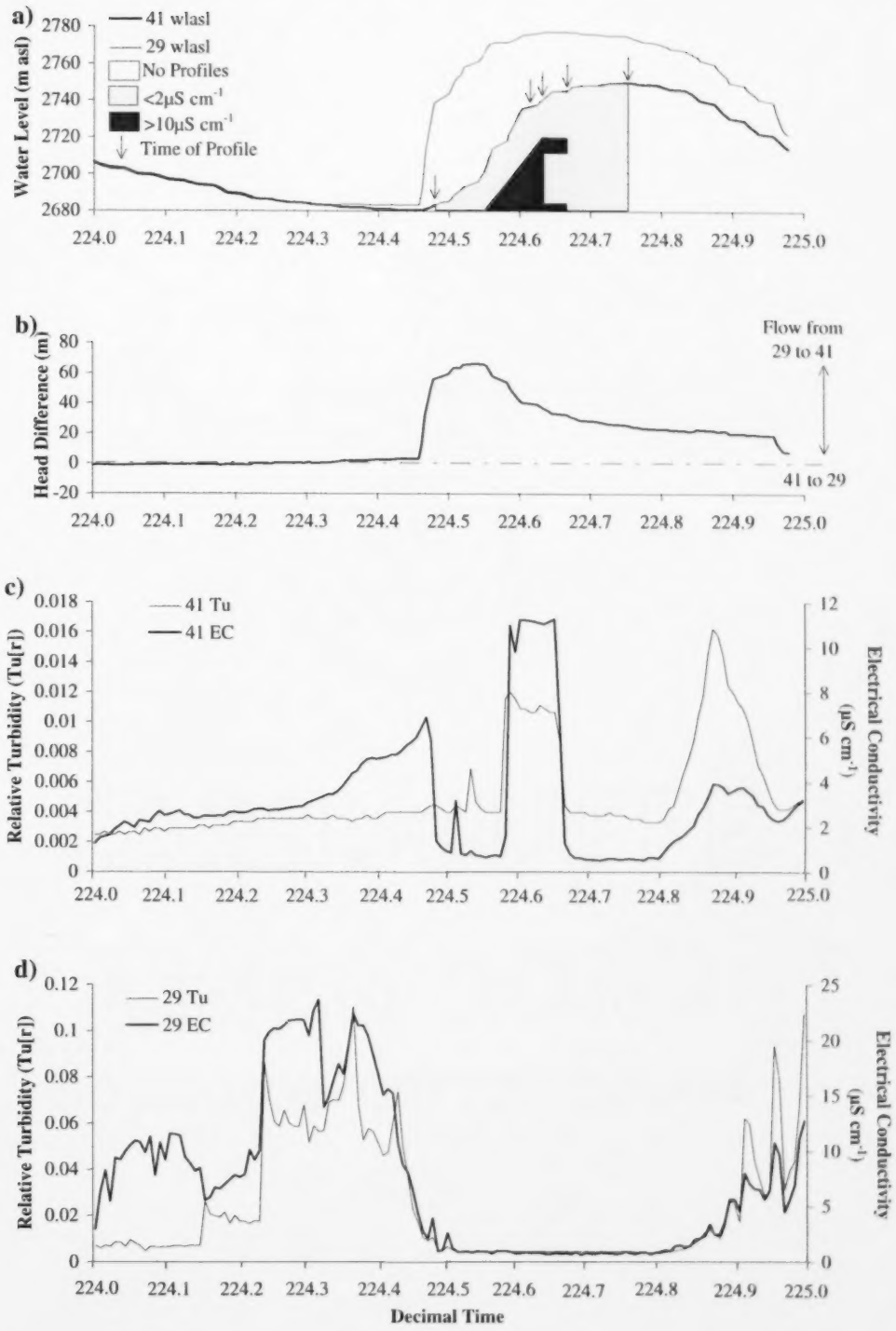


Figure 4.15: a) H29 WL and H41 WL and EC profiles, b) H29-H41 HD, c) H41 in-situ Tu and EC, and d) H29 in-situ Tu and EC on JD 224.

This appears to be due to the larger HD between H29 and H41, which resulted in basal water being driven further up the borehole than on JD 218. This allowed basal water within the borehole to mix with dilute waters derived from the englacial channel.

During Period 4, H34 began to be influenced by the inflow of basal water. Throughout the daily WL peak, the H29-H34 HD was directed towards H34 and the peak HD was much greater than on JD 218 (60m compared to 8m) (Figure 4.16). Low in-situ EC values measured when the WL started to rise suggests that the initial part of the WL rise was supraglacially/englacially fed. At JD 224.56, however, water with high Tu and EC of ~16μS $cm^{-1}$ entered the base of the hole and rose to 40m ab. This water was overlain by a cap of more dilute water which thickened slightly during the day, suggesting continued supraglacial/englacial input to the borehole, but 80% of the observed WL rise was fed by basally-derived water. In-situ EC fell as the WL fell, suggesting that water may have drained from the base of the borehole even during periods of rising WL, thus lowering the level of the condocline. Very low EC values recorded before the borehole went dry probably represent the remnants of the dilute cap before the hole drained. As HD was directed towards H29 before the WL started to rise and H34 was virtually dry, this part of the subglacial drainage system may have drained completely overnight.

During Period 4, borehole WLs responded more directly to diurnal forcing from the subglacial drainage system than in previous periods. The efficiency of this drainage system between H29, H41 and H34 was apparently improved, and there was significant flux of water through this system. Boreholes received significant inputs of basally-derived water during periods of rising pressure. Complex patterns of water circulation developed within boreholes and these must be understood if in-situ water quality records are to be interpreted.

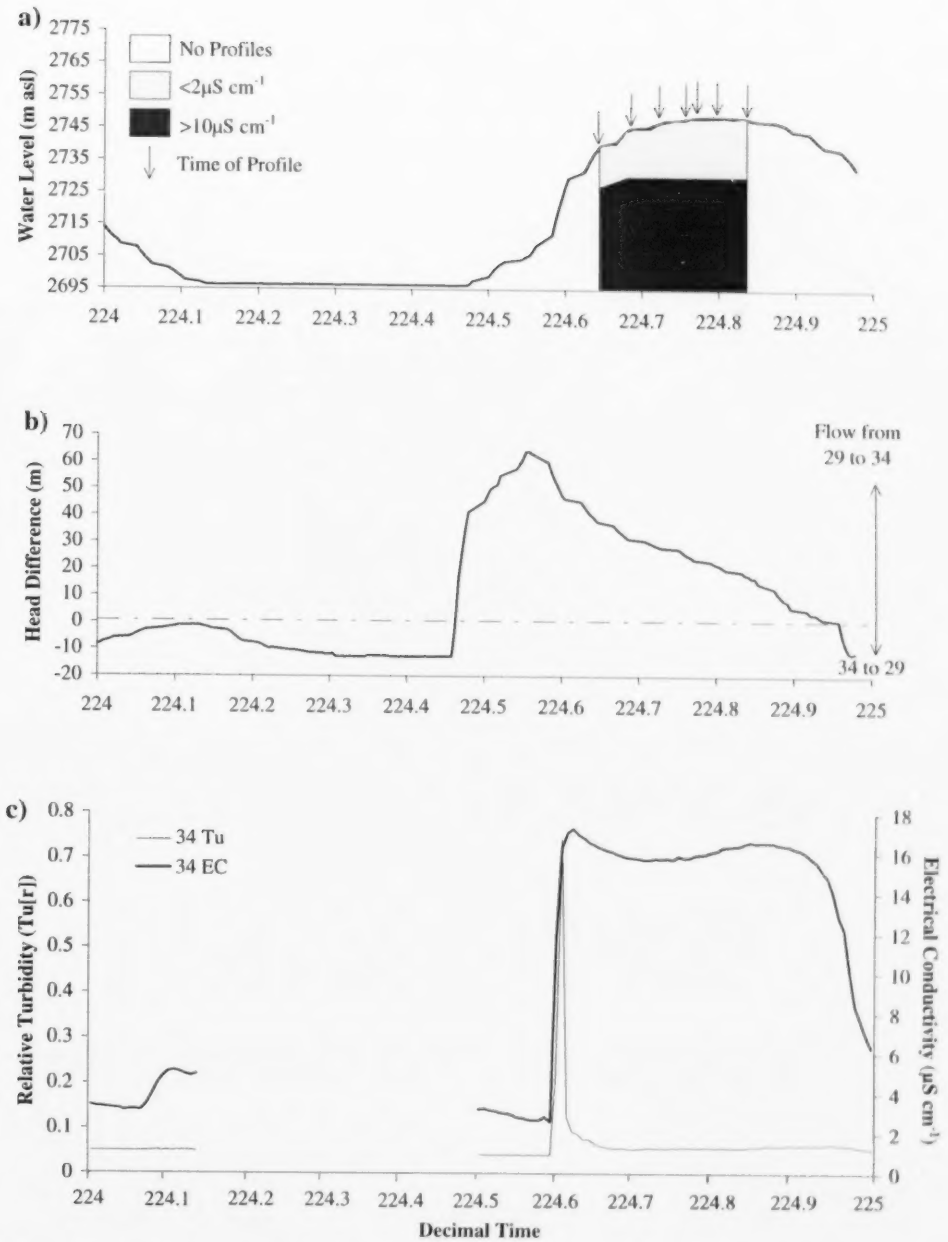


Figure 4.16: H34 a) WL and EC profiles, b) H29-H34 HD, and c) in-situ Tu and EC on JD 224.

***Period 5***

In general, the patterns recorded in borehole measurements from Period 5 were very similar to those described for Period 4. There are, however, a few significant differences. These can be seen by comparing results from JD 224 (Figures 4.15 and 4.16) with those from JD 229 (Figures 4.17 and 4.18). H29 is again substituted for H35.

Although WL in H41 still peaked after that in H29 on JD 229, it began to rise simultaneously in the two holes (Figure 4.17). In H41, basal water (with high EC and Tu) entered the base of the borehole as soon as WL began to rise. The dilute layer at the top of the water column was much thinner than on JD 224, and there was no fall in in-situ EC as WL started to rise. This suggests that the transmissivity of the drainage system between H41 and H29 had increased sufficiently since JD 224 that the diurnal rise in pressure was felt almost immediately at H41.

By contrast, differences in the results from H34 between JD 224 and JD 229 suggest either a decrease in the transmissivity of the subglacial drainage system between H29 and H34 or an increase in supraglacial inputs (Figure 4.18). The dilute water cap to the borehole water column was thicker than on JD 224 and the basal input was more dilute than on the earlier date. The rise of the basally-derived water seems to have been halted by the input of supraglacial/englacial waters. This input may have started to force the high EC water out of the base of the borehole even whilst the WL was rising as in-situ EC fell rapidly when the WL started to fall.

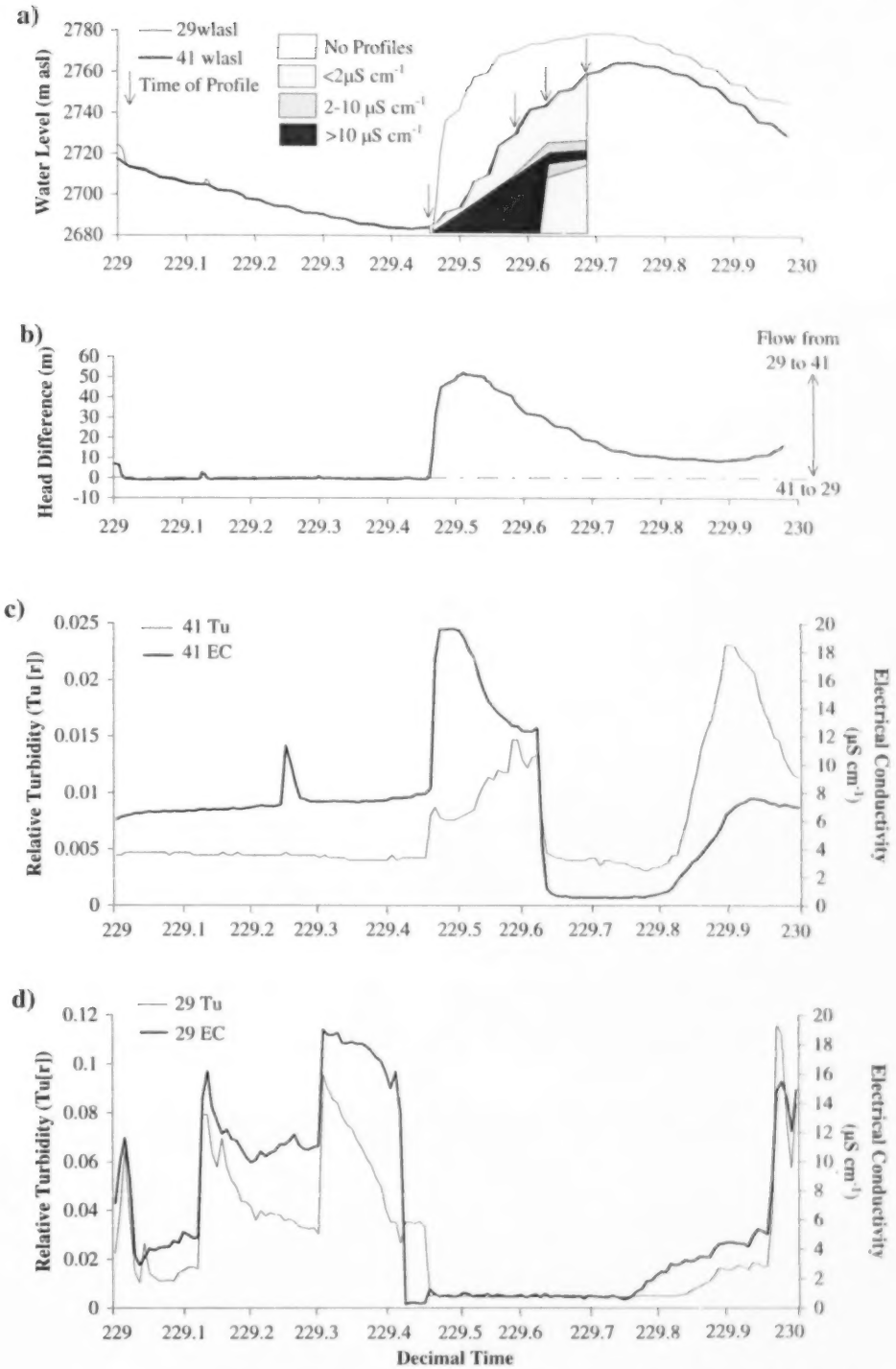


Figure 4.17: a) H29 WL and H41 WL and EC profiles, b) H29-H41 HD, c) H41 in-situ Tu and EC, and d) H29 in-situ Tu and EC on JD 229.

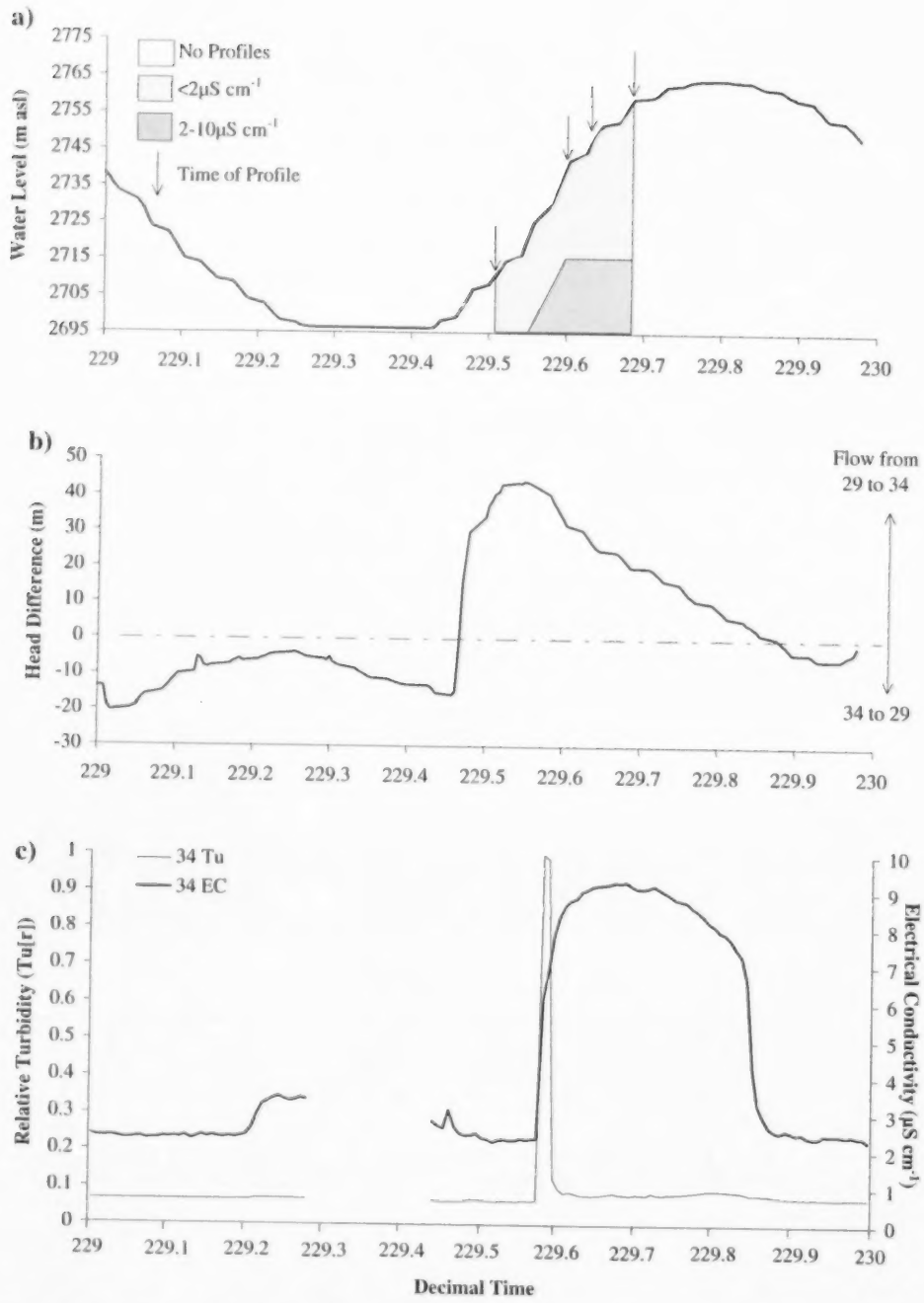


Figure 4.18: H34 a) WL and EC profiles, b) H29-H34 HD, and c) in-situ Tu and EC on JD 229.

***Summary:***

The combination of borehole WL, in-situ water quality and EC profiling measurements provide a reasonably clear picture of the evolution of the subglacial drainage system in the borehole array over the 1993 summer observation period. At the start of the season, the boreholes discussed in this section were connected to the glacier drainage system by either englacial (H35) or subglacial (H41, H34) pathways. WL variations in all boreholes were driven by fluctuations in the inflow of supraglacial/englacial waters, and were little affected by basal water flow. Where diurnal WL cycles occurred, variations in in-situ EC were attributable to variable dilution of small volumes of *true* basal water by water draining from the base of the boreholes.

In Period 3, the WL and water quality in H41 were influenced by basal inputs as basal water was forced into the borehole during periods of rising WL. A comparable basal influence was not detected in H34, demonstrating that this part of the bed was not yet efficiently connected to the subglacial drainage system that was influencing WL and water quality behaviour in H41. As the season progressed, the basal influence became stronger and basal water rose higher within both the boreholes (except for Period 5 in H34). On occasion, englacial channels could introduce dilute water to the rising column of more concentrated water, diluting it and forcing it back down the borehole and into the subglacial drainage system. The resulting patterns of water circulation were complex and made EC profiling results an essential basis for the interpretation of in-situ water quality records.

## 4.6 POSSIBLE EXPLANATIONS FOR THE OBSERVED EVOLUTION OF THE SUBGLACIAL DRAINAGE SYSTEM:

The observations discussed clearly demonstrate that the WL behaviour in all the boreholes changed over the summer observation period. Before these changes occurred, WL fluctuations were of a low amplitude and were generally poorly correlated with each other. Sustained high temperatures followed by heavy rainfall in Period 2 appear to have initiated the changes in WL behaviour which were dominated by the significant drop in H35 WL. Following Period 2, WL behaviour in H35, H41, H34 and H36 became coherent and WL fluctuation amplitudes increased. Analyses of water quality data and EC profiles demonstrate that the forcing which drove the WL variations in these boreholes (except H36) at the start of the observation period was different to that which drove the WL variations at the end of the observation period. Supraglacial/englacial inputs supplied H35, H34 and H41 with water in Periods 1 and 2, whilst subglacial inputs clearly contributed water to the boreholes in Periods 3, 4 and 5. In contrast, H40a, H42 and H36 (in Period 5) WL behaviours did not respond in the same way as H35, H41, H34 and H36 (in Periods 3 and 4) WLs after Period 2 which suggests a more complicated relationship between the forcing mechanism and the WL behaviour in these holes.

The presence of a subglacial channel located within the centre of the 1993 VPA at the end of the observation season (i.e. Period 5) was inferred from borehole measurements, both in Chapter 2 and by Hubbard et al. (1995). This channel was characterised by daily water pressure variations which produced a hydraulic gradient between the channel and the surrounding areas of the bed which appeared to drive water out of the channel during the afternoon and back to it overnight. If this drainage configuration is accepted, the changes in WL behaviour that were observed over the observation period are likely to represent the evolution of the subglacial drainage system from an unknown configuration to a channelised configuration. This channelised configuration must have been attained by Period 5 at the latest, but was probably initiated earlier. The significant changes in WL behaviour in Period 2 are likely to have occurred in response to some sort of re-organisation of the subglacial drainage system. However, it must be ascertained whether a channelised system existed before Period 2 or whether the changes in WL behaviour in Period 2 were a response to the formation of a channel within the borehole array.

### 4.6.1 Evidence for channel formation:

Aside from the borehole measurements described above, the best evidence for subglacial drainage evolution comes from dye tracing studies conducted in 1990 and 1991. Nienow (1993) found that when repeated dye injections were made at individual moulins, the dye travel time from moulin to glacier snout decreased progressively over the melt season, until it eventually reached a stable minimum value. This value increased in magnitude and was reached later in the season at moulins located further upglacier. The decrease in travel time began before the transient summer snowline passed each moulin, but the minimum value was not reached until up to 5 days after the snowline had passed. Nienow concluded that by the time the minimum value was reached, a system of major subglacial channels connected the moulin to the glacier snout. Before this date, the channel system was growing headwards towards the moulin, but a section of inefficient distributed drainage system lay between the moulin and the channel system. Nienow (1993) argued that channel formation was stimulated by changes in the magnitude and diurnal variability of water inputs to moulins which occurred following exposure of an impermeable, low albedo ice surface in the drainage catchment upstream of the moulin. The data presented in this chapter allow testing of this hypothesis.

Since the snowline passed through the drill site around JD 200 (July 19) in 1993, Nienow's (1993) model predicts the probable existence of a major channel in this area by JD 205. However, borehole measurements provide no clear evidence for the existence of such a channel before JD 212 after which daily WL fluctuation amplitudes increased and became more coherent (except in H40a and H42). This raises the question of whether a channel existed in the borehole array before JD 212, or whether the process of channel formation was slower in 1993 than in 1990/91.

There are four reasons for suspecting that the events of JD 212-214, when the WL behaviours changed, were a response to the formation of a major subglacial channel, and that channelisation occurred rather later in 1993 than in previous years:

a) Boreholes were drilled at approximately 20m intervals across the area in which the channel was located at the end of the season. Given the density of boreholes, it would be surprising if the channel had existed, but not been found before JD 212.

b) The WL drop in H35 after JD 212 was associated with major changes in the behaviour recorded in all the boreholes studied, and not just in H35. It thus seems more likely that the WL drop resulted from a change in the subglacial drainage system, than from the development of a basal connection between H35 and a pre-existing drainage channel. Although such a connection could have resulted from advection of H35 into a better connected area of the glacier bed (Hantz and Lliboutry, 1983; Fountain, 1994), or from the growth of a link between borehole and channel resulting from overpressuring of the glacier bed by the borehole (Engelhardt, 1978), it seems unlikely that such events would have triggered major changes in the behaviour of other boreholes. In addition, the three day duration of the WL drop seems inconsistent with a sudden connection event of this type (c.f. examples of sudden drainage events reported by Hodge (1976), Engelhardt (1978), Stone and Clarke (1993), and Fountain (1994)).

c) The period JD 192-210 was one of generally low air temperatures (sub-freezing temperatures were recorded on 11 nights in this period) (Figure 4.2a) and low bulk meltwater discharges (typically $<3m^3 s^{-1}$, and as low as $1.5m^3 s^{-1}$ on several days; Figure 4.2c). Thus, although the snowline passed through the drill site around JD 200, moulins located upglacier from the borehole array may not have begun to receive large meltwater inputs until around JD 212, when peak daily discharge reached a typical late summer value of $5m^3 s^{-1}$. This suggestion is confirmed by numerical modelling of meltwater discharge into a moulin located ~220m upstream from the drill site in 1993, which shows a significant increase in inputs around JD 212 (Figure 4.19) (Arnold et al., submitted).

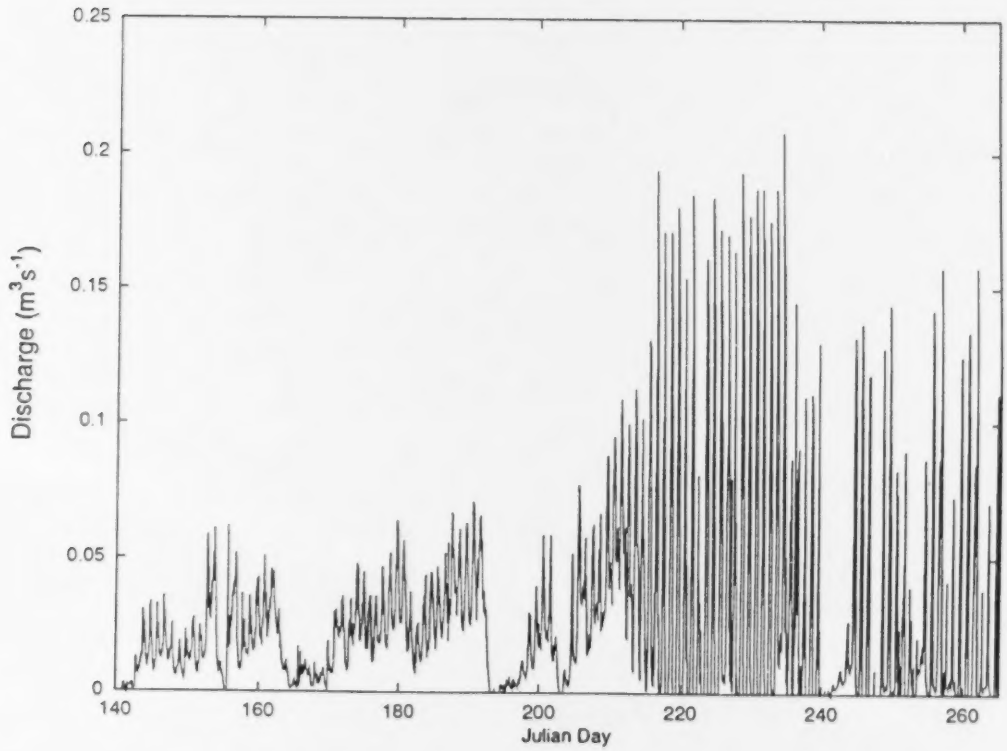


Figure 4.19: Modelled moulin input hydrograph for a moulin located ~220m upglacier from the borehole array in 1993. (From Arnold et al., submitted).

Major input peaks which occurred around JD 216 (Figure 4.19) likely reflect the removal of the snowpack in the upper glacier catchment. If, as suggested by Nienow (1993), large and diurnally variable discharges are required to stimulate channel growth, this could account for delayed channel formation.

d) Although Nienow's (1993) model of up-glacier channel growth may be valid at a glacier-wide scale, it may be that, at a local scale, channel segments are more likely to grow downglacier from individual moulins, eventually connecting to a main channel system which is already established further downstream. Since the borehole array is located mid-way between two sets of moulins, a channel might not develop in this area of the glacier until the catchment of the upstream moulins was at least partially snow-free. Given the weather conditions and resultant slow rate of snowline retreat in the period JD 200-220, 1993, this may not have occurred until significantly later than JD 200. If this suggestion is correct, the WL drop in H35 might be viewed as a response to the breaking of a seal which separated an incipient channel from an integrated channel system which was already established further downglacier. This would have permitted free drainage of water through the borehole array area, allowing drainage of water stored in crevasses and subglacial cavities, and the onset of diurnal water pressure cycling. Clarke (in press, his Figure 9) has simulated similar behaviour using a lumped element model of a subglacial drainage circuit.

In the light of these arguments, it is suggested that the events of JD 212-214 represent the development of a subglacial channel within the borehole array. This may have been the result of a channelised system located upglacier of the borehole connecting to a channelised system downglacier of the borehole array. However, modelling of subglacial water pressures over the 1993 observation season (Arnold et al., submitted) show that the changes in borehole WL behaviour could also have been the result of changing discharge regimes in a channel which may have existed at the start of the observation period. The changes in the borehole WL behaviour may therefore have not been the result of the formation of a channel.

**4.6.2 The character of the subglacial drainage system before channelisation:**

From the data presented it is possible to draw some conclusions about the character of the subglacial drainage system prior to channelisation:

a) Since the VPA existed before JD 212, it appears that the area of the borehole array was a region of preferential water flow even before channelisation as WLs fell on a diurnal basis when supraglacial and/or englacial inputs ceased. However, the absence of large diurnal WL variations in this period suggests either (i) that the flow was fed by a source (such as basal melt or seepage from the supraglacial snowpack) which generated only minor diurnal variations in water flux, or (ii) that the drainage system contained sufficient unused storage volume to accommodate diurnal flux variations without large accompanying changes in water pressure.

b) Where diurnal WL changes did occur, they resulted from the direct input of surface-derived waters to boreholes. Engelhardt (1978) modelled the response of borehole WL to both sudden and periodic changes in water input, and found that maximum WL response was produced by cyclic input changes with a period of 8.4 hours. This reflects the fact that the dimensions of boreholes and passageways draining from them are unable to adjust to changing water inputs by melting and contraction on such short timescales.

c) H34, H41 and H36 drained to or close to the bed after drilling, and did so repeatedly overnight thereafter (except for H36), confirming that some parts of the subglacial drainage system had significant storage capacity. Drainage of a full borehole 50m deep, with a diameter of 0.1m, would require the system to absorb $0.5m^3$ of water. Such a volume could probably be accommodated by cavities on the lee side of bedrock bumps, or by the pore space in permeable sediments.

d) H35 failed to develop a near-basal connection until after channelisation. This suggests that i) the inferred englacial connection in H35 located at 5m ab may have formed in response to high channel pressures which caused the ice to fracture along a line of weakness to form a connection between the channel and H35, and ii) the bed was hydraulically patchy before channelisation, with some areas of extremely low hydraulic conductivity. Those boreholes which drained to the bed overnight refilled with supraglacially/englacially-derived water during the day, suggesting that available subglacial storage spaces were not well connected to an efficient drainage system. Patches of low hydraulic conductivity bed may have isolated storage spaces from each other. A drainage system in which cavities developed in the lee side of isolated bedrock bumps protruding through a pervasive till layer would have these characteristics (c.f. Murray and Clarke, 1995, p 10234). It would also be consistent with Nienow's (1993) conclusions about the type of drainage system which underlay much of Haut Glacier d'Arolla prior to the formation of subglacial channels during each melt season.

e) The failure of basal water to enter boreholes until after channelisation suggests that, in the absence of inputs from boreholes, water fluxes through the subglacial system were extremely low. This suggests that surface-derived waters may not have penetrated much of the VPA until after channel formation.

**4.6.3 The character of the subglacial drainage system after channelisation:**

The WL behaviour measured after channelisation in the 7 boreholes observed can be grouped into 4 categories on the basis of their WL responses to channel forcing. These categories are: direct response, lagged response, damped response and inverse response. Discussion of these categories provides information concerning the character of the drainage system after channelisation.

4.6.3.1 *Direct Response:* The WL behaviour in H29 and H35 falls into this category as these measurements represent near-channel water pressure conditions. This is demonstrated by the fact that H35 registered the highest WL fluctuation amplitudes after the middle of Period 3 (Figure 4.8) and was generally the first borehole to reach peak diurnal WL (except in Period 5; Figure 4.9). The F-R plot of H29/H35 (Figure 4.11a) shows minimal hysteresis and demonstrates that the WL records are almost identical.

Low in-situ EC registered in H29 on JD 224 and JD 229 (Figures 4.15d and 4.17d) is therefore likely to represent the propagation of dilute channel water to surrounding areas of the bed as channel pressures rose during the day, whilst higher in-situ EC measured on the falling WL limb, represents basal water flowing along the bed towards the channel as the HD between the channel and the surrounding areas of the bed fell overnight. Lags associated with CCCs between temperature and H35 WL in Periods 3-5 are the lowest for all the pairings (Table 4.2). This also demonstrates that H35 (and hence H29) was located closer to the channel than the other boreholes as the daily meltwater pulse was registered by H35 sooner than the other boreholes. WL behaviour of the remaining boreholes can therefore be compared to that of H35 or H29 when considering the response of borehole WLs to channel forcing.

4.6.3.2 *Lagged Response:* H41 and H34 WL behaviour falls into this category. After the period of re-organisation in Period 3, H41 and H34 WL fluctuation amplitudes were lower than those in H35 (Figure 4.8a) and peak daily WLs were attained after those in H35 (Figure 4.9a). This suggests that these holes were located at some distance from the channel. As H41 demonstrated higher WL amplitudes than H34 and reached diurnal peak WL before H34, H41 was likely to have been located closer to the channel than H34. These interpretations are supported by the F-R plots of H41/H35 and H34/H35 (Figures 4.11b and c). The hysteresis loops in both plots demonstrate that there was a lag between when the diurnal pressure wave was registered near the channel in H35 and when it was registered at more distant locations, first in H41 and then in H34.

In-situ water quality and EC profiling data for H41 and H34 can be used to determine when basal water was first introduced to the base of these holes, and thus when channel influences were first registered at these parts of the bed. In H41, basal water was likely to have been first registered on JD 215 when a high in-situ EC peak of ~14μS $cm^{-1}$ was measured (Figure 4.4b). Profiling data on JD 218 (Figure 4.13a) suggest that this input of basal water was forced up the borehole. In-situ EC measurements in H34 (Figure 4.5b) suggest that a basal influence was not registered until JD 221 when an EC peak of ~22μS $cm^{-1}$ was recorded. As with H41, profiling data on JD 224 (Figure 4.16a) suggest that this basal water was also forced into the borehole via its base. Thus H34 registered basal water inputs 6 days after they were registered in H41. This is consistent with the inference that H41 was located closer to the channel than H34.

The transmissivity of the drainage system between the channel and H41 seemed to increase after Period 3. This may have resulted from either a) the flushing of fines from subglacial sediment by diurnally reversing water flows in the vicinity of the channel (Figure 4.4d) which would have increased the hydraulic conductivity of the subglacial sediment (Hubbard et al., 1995), or b) the development of areas of flow concentration or micro-channels at the ice-sediment interface (Hubbard et al., 1995). In contrast, the transmissivity of the drainage system between the channel and H34 appeared to increase

and then decrease, suggesting that at this distance from the channel, diurnally reversing flows (Figure 4.5d) were either too weak or too infrequent to maintain a highly conductive drainage system. This is consistent with the findings of Hubbard et al., (1995) that the hydraulic conductivity of subglacial sediment appeared to decrease exponentially with distance from the channel.

4.6.3.3 *Damped Response:* H42 WL falls in this category because WL fluctuations fell from 2-13m before JD 212 to <2m after JD 212 (Figure 4.8b). This contrasts the WL responses in H35, H41, H34 and H36. In Chapter 3, H42 was classified as *englacially connected* as the base WL coincided with the level at which an englacial connection was made during drilling (~26m bs). As insufficient EC profiling data are available to determine whether a basal connection existed or not, the WL variations were likely to have been supplied by englacial and/or supraglacial inputs. The reduction in the WL fluctuation amplitude may thus represent either a reduction in these inputs or the development of a more efficient englacial outflow such that the supraglacial inputs were drained more easily. However, inspection of the F-R plot for H42/H35 (Figure 4.11e) provides interesting information concerning the nature of the relationship between H35 and H42 WLs. H42 WL initially remained stable at its base level while H35 WL rose. H42 WL only started to rise when H35 WL reached ~2757m.a.s.l.. This elevation coincides with the location of the inferred englacial channel in H42. Thus, it appears that the englacial channel in H42 was connected directly to the subglacial channel such that water backed-up the englacial channel as water pressure in the subglacial channel increased. When the WL in the englacial channel reached the level at which it entered H42, a WL increase was registered in H42. However, two problems arise from this interpretation: a) the WL in H42 would be expected to match that in H35, but H42 peak WL was ~18m less than the peak WL attained in H35, and b) the WL in H42 would be expected to fall synchronously with that in H35, but the F-R plot shows that there was a lag between the falling WLs. These discrepancies are difficult to reconcile.

Another interpretation may be that the small WL fluctuation amplitudes measured in H42 represent the lagged arrival of the pressure wave across the bed from the channel, but that no water entered the base of the hole. This is supported by Hubbard et al. (1995) who found that although the pressure wave was registered in H42 at a time consistent with the outward propagation of the pressure wave from the channel, the WL amplitude in H42 between JD 228 and JD 234 was smaller than they predicted when modelling WL amplitudes away from the channel with flow through subglacial sediment of decreasing hydraulic diffusivity with distance from the channel. They concluded that the drainage system beneath H42 was unable to transport the water flux that was required to accurately reflect the magnitude of the subglacial pressure wave.

From the data available it is difficult to understand exactly why the WL amplitude in H42 decreased. However, it is likely that an interpretation should include the influence of the englacial channel as the base WL in H42 was obviously governed by this connection.

4.6.3.4 *Inverse Response:* H36 and H40a fall into this final category; H36 because of its anomalous WL behaviour at the end of Period 4 and through Period 5 (Figure 4.6a), and H40a because of its apparent disconnection on JD 214 and subsequent inverse behaviour (Figure 4.7b).

Although few profiling data are available for H36, it was thought to be basally connected as the borehole went dry immediately after it was drilled. WL fluctuations after channelisation are therefore assumed to have been basally driven. Three significant changes in H36 WL occurred in Period 5: a) base WL increased from ~30m to ~70m ab, b) rapid drainage events started to occur during periods of rapidly rising WL in H35 (first seen on JD 224), and c) a semi-diurnal WL cycle emerged on JD 229 where the second peak preceded the drainage. The H36/H35 F-R plot (Figure 4.11d) can be used to help explain these features. Initially, H36 WL seemed to drain slowly as H35 WL increased, but drained slightly faster when H35 WL reached ~2755m.a.s.l.. H36 drained rapidly for a short period when H35 WL was ~2772m.a.s.l.. This was followed by rapid re-filling.

The rapid drainage event appears to have occurred when the water pressure in H35 came close to ice overburden pressure (IOP) at H35. Just prior to H36 draining rapidly, the WL in H35 was 85m ab. If the depth of H35 was 96m, IOP at H35 would be reached when the WL was at the equivalent of 88m ab (0.917 x ice thickness). Thus, it is inferred that rapidly rising channel water pressure to levels close to IOP caused unloading of the bed close to the channel. This process produced a consequent loading of the bed away from the channel causing an increase in pressure (small peak in H36 WL before it drained). Subsequent pressure wave propagation from the channel opened up areas of the bed ahead of the pressure wave. This likely created a void space at the base of H36 allowing water to drain rapidly. However, when the pressure wave reached the base of H36, drainage was impeded and the WL in H36 rose. The eventual fall in H36 WL lagged that in H35 and occurred at a slower rate presumably due to the fact that as H35 drained, the bed near the channel was re-loaded which impeded drainage of the surrounding bed. It seems that through Period 5, the period of time during which H36 could drain decreased, thus causing the base WL in H36 to rise. This may have occurred due to the increasing velocity at which the pressure wave propagated along the bed (caused by increasing hydraulic conductivity of the subglacial sediment, or the formation of micro-channels at the ice-sediment interface; Hubbard et al, 1995). This would allow less time for H36 to drain between the time that the void space was created and the time at which the pressure wave actually reached the base of H36.

From this interpretation, the WL behaviour in H36 appears to have undergone four phases:

a) Unloading of the bed near the channel caused loading of the bed at H36 which was registered as a small increase in H36 WL.

b) Pressure wave propagation opened up parts of the bed ahead of the pressure wave. This created a void space at the base of H36, allowing it to drain rapidly.

c) The pressure wave reached the base of H36, impeding drainage and causing the WL in H36 to rise.

d) As channel pressure fell, the bed near the channel was re-loaded causing the WL in H36 to fall at a slow rate.

On JD 214 H40a appeared to disconnect as the WL increased steadily until it was almost full (Figure 4.7b). Subsequent minor WL variations occurred on a diurnal basis, but they were negatively correlated with WL variations in H35 (Figure 4.7b), H41 and H34 (Table 4.1). The H40a/H35 F-R plot for JD 218 (Figure 4.11f) demonstrates a predominantly negative correlation between H40a and H35 WL behaviour. This suggests that an unloading/loading process similar to that used to explain H36 WL behaviour also influenced the behaviour in H40a. However, H40a appears only to have undergone the first two phases. During the initial rise in H35 WL, the bed at H40a was loaded causing a small increase in H40a WL. As the propagating pressure wave opened up more areas of the bed, the WL in H40a fell. It appears that there was no efficient hydraulic pathway between the channel and H40a to register a consequent WL increase.

The inverse behaviour seen in H40a resembles that seen by Murray and Clarke (1995) in a borehole thought to be located between two areas of the bed which were well connected to the subglacial drainage system. An inverse relationship between this hole (A1) and a hole located in the connected area (C1) showed that increasing pressure at C1 unloaded the area around A1 allowing pressure to fall at this hole, whilst falling pressure at C1 re-loaded the area around A1 causing an increase in pressure at this hole. However, loading of the bed at A1 when pressure in C1 initially increased was not observed. This may suggest that A1 was located closer to C1 than H40a was located to H35.

**4.6.4 Summary:**

Although WL behaviour in the observed boreholes did not all respond in a similar fashion to the establishment of a channelised system in the borehole array in Period 2, it has been demonstrated that the WL behaviour that did occur was driven by a common forcing: daily channel pressure fluctuations. The daily pressure wave propagated away from the channel during the day to the surrounding areas of the bed and returned towards the channel overnight. In H35, H41 and H34 the arrival of the pressure wave was registered progressively later in the day and by decreasing WL fluctuation amplitudes with distance from the channel. H42 WL appears to have responded to channel pressure forcing either via an englacial channel or via the bed. However, the nature of this relationship is unclear and it is likely that the presence of the englacial channel in H42 imposed a significant influence on the WL behaviour. Inverse WL behaviour measured in H36 and H40a can be explained by the daily loading and unloading of the bed in areas surrounding the channel by the daily propagation of the channel pressure wave. In H36, unloading established a connection between the base of H36 and the channel such that the WL in H36 was driven by rising channel pressures. In H40a, unloading allowed slight drainage from the borehole, but it appears that this hole was located too far from the channel to register an increase in WL from the rising channel pressure. Instead, the WL in H40a rose in response to falling channel pressure which had the effect of re-loading the bed at the base of H40a.

## 4.7 SUMMARY:

Evolution of the subglacial drainage system within the borehole array over the 1993 summer observation season has been demonstrated. This evolution occurred in response to the development of a subglacial channel between JD 212 and JD 214. Prior to channelisation, borehole WL fluctuations were low in amplitude and poorly correlated, suggesting that the WL fluctuations occurred independently of each other. The period over which channel development was inferred to have occurred culminated in a significant change in the WL behaviour of all boreholes observed, especially the marked drop in H35 WL. After channel development, borehole WLs did not all behave in the same fashion. WL fluctuation amplitudes increased and time to peak WL decreased in H35, H41, H34 and H36 (in Period 3 until the end of Period 4). In contrast, WL fluctuation amplitudes decreased in H42. WL behaviour in H36 (at the end of Period 4 and through Period 5) and H40a occurred in response to the loading and unloading of the bed close to and away from the channel. Despite these differences in WL behaviour, it was demonstrated that all the WLs observed (but possibly not that in H42) were driven by a common forcing: daily pressure fluctuations in the channel.

Analysis of profiling data was vital for the interpretation of in-situ water quality data and aided the understanding of water circulation patterns within boreholes and between boreholes. This chapter has demonstrated that the integration of various borehole-derived data sources is a necessity when attempting to interpret borehole WL measurements to determine the configuration of the subglacial drainage system in an area, otherwise unreliable interpretations may be reached.

# CHAPTER 5: CONCLUSION

A range of data derived from boreholes drilled to the bed of Haut Glacier d'Arolla in the summer ablation periods of 1992, 1993 and 1995, has been used to infer the nature and evolution of the subglacial drainage system under a part of the glacier.

Borehole WL behaviour was initially classified and mapped for a five day period at the end of each observation period. A VPA was identified in the borehole array in each year. In general, base WLs increased and WL fluctuation amplitudes decreased away from the centre of the VPA. It was inferred that, in each year, a channel existed in the centre of the VPA and the surrounding areas of the bed were drained by a distributed drainage system. Different WL behaviour exhibited in each year demonstrated that the inferred channel was not pressurised to the same degree each year. This was due to different melt conditions both before and during the five day classification period. Classification of WL behaviour over an entire observation period demonstrated the evolution of the subglacial drainage system within the borehole array.

In order to use in-situ WL and water quality data to provide a detailed description and explanation of the nature and evolution of the subglacial drainage system identified, it was first necessary to determine the water source and circulation patterns of each borehole so that the WL and water quality data could be interpreted more reliably. Where possible, information from seven types of borehole-derived data was combined to identify five plumbing categories. In-situ water quality measurements taken in actively connected boreholes were most likely to have recorded *true* basal water quality signals, but not continuously, as the patterns of water circulation within these boreholes were often complex. For example, in a borehole that was inferred to be fed primarily from the bed with no englacial influences (93/37), *true* basal water quality was measured only on the rising limb of the daily WL cycle. In another actively connected hole (93/41), water was inferred to exit the base of the borehole even under conditions of rising WL. The initial determination of borehole plumbing was thus proven to be a vital requirement before attempts at interpreting in-situ WL and water quality data could be made.

With the added knowledge of borehole plumbing it was possible to construct a detailed description and explanation of the nature and evolution of the subglacial drainage system under the borehole array over the 1993 summer observation period. Based on changing trends in the WL and HD data, the observation period was divided into five sub-periods. By combining the in-situ water quality measurements and EC profiles with the WL and HD data in these sub-periods, it was inferred that the formation and subsequent evolution of a major subglacial channel occurred within a distributed drainage system under the borehole array. Channel formation simultaneously influenced the WL behaviour in all the boreholes observed. It was demonstrated that before channel formation, WL fluctuations occurred independently of each other, whereas after channel formation, WLs were driven by a common forcing: channel pressure. Channel pressure variations generated a diurnally reversing transverse hydraulic gradient, which drove water away from the channel into the surrounding distributed system during periods of rising pressure, and allowed water to return to the channel overnight. However, this process did not influence all the WL behaviours in the same manner.

## 5.1 IMPLICATIONS:

This study has demonstrated that although boreholes drilled to the bed of warm-based glaciers do provide direct access to the glacier bed, the data derived from them must be used with caution as each borehole has been shown to be uniquely plumbed into the glacier's supraglacial, englacial and subglacial drainage system. It is therefore imperative that the plumbing of each borehole into a glacier's drainage system is first determined before any borehole-derived data are used to make inferences about the subglacial drainage system in the area. Interpretations about the nature of the subglacial drainage system made by studies such as Engelhardt (1978), Hantz and Lliboutry (1983), and Fountain (1994), may therefore be unreliable as borehole plumbing was not considered. EC profiling is the most valuable tool for determining the plumbing of a borehole as this method provides information about the water sources and circulation patterns within a borehole. By supplementing EC profiling data with additional borehole-derived data such as drilling records, salt tracing and down-borehole video imagery an even more accurate

determination of borehole plumbing can be reached.

This study has also demonstrated that evolution of the subglacial drainage system under a part of Haut Glacier d'Arolla occurred over the summer observation period in 1993. Such evolution has also been described by Nienow (1993) and Nienow et al. (submitted) for Haut Glacier d'Arolla, and by Fountain (1994) for South Cascade Glacier, U.S.A.. However, detailed analysis of continuous time series measurements in this study has allowed the influence of short-term events (e.g rainfall and periods of high temperature) on the evolution of the subglacial drainage system to be highlighted. In addition, detailed analysis of daily time series measurements enabled changing relationships between the data series to be observed. For example, changes in the time at which EC spikes occurred during the daily WL cycles over the observation period helped to demonstrate the evolution and improved efficiency of the subglacial drainage system. Such detailed analyses provide interpretations that go one step beyond those made by dye tracer studies (e.g. Nienow, 1993; Willis et al., 1990), bulk meltwater chemistry analysis (e.g. Collins, 1979) and forefield mapping (e.g. Walder and Hallet, 1979; Sharp et al., 1989) as short-term processes and the forces causing them can be studied in detail and fitted into the broader long-term perspective (e.g. analysing daily cycles and determining how and why they piece together to produce observed seasonal trends).

If WL and in-situ water quality data derived from boreholes drilled in warm-based glaciers are supplemented by additional borehole-derived data, they have a significant potential for being used to make reliable inferences about the configuration and behaviour of the subglacial drainage system in the area. These inferences could be consequently combined with interpretations derived from other data such as dye tracing measurements, surface velocity measurements, chemical analyses of water taken from the base of boreholes and proglacial stream measurements to construct a comprehensive picture of the configuration of the subglacial drainage system of a glacier and an understanding of the processes that occur within it.

## BIBLIOGRAPHY

Alley, R.B. 1996. Towards a hydrologic model for computerized ice-sheet simulation. **Hydrological Processes,** 10(4), 649-660.

Braithwaite, R.J. 1981. On glacier energy balance, ablation and air temperature. **Journal of Glaciology,** 27(97), 381-391.

Brown G.H., Sharp, M., Tranter, M., Gurnell, A.M. and Nienow, P. 1994. Impact of post-mixing channel reactions on the major ion chemistry of bulk meltwaters draining the Haut Glacier d'Arolla, Valais, Switzerland. **Hydrological Processes,** 8, 465-480.

Clarke, G. K.C. In press. Lumped-element analysis of subglacial hydraulic circuits. **Journal of Geophysical Research.**

Collins, D.N. 1979. Quantitative determination of the subglacial hydrology of two Alpine glaciers. **Journal of Glaciology,** 23(89), 347-362.

Copland, L., Harbor, J., Gordon, S. and Sharp, M. In press. The use of borehole video in investigating the hydrology of a temperate glacier. **Hydrological Processes.**

Engelhardt, H. 1978. Water in glaciers: Observations and theory of the behaviour of water levels in boreholes. **Zeitschrift für Gletscherkunde und Glazialgeologie,** 14(1), 35-60.

Fenn, C.R. 1987. Electrical conductivity. In Gurnell, A.M. and Clarke, M.J. (eds.) *Glacio-fluvial sediment transfer: An alpine perspective.* Chichester, John Wiley and Sons, 377-414.

Fischer, U.H. and Clarke, G.K.C. 1994. Ploughing of subglacial sediment. **Journal of Glaciology,** 40 (134), 97-106.

Fountain, A.G. 1992. Subglacial water flow inferred from stream measurements at South Cascade Glacier, Washington, USA. **Journal of Glaciology,** 38(128), 51-64.

Fountain, A.G. 1993. Geometry and flow conditions of subglacial water at South Cascade Glacier, Washington State, USA.; an analysis of tracer injections. **Journal of Glaciology,** 39(131), 143-156.

Fountain, A.G. 1994. Borehole water-level variations and implications for the subglacial hydraulics of South Cascade Glacier, Washington State, U.S.A. **Journal of Glaciology,** 40 (135), 293-304.

Gurnell, A.M. and Fenn, C.R. 1985. Spatial and temporal variations in electrical conductivity in a proglacial stream. **Journal of Glaciology,** 31(108), 108-114.

Hallet, B. and Anderson, R.S. 1980. Detailed glacial geomorphology of a proglacial bedrock area at Castleguard Glacier, Alberta, Canada. **Zeitschrift für Gletscherkunde und Glazialgeologie,** 16(2), 171-84.

Hantz, D. and Lliboutry, L. 1983. Waterways, ice permeability at depth, and water pressures at Glacier D'Argentiere, French Alps. **Journal of Glaciology,** 29(102), 227-239.

Harper, J.T. and Humphrey, N.F. 1995. Borehole video analysis of a temperate glacier's englacial and subglacial structure: Implications for glacier flow models. **Geology,** 23(10), 901-904.

Hodge, S.M. 1976. Direct measurement of basal water pressures: a pilot study. **Journal of Glaciology,** 16(74), 205-218.

Hooke, R. Leb, Wold, B. and Hagen, J.O. 1985. Subglacial hydrology and sediment transport at Bonhusbreen, southwest Norway. **Geological Society of America Bulletin,** 96, 388-397.

Hooke, R. Leb, Miller, S.B. and Kohler, J. 1988. Character of the englacial and subglacial drainage system in the upper part of the ablation area of Storglaciaren, Sweden. **Journal of Glaciology,** 34(117), 228-231.

Hooke, R. LeB., Laumann, T. and Kohler, J. 1990. Subglacial water pressures and the shape of subglacial conduits. **Journal of Glaciology,** 36(122), 67-71.

Hubbard, B.P. 1992. Basal ice facies and their formation in the western Alps. (Ph.D. thesis, University of Cambridge).

Hubbard, B.P., Sharp, M.J., Willis, I.C., Nielsen, M.K. and Smart, C.C. 1995. Borehole water-level variations and the structure of the subglacial hydrological system of Haut Glacier d'Arolla, Valais, Switzerland. **Journal of Glaciology,** 41 (139), 572-583.

Humphrey, N., Raymond, C. and Harrison, W. 1986. Discharges of turbid water during mini-surges of Variegated Glacier, Alaska, U.S.A. **Journal of Glaciology,** 32(111), 195-207.

Iken, A. 1981. The effect of the subglacial water pressure on the sliding velocity of a glacier in an idealized numerical model. **Journal of Glaciology,** 27(97), 407-421.

Iken, A. and Bindschadler, R.A. 1986. Combined measurements of subglacial water pressure and surface velocity of Findelengletcher, Switzerland: conclusions about drainage system and sliding mechanism. **Journal of Glaciology,** 32(110), 101-119.

Kamb, B., Raymond, C.F., Harrison, W.D., Engelhardt, H., Echelmeyer, K.A., Humphrey, N., Brugman, M.M. and Pfeffer, T. 1985. Glacier surge mechanism: 1982-1983 surge of Variegated Glacier, Alaska. **Science,** 227(4686),469-479.

Kamb, B. 1987. Glacier surge mechanism based on linked-cavity configuration of the basal water conduit system. **Journal of Geophysical Research,** 92(B9), 9083-9100.

Ketterling, B. 1995. Electrical conductivity of waters in glacier boreholes. (M.Sc. thesis, University of Western Ontario).

Murray, T. and Clarke, G.K.C. 1995. Black-box modelling of the subglacial water system. **Journal of Geophysical Research,** 100(B7), 10,231-10245.

Nielsen, M.K. 1995. Instrumentation for the investigation of subglacial hydrology. (M.Sc thesis, University of Bristol).

Nienow, P. 1993. Dye-tracer investigations of glacier hydrological systems. (Ph.D thesis, University of Cambridge).

Nienow, P., Sharp, M. and Willis, I. In Press. Temporal switching between englacial and subglacial drainage pathways: dye tracer evidence from the Haut Glacier d'Arolla, Switzerland. **Geografiska Annaler.**

Nienow, P., Sharp, M. and Willis, I. Submitted. Dye tracer investigations at the Haut Glacier d'Arolla, Switzerland. II. Seasonal changes in the morphology of the subglacial drainage system. **Earth Surface Processes and Landforms.**

Nye, J.F. 1973. Water at the bed of a glacier. In `Symposium on the Hydrology of Glaciers' (Proceedings of the Cambridge Symposium, 7-13 September 1969). **IAHS Publication,** 95, 189-194.

Paterson, W.S.B. 1994. *The Physics of Glaciers,* 3rd Edition, Pergamon, Oxford, 480pp.

Pohjola, V.A. 1993. TV-video observations of bed and basal sliding on Storglaciaren, Sweden. **Journal of Glaciology,** 39(131), 111-118.

Pohjola, V.A. 1994. TV-video observations of englacial voids in Storglaciaren, Sweden. **Journal of Glaciology,** 40(135), 231-240.

Raiswell, R. 1984. Chemical models of solute acquisition in glacial meltwaters. **Journal of Glaciology,** 30(104), 49-57.

Raymond, C.F., Benedict, R.J., Harrison, W.D., Echelmeyer, K.A. and Sturm, M. 1995. Hydrological discharges and motion of Fels and Black Rapids Glacier, Alaska, U.S.A.: implications for the structure of their drainage systems. **Journal of Glaciology,** 41(138), 290-304.

Röthlisberger, H. 1972. Water pressure in intra- and subglacial channels. **Journal of Glaciology,** 11(62), 177-203.

Sharp, M.J. 1991. Hydrological inferences from meltwater quality data: the unfulfilled potential. **Proc. British Hydrol. Soc. National Symp., Southampton, 16-18 Sept. 1991,** 5.1-5.8.

Sharp, M.J., Gemmell, J.C. and Tison, J-L. 1989. Structure and stability of the former subglacial drainage system of the Glacier de Tsanfleuron, Switzerland. **Earth Surface Processes and Landforms,** 14, 119-34.

Sharp, M.J., Richards, K.S., Willis, I.C., Nienow, P., Lawson, W. and Tison, J-L. 1993. Geometry, bed topography and drainage system structure of the Haut Glacier d'Arolla, Switzerland. **Earth Surface Processes and Landforms,** 18, 557-72.

Shreve, R.L. 1972. Movement of water in glaciers. **Journal of Glaciology,** 11(62), 205-214.

Smart, C.C. 1996. Statistical evaluation of glacier boreholes as indicators of basal drainage systems. **Hydrological Processes,** 10(4), 599-613.

Stenborg, T. 1969. Studies of the internal drainage of glaciers. **Geografiska Annaler,** 51A(1-2), 13-41.

Stone, D.B. 1993. Characterization of the basal hydraulic system of a surge-type glacier: Trapridge Glacier, 1989-1992. (M.Sc. thesis, University of British Columbia)

Stone, D.B., Clarke, G.K.C. and Blake, E.W. 1993. Subglacial measurement of turbidity and electrical conductivity. **Journal of Glaciology,** 39(132), 415-420.

Stone, D.B. and Clarke, G.K.C. 1993. Estimation of subglacial hydraulic properties from induced changes in basal water pressure: a theoretical framework for borehole response tests. **Journal of Glaciology,** 39(132), 327-340.

Stone D.B. and Clarke, G.K.C. 1996. In situ measurements of basal water quality as an indicator of the character of subglacial drainage systems. **Hydrological Processes,** 10(4), 615-628.

Tranter, M., Brown, G., Raiswell, R., Sharp, M. and Gurnell, A. 1993. A conceptual model of solute acquisition by Alpine glacial meltwaters. **Journal of Glaciology,** 39(133), 573-581.

Tranter, M., Sharp, M.J., Brown, G.H., Willis, I.C., Hubbard, B.P., Nielsen, M.K., Smart, C.C., Gordon, S., Tulley, M. and Lamb, H.R. In Press. Variability in the chemical composition of in situ subglacial meltwaters. **Hydrological Processes.**

Walder, J.S. 1986. Hydraulics of subglacial cavities. **Journal of Glaciology,** 32(112), 439-45.

Walder, J.S. and Hallet, B. 1979. Geometry of former subglacial water channels and cavities. **Journal of Glaciology,** 23(89), 335-46.

Walder, J.S. and Fowler, A. 1994. Channelized subglacial drainage over a deformable bed. **Journal of Glaciology,** 40 (134), 3-15.

Weertman, J. 1972. General theory of water flow at the base of a glacier or ice sheet. **Reviews of Geophysics and Space Physics,** 10(1), 287-333.

Willis, I.C., Sharp, M.J. and Richards, K.S. 1990. Configuration of the drainage system of Midtdalsbreen, Norway as indicated by dye-tracing experiments. **Journal of Glaciology,** 36(122), 89-101.

## APPENDIX I: DRILLING PROCEDURE

The drill used was a commercial high pressure hot water cleaner, model HDS 100B manufactured by Kärcher. It consisted of a petrol-fuelled pump which sucked water up a short inlet hose, passed it through a diesel-fuelled boiler and forced it out of an outlet pipe. The intake hose drew water from the bottom of a 30 gallon bucket filled with supraglacial water which provided additional head to drive water into the drill system. The ends of two 100m sections of thick-walled rubber hose (Conti Asymflex 3TE 12DIN) were fitted with hose tails so that they could be linked by threaded connectors, and joined to the drill outlet pipe and the stainless steal drill stem (2x1m). A tapered, brass drill head with a drill tip was screwed onto the end of the drill stem. Two types of drill tip were used: one with a small central hole that produced a straight jet of water and was used for drilling new boreholes, and one with a slightly wider hole that produced a 45° cone of water that was used for reaming old boreholes to widen them or loosen in-situ instruments if they were stuck.

This drilling system was able to generate a water pressure of between 60 and 80 bars at a temperature ranging from 80 to 150°C. The water pressure and temperature could be adjusted to produce an average drilling rate of c. 2m $min^{-1}$ through the upper 60m of the ice. This slowed to c. 1m $min^{-1}$ for the next 50m and then slowed further for any remaining distance to the bed. The bed was considered to have been reached and drilling was halted when no further progress could be made at a depth consistent with radio-echo sounding (Sharp et al., 1993) and the depth of neighbouring boreholes.

## APPENDIX II: EC PROFILERS

The EC profilers used were hand made instruments designed by Chris Smart and Brad Ketterling. As the profilers were to be used continuously and vigorously they needed to be robust and durable if they were to last through the observation season.

The profilers consisted of three main components (Figure II.1):

a) **Sensor module**: where a voltage was applied to the water to measure resistance. This module had to be especially robust in order to withstand repeated contact with the bed and/or ice obstructions and constrictions in the borehole itself. In addition the module had to be corrosion-proof so that the voltage transmission/reception capacity did not deviate over the observation season.

b) **Support module:** to which the sensor module and cable were attached. This housed the wiring for the instrument and provided the necessary strain relief for the cable as well as the sufficient weight to allow the probe to plumb the boreholes freely.

c) **Cable:** this had to be very strong and thick to support the considerable weight of the probe that can occur at great depths in a dry borehole, but it also needed to be flexible enough to be handled with ease. The profilers were attached to 150m of cable that was marked off at 5m intervals with electrical tape using a colour code system.

The profiler cable was attached to a Campbell Scientific CR-10 data logger which was programmed to provide an excitation voltage to the sensor module, take readings of resistance at one second intervals, convert the resistance to conductance and multiply the conductance with a cell constant specific to each profiler. This provided an output of specific conductivity in $\mu S\ cm^{-1}$. Solutions of known EC were used to calibrate the profilers and provide cell constants for the logger programme.

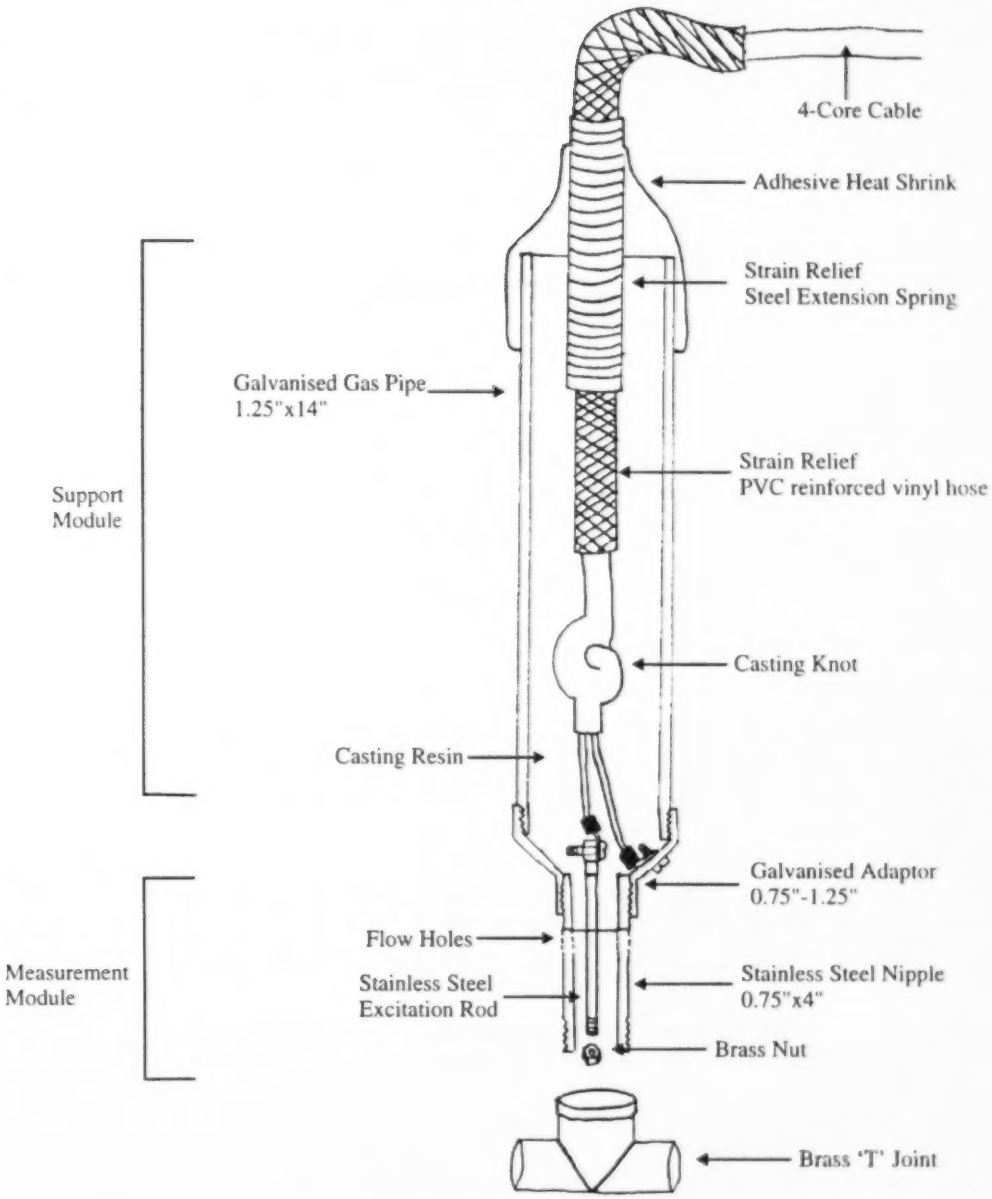


Figure II.1: EC profiler components.

# APPENDIX III: IN-SITU WATER PRESSURE, ELECTRICAL CONDUCTIVITY AND TURBIDITY SENSORS

In-situ sensors used in 1993 were designed and built by M. Nielsen. Three probes which measured water pressure, EC and turbidity were fitted into PTFE cylinder casings and connected together forming a single sensor head with a diameter of 4.5cm (Figure III.1). Weights were attached to the base of the casing to reduce buoyancy. A detailed description of each sensor head is provided by Nielsen (1995). The sensors were attached to 210m of 15-core cable and wired into Campbell Scientific CR-10 data loggers which were programmed to record the means of 30 readings every 10 minutes. Water pressures and ECs were calibrated against known values and were accurate to within 0.5m of water head and 5$\mu S\ cm^{-1}$, respectively.

In 1995, six in-situ water pressure and EC sensors were constructed by Bryn Hubbard, Bernd Kulessa and the author. The pressure sensors were 10bar and 1.6bar 'TransInstruments' transducers. These were soldered onto 4-core cable and set in casting resin. Calibration was undertaken in the field by lowering the sensors down a full borehole at 10m intervals and recording the measured mV readings. Water pressure in mV was later converted to water level in metres. The in-situ EC sensors were constructed following the guidelines of Stone et. al (1993) with minor revisions (Figure III.2) and calibrated in the same way as the EC profilers. In order to measure both water pressure and EC in a single borehole, the cables of pairs of in-situ and water pressure sensors were taped together. The sensors were attached to Campbell Scientific CR-10 data loggers which recorded the means of 30 readings every 10 minutes.

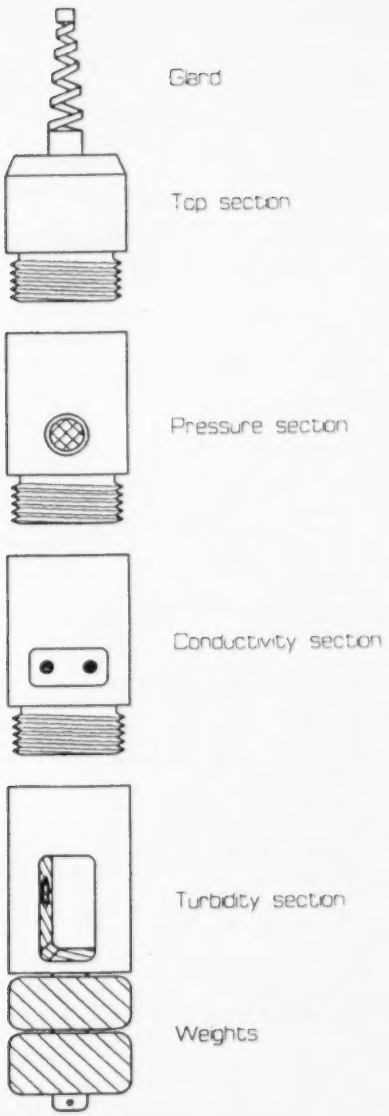


Figure III.1: Combined water pressure, electrical conductivity and turbidity sensor used in 1993.

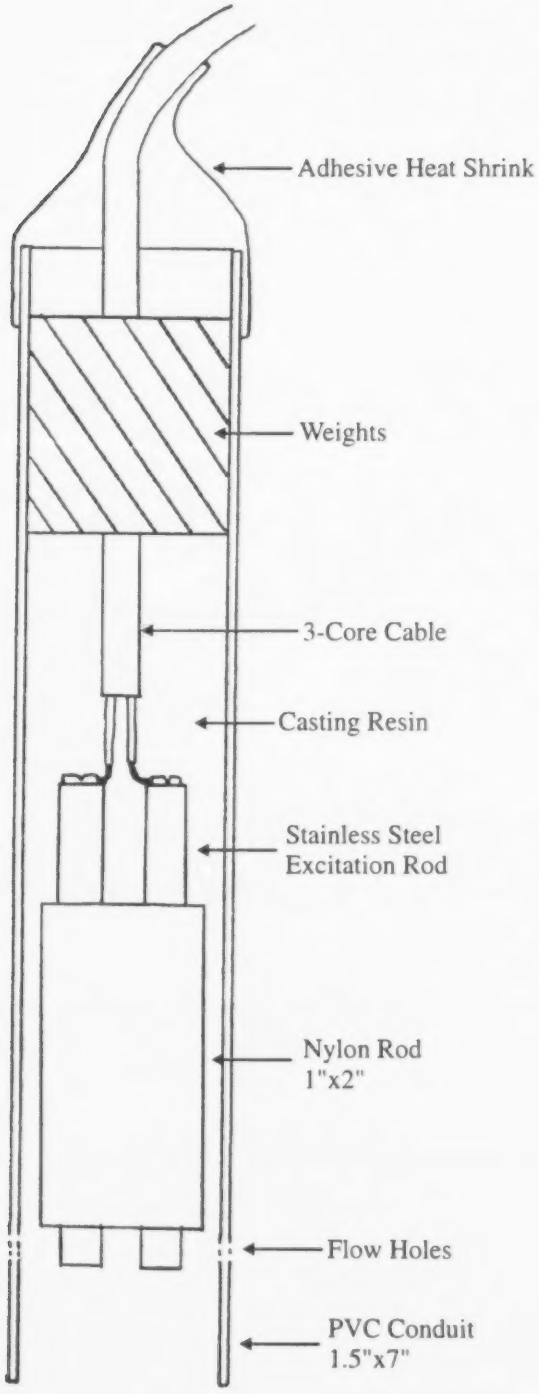


Figure III.2: In-situ EC sensor constructed in 1995.

## APPENDIX IV: VIDEO IMAGERY SYSTEM

In 1995, eleven boreholes were viewed with a commercially available borehole video camera system supplied by Colog Inc., and manufactured by Marks Products Inc.. The Geo Vision Micro™ system consisted of a miniature colour video camera housed in a 3cm wide by 30cm long waterproof stainless steel container, 230m of cable on a hand-operated winch, a small combined colour monitor/VCR, a microphone, two lighting attachments, several side-looking mirrors, and a mounting tripod (Figure IV.1). System power came from an inverter attached to a 12 volt car battery. An out-front lighting attachment, consisting of a small bulb on the end of a thin rod, allowed exploration of boreholes at least 3cm in diameter. Alternatively, a 7.6cm diameter ring lighting attachment of four high-intensity bulbs could be mounted around the end of the camera. A side-looking mirror could also be attached to give a 360° view of the side of the borehole when the camera was rotated. During recording, a display on the colour monitor showed the depth of the video camera below the ice surface. The borehole video images were recorded on standard small-sized video cassettes for later viewing and analysis.

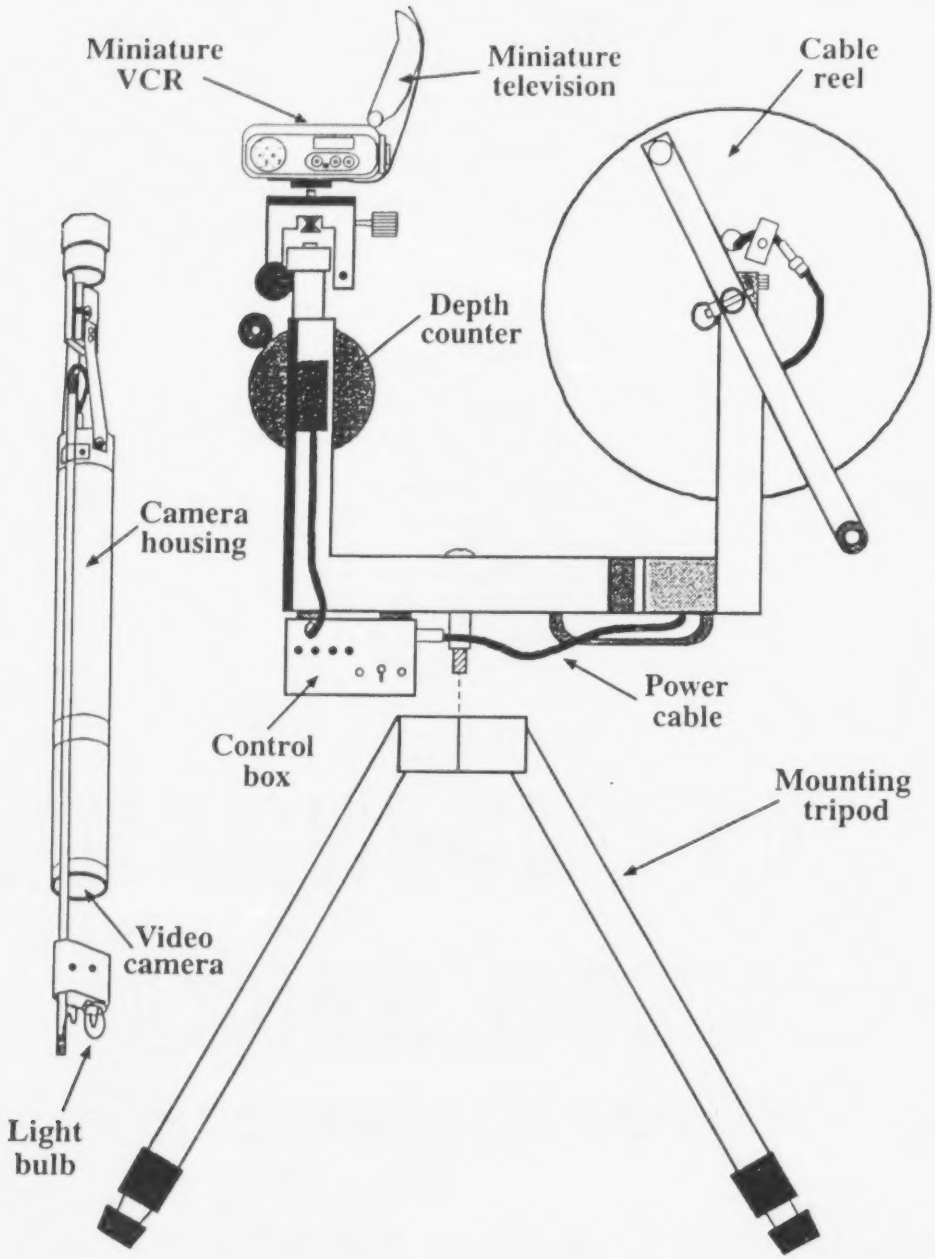


Figure IV.1: Components of the Geo Vision Micro$^{TM}$ borehole video imagery system.